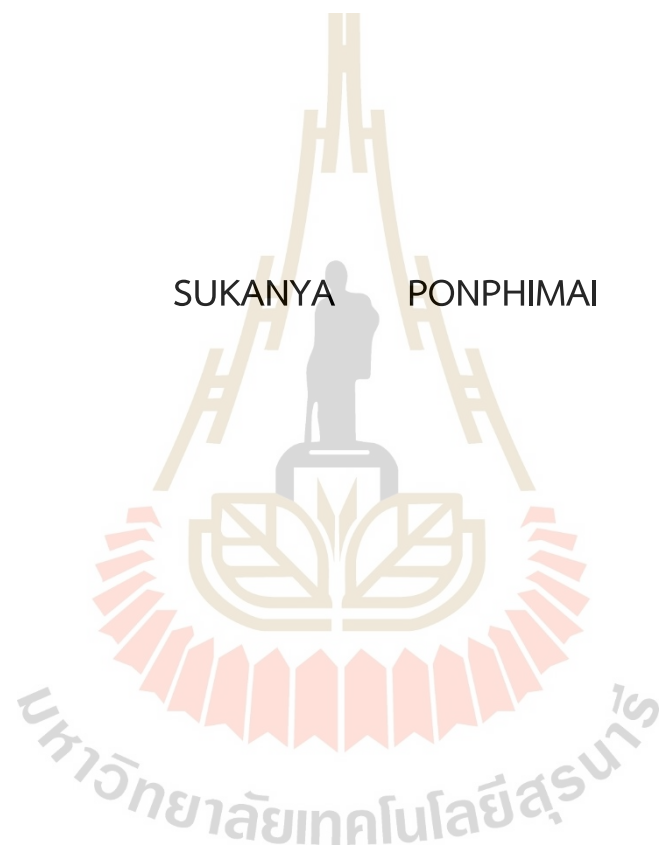
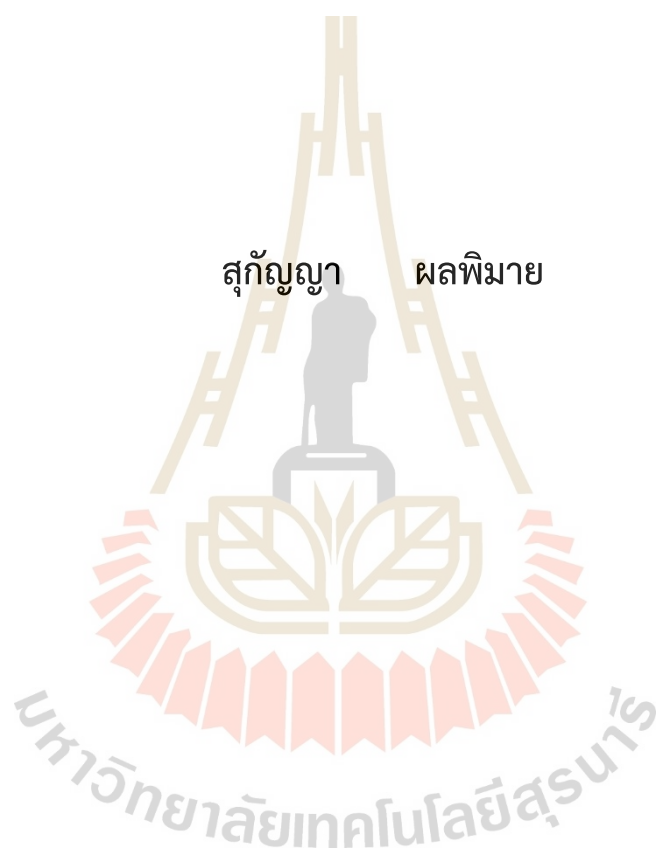


PRODUCTION AND CHARACTERIZATION OF MURINE SINGLE-
CHAIN VARIABLE FRAGMENT (MuscFV) ANTIBODY AGAINST
ACRYLAMIDE IN COFFEE



A Thesis Submitted in Partial Fulfillment of the Requirements for the
Degree of Translational Medicine
Suranaree University of Technology
Academic Year 2023

การผลิตและการแสดงคุณลักษณะของ MuscFv ต่ออะคริลาไมด์ในกาแฟ



วิทยานิพนธ์นี้เป็นส่วนหนึ่งของการศึกษาตามหลักสูตรปริญญาปรัชญาดุษฎีบัณฑิต

สาขาเวชศาสตร์ปริวรรต

มหาวิทยาลัยเทคโนโลยีสุรนารี

ปีการศึกษา 2566

PRODUCTION AND CHARACTERIZATION OF MURINE SINGLE-
CHAIN VARIABLE FRAGMENT (MuscFV) ANTIBODY AGAINST
ACRYLAMIDE IN COFFEE

Suranaree University of Technology has approved this thesis submitted in
partial fulfillment of the requirements for a Doctoral' s Degree

Thesis Examining Committee

Kantaphon G.

(Dr. Kantaphon Glab-ampai)

Chairperson

Kanyarat T.

(Dr. Kanyarat Thueng-in)

Member (Thesis Advisor)

Jeeraphong T.

(Assoc.Prof. Dr.Jeeraphong Thanongsaksrikul)

Member (Thesis Co-advisor)

Sanong

(Dr.Sanong Suksaweang)

Member (Thesis Co-advisor)

T. Sim

(Dr.Theeraya Simawaranon)

Member (Thesis Co-advisor)

Krajang

(Assoc. Prof. Dr. Krajang Talabnin)

Member

Yupaporn Ruksakulpiwat

(Assoc. Prof. Dr. Yupaporn Ruksakulpiwat)

Vice Rector for Academic Affairs and

Quality Assurance

Sutham Pinjaroen

(Assoc. Prof. Sutham Pinjaroen, M.D.)

Dean of Institute of Medicine

สุกัญญา ผลพิมาย: การผลิตและการแสดงคุณลักษณะของ MuscFv ต่ออะคริลาไมด์ในกาแฟ (PRODUCTION AND CHARACTERIZATION OF MURINE SINGLE-CHAIN VARIABLE FRAGMENT (MuscFV) ANTIBODY AGAINST ACRYLAMIDE IN COFFEE)
 อาจารย์ที่ปรึกษาวิทยานิพนธ์: ดร.กัญญารัตน์ ถึงอินทร์ ,146หน้า

คำสำคัญ: สารอะคริลาไมด์/เฟจ/ MuscFv/แอนติบอดี

อะคริลาไมด์ (AA) พบว่าเกิดขึ้นเองตามธรรมชาติในอาหาร โดยเฉพาะอาหารจำพวกน้ำตาลและแป้งที่ผ่านกระบวนการปรุงที่อุณหภูมิสูงจะก่อเกิดอะคริลาไมด์ในอาหารได้ นอกจากนี้ยังพบว่าอะคริลาไมด์เป็นสารก่อมะเร็งที่เป็นอันตราย เป็นพิษต่อระบบประสาท เป็นพิษต่อระบบสืบพันธุ์ และเป็นสารก่อมะเร็งในสัตว์ ผู้วิจัยจึงมีความสนใจในการสร้างแอนติบอดีต่ออะคริลาไมด์เพื่อจุดประสงค์ในการตรวจจับสารปนเปื้อนอะคริลาไมด์ในกาแฟ

ในการวิจัยครั้งนี้ ทำการคัดเลือกหาเฟจจากคลังแอนติบอดี เพื่อการคัดหาเฉพาะ antibody ส่วน single chain fragment variable (scFv) ที่จำเพาะต่ออะคริลาไมด์จากคลังแอนติบอดีของหนู (MuscFv) ผู้วิจัยใช้สารอะคริลาไมด์มาตรฐาน (AA) เป็นแอนติเจนสำหรับการคัดเลือกแบคทีเรียเฟจ ซึ่งการคัดเลือกหาเฟจจากคลังแอนติบอดีของหนูนั้นจะสามารถแสดงออกถึงแอนติบอดีเป้าหมายใน *E. coli* ได้ หลังจากนั้นได้มีการนำมาคัดแยก scFv แอนติบอดีที่จำเพาะต่ออะคริลาไมด์ ยืนยันความจำเพาะด้วยเทคนิค Western blot และทดสอบการจับกันด้วยเทคนิค ELISA รวมถึงได้รับการทดสอบการเกิดปฏิกิริยาข้ามกับ BSA แล้วนั้น ทำให้การสร้างแอนติบอดี (MuscFv) ของหนูที่จำเพาะต่ออะคริลาไมด์ในกาแฟถูกสร้างขึ้นสำเร็จแล้ว และตรวจสอบได้โดยวิธี ELISA และ HPLC

การสร้างคลังข้อมูลของชิ้นส่วนแอนติบอดีรีคอมบิแนนท์ที่แสดงบนพื้นผิวของแบคทีเรียเฟจ เพื่อการคัดเลือกหาเฟจจากคลังแอนติบอดีต่อแอนติเจนเป้าหมาย เป็นเครื่องมือทางเทคโนโลยีชีวภาพที่สำคัญในการสร้างแอนติบอดีโมโนโคลนัล ซึ่งการวิจัยครั้งนี้เป็นการศึกษาครั้งแรกที่ได้อธิบายถึงการคัดเลือกแอนติบอดีต่ออะคริลาไมด์จากคลังข้อมูลแอนติบอดีของหนู และสามารถตรวจจับอะคริลาไมด์ในกาแฟได้

สาขาวิชาเวชศาสตร์ปริวรรต
 ปีการศึกษา 2566

รายชื่อชื่อนักศึกษา *Sikanya*
 รายชื่อชื่ออาจารย์ที่ปรึกษา *Kanyard T.*
 รายชื่อชื่ออาจารย์ที่ปรึกษาร่วม *Jeeraphong T.*
 รายชื่อชื่ออาจารย์ที่ปรึกษาร่วม *T. Sam*
 รายชื่อชื่ออาจารย์ที่ปรึกษาร่วม..... *[Signature]*

SUKANYA PONPHIMAI: PRODUCTION AND CHARACTERIZATION OF MURINE SINGLE-CHAIN VARIABLE FRAGMENT (MuscFv) ANTIBODY AGAINST ACRYLAMIDE IN COFFEE. THESIS ADVISOR: Dr. KANYARAT THUENG-IN ,140 page PP.

Keyword: Acrylamide/Phage bio-panning/ MuscFv/Antibody

Ingredients of food, especially sugar and starch at high temperature cooking process could lead to the formation of acrylamide (AA). This chemical is harmful carcinogens, a neurotoxicant, reproductive toxicant, and carcinogen in animal species. However, the detection of acrylamide contaminated in food is unnoticed.

In this work, Phage bio-panning was performed in order to select scFv specific to acrylamide from murine scFv (MuscFv) phage-displayed library. Acrylamide standard (AA) used as antigen for bio-panning and was expressed in *E. coli* system. Several scFvs were isolated and specificity towards acrylamide was confirmed by Western blot and the binding tested by ELISA. The anti-AA MuscFv phage clones did not show any cross-reactivity with BSA from bio-panning process. Further, biochemical and functional investigations demonstrated that the binding of specific MuscFv with acrylamide. Moreover, we tested the anti-AA MuscFv specific to acrylamide could detect acrylamide in coffee using ELISA and verified by High- performance liquid chromatography (HPLC).

The construction of libraries of recombinant antibody fragments that are displayed on the phage surface. The selection of phage antibodies against target antigens has become an important biotechnological tool to generate novel monoclonal antibodies for research. For the first time, this study describes the selection of antibodies against acrylamide from murine scFv phage-displayed library which can detect acrylamide in coffee.

School of Translational Medicine
Academic Year 2023

Student's Signature
Advisor's Signature
Co-advisor's Signature
Co-advisor's Signature
Co-advisor's Signature

ACKNOWLEDGEMENT

First, I wish to express my deepest appreciation to my advisor, Dr. Kanyarat Thueng-in, who gave me the opportunity to do challenging and interesting study and always add valuable suggestions and guidance throughout. Moreover, I would like to express sincere appreciation to my co-advisors, Asst.Prof. Dr.Jeeraphong Thanongsaksrikul Dr.Sanong Suksaweang and Dr.Theeraya Simawaranon, who patiently educated, encouraged, guided, and strengthened my knowledge in order for me to complete my doctoral 's degree in Translational medicine.

I would like to acknowledge Dr. Kantaphon Glab-ampai, who offered consultation on a molecular docking model and my internal examiner, Assoc. Prof. Dr. Krajang Talabnin, who provided valuable suggestions.

I would like to thank to mouse scFv phage-displayed library from Faculty of Allied Health Sciences, Thammasat University, Thailand. I would like to acknowledge to the Thailand Research Fund and best student scholarships. Moreover, sincere thanks to the Translational medicine Unit, Suranaree University of Technology for supporting the equipment and laboratory facilities.

I would like to thank to "This research and innovation activity is funded by National Research Council of Thailand (NRCT) and Suranaree University of Technology (SUT)" for this sturdy.

I would also like to thank my friends for providing invaluable encouragement. Finally, I would like to thank my husband, my daughter and my parents for their continued love, support, guidance, and encouragement.

SUKANYA PONPHIMAI

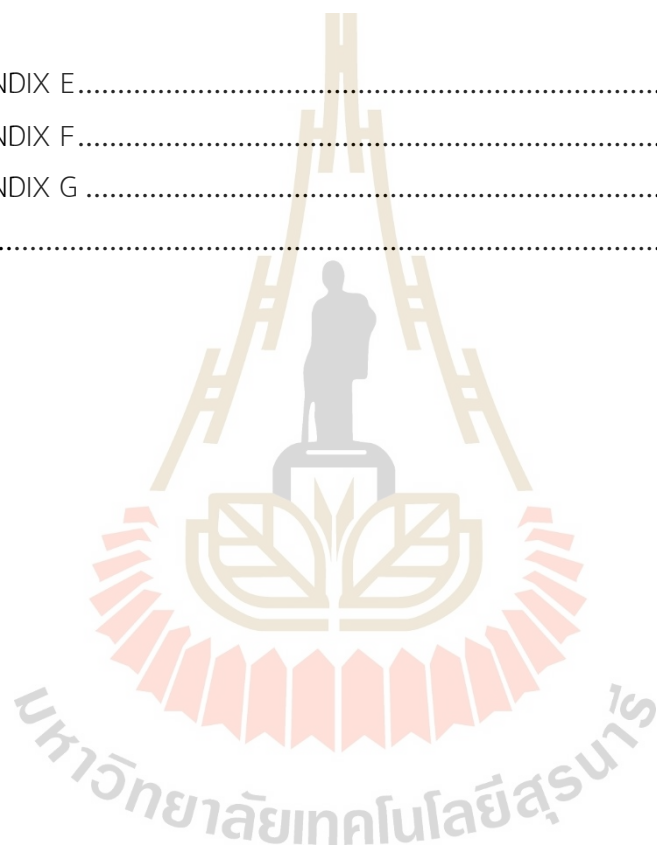
TABLE OF CONTENTS

	Page
ABSTRACT (THAI).....	II
ABSTRACT (ENGLIST).....	I
ACKNOWLEDGEMENT.....	II
TABLE OF CONTENTS.....	IV
LIST OF FIGURES.....	VIII
LIST OF ABBREVIATIONS.....	XI
CHAPTER	
1. INTRODUCTION.....	1
1.1 General introduction	2
1.2 Research objective	2
1.3 Scope and limitations of the study	2
1.4 Expected results	3
2. LITERATURE REVIEWS	4
2.1 Acrylamide.....	4
2.2 Conventional antibody	12
2.3 Phage display technology.....	18
2.4 Principle of enzyme-linked immunosorbent assay (ELISA)	23
2.5 Formation of acrylamide (AA) in Coffee	30
3. RESERCH METHODLOGY	35
3.1 MuscFv antibody production.....	35
3.1.1 Selection of Phage clone displaying murine scFv that bound to AA by bio-panning.....	34
3.2 Sub-cloning of muscFv antibodies	39
3.2.1 Sub-cloning of muscFv- AA from pSEX81 vector to pOPE101 vector.....	39
3.3 Expression and purification of anti-AA MuscFv antibodies.....	43
3.3.1 Small scale expression of the anti-AA MuscFv antibodies.....	43

3.3.2 Large-scale expression of anti-AA MuscFv antibodies.....	43
3.3.4 Purification of anti-AA MuscFv antibodies	44
3.4 Protein determination and characterization.....	44
3.4.1 Sodium dodecyl sulfate-polyacrylamide gel electrophoresis.....	44
3.4.2 Characterization and Homology modeling and intermolecular docking.....	45
3.5 Production of ELISA detect AA in coffee.....	46
3.5.1 Determination of the cutoff value of Anti-AA MuscFv antibody by indirect ELISA	46
3.5.2 Validation of AA standard and anti-AA MuscFv antibody	47
3.5.3 Determination of Anti-AA MuscFv specific to acrylamide in coffee	47
3.6 Other of related experiments.....	47
3.6.1 Production of polyclonal antibody against acrylamide	47
3.6.2 Preparation of Glutathione S-transferase conjugation AA standard.....	48
3.6.3 Production of AuNPs conjugation MuscFv- anti AA.....	48
3.6.4 Preparation of immunochromatographic strip test for AA detection	49
4. RESULT AND DISCUSSION.....	50
4.1 MuscFv antibody production.....	50
4.1.1 Screening of Phage clone displaying MuscFv that bound to AA.....	50
4.1.2 Selection for phage transformed E. coli clones that carried recombinant phagemids with the inserted murine scFv (MuscFv)-coding sequences	52

4.1.3 Binding of the muscFv-AA phage by indirect ELISA.....	54
4.2 Sub-cloning of muscFv antibodies	54
4.2.1 Sub-cloning of muscFv- AA phage from pSEX81 vector to pOPE101 vector	54
4.3 Expression and purification of anti-AA MuscFv antibodies.....	56
4.4 Characterization and Homology modeling and intermolecular docking.....	58
4.4.1 Complementary determining regions (CDRs) and immunoglobulin framework regions (FRs) of the MuscFv-N11.1	58
4.4.2. Computerized simulations to determine the presumptive epitopes of the MuscFv-N11.1 bound AA	59
4.5 Production of ELISA detect AA	62
4.5.1 Validation of AA standard and MuscFv-N11.1 antibody	62
4.5.2 Determination of the cutoff value of MuscFv-N11.1 by indirect ELISA.....	63
4.5.3 Determination of MuscFv-N11.1 specific to acrylamide in coffee	64
4.6 The result of related experiments	70
4.6.1 Production of polyclonal antibody against AA.....	70
4.6.2 Preparation of Glutathione S-transferase conjugation AA standard	71
4.6.3 Production of AuNPs conjugation MuscFv- anti AA	71
4.6.4 Preparation of immunochromatographic strip test for AA detection	72
4.7 Discussion	73
5. CONCLUSION AND RECOMMENDATION	77
5.1 Conclusion	78
5.2 Recommendation	80

REFERENCES.....	81
APPENDIX.....	101
APPENDIX A.....	102
APPENDIX B.....	125
APPENDIX C.....	126
APPENDIX D	128
APPENDIX E.....	129
APPENDIX F.....	130
APPENDIX G	132
VITAE.....	134



LIST OF FIGURES

Figure	Page
2.1	Chemical structure of acrylamide4
2.2	Formation of acrylamide through 3-APA.....6
2.3	Formation of acrylamide from acrolein6
2.4	Maillard reactions7
2.5	Metabolism of acrylamide.....10
2.6	Schematic diagrams of the antibody structure13
2.7	Schematic diagrams of all human antibody classes / types: IgM, IgD, IgG, IgE, and IgA.....14
2.8	Antibody model showing subunit composition and domain distribution along the polypeptide chains17
2.9	Bacteriophage (phage)19
2.10	<i>E.coli</i> filamentous bacteriophages.....21
2.11	steps for phage display technology23
2.12	Steps of ELISA.....25
2.13	Indirect ELISA.....25
2.14	Direct ELISA.....26
2.15	Sandwich ELISA.....27
2.16	Competitive ELISA28
2.17	Potential pathways of acrylamide formation during coffee processing30
2.18	A review of studies investigating acrylamide inhibition during coffee processing32
4.1	PCR amplicon of the phagemid <i>muscfv</i> sequence50
4.2	PCR amplicon of the phagemid <i>muscfv</i> sequence. (Continued)51
4.3	PCR amplicon of the phagemid <i>muscfv</i> sequence. (Continued)52

LIST OF FIGURES (Continued)

Figure	Page
4.4	PCR amplicon of muscfv (~750 -900 bp) in picked pSEX81 -transformed <i>E. coli</i> derived from phage bio-panning53
4.5	Results of indirect ELISA for determining binding of muscfv-AA phage54
4.6	PCR amplicon of pOPE10: muscfv (~750 -900 bp) in picked pOPE101 - transformed <i>E. coli</i> derived from Sub-cloning55
4.7	anti-AA Muscfv antibodies (~25-30 kDa) expressed by <i>E. coli</i> inserted murine scFv (Muscfv) clones as determined by WB.....56
4.8	Purified anti-AA Muscfv antibodies57
4.9	The ELISA binding result of Muscfv-N11.1 showed statistically significant specific binding of Muscfv to acrylamide when compared with BSA.....58
4.10	The deduced amino acid (aa) sequence of Muscfv-N11.1 was shown including the VH and VL domains joined by a (Glu4 Gly1 Phe1 Ser1) linker, the complementary determining region 1-3 (CDR1-3).59
4.11	The Molecular docking model of Muscfv-N11.1 interacts with acrylamide.60
4.12	Checker board titration of anti-AA Muscfv antibody62
4.13	Acrylamide standard test linearity plot correlation between concentration and area, with an $R^2 = 0.9303$63
4.14	The cutoff value of Muscfv-N11.1 specific to acrylamide was performed by ELISA.....64
4.15	The determination of Muscfv-N11.1 specific to acrylamide in coffee was performed using the dark roasted coffee beans containing 2 coffee brands.....65

LIST OF FIGURES (Continued)

Figure		Page
4.16	Chromatograms of acrylamide standard 1000 ng/ml, (RT: 3.827 min)	66
4.17	Linearity plot for acrylamide standard	67
4.18	Chromatograms of coffee A1 spiked with AA standard at concentrations 0.5 mg/ml. showed an acrylamide (RT: 3.840 min) and interference	68
4.19	Chromatograms of coffee A2 non-spiked with AA standard found that an acrylamide (RT: 3.854 min) and interference	68
4.20	Chromatograms of coffee B1 spiked with AA standard at concentrations of 0.5 mg/ml show acrylamide (RT: 3.854 min) and interference	69
4.21	Chromatograms of coffee B2 non-spiked with AA standard found that an acrylamide (RT: 3.854 min) and showed interference.....	69
4.22	Checker board titration results showed the lowest amount of polyclonal antibody against acrylamide in rabbit No.1 and rabbit No.2.....	70
4.23	Glutathione S-transferase conjugation AA standards were checking binding anti-GST, mAb anti- AA and anti- AA from rabbit No.1 by dot blot assay.....	71
4.24	The results from the immunochromatographic strip tests showed the absences of bands in both groups	72

LIST OF ABBREVIATIONS

AA	=	Acrylamide standard
Ab	=	Antibody
aa	=	amino acid
Amp	=	Ampicillin
AuNPs	=	Colloid gold nanoparticles
bp	=	Base pair
BSA	=	Bovine serum albumin
CDRs	=	Complementarity determining regions
Conc.	=	concentration
CBB	=	Coomassie staining
DI water	=	Distilled water
<i>E. coli</i>	=	Escherichia coli
ELISA	=	Enzyme-linked immunosorbent assay
Fab	=	Fragment antigen-binding
GST	=	Glutathione S-transferase
g	=	Gram
hr	=	Hour
HRP	=	Horseradish Peroxidase
HPLC	=	high-performance liquid chromatography.
IPTG	=	Isopropyl β -D-thiogalactopyranoside
kDa	=	kilo Dalton
Kb or bp	=	Kilobase or base pair
kcal/mol	=	kilocalorie per mole
LB	=	Lysogeny broth/Luria-Bertani
LB-AG	=	LB-ampicillin-glucose agar
LOD	=	Limit of detection
mAb	=	Monoclonal antibody
MuscFv	=	Murine Single-chain variable fragment

LIST OF ABBREVIATIONS (Continued)

mg/ml	=	Milligram per milliliter
µg/ml	=	Microgram per milliliter
µl	=	Microliter
PBS	=	Phosphate buffered saline
µm	=	Micrometer
Ni-NTA	=	Nickel-nitrilotriacetic acid
nm	=	nanometer
OD	=	Optical density
RT	=	room temperature
RT	=	Retention time
rpm	=	Revolution per minute
SD	=	Standard deviation
SDS-PAGE	=	Sodium dodecyl sulfate-polyacrylamide gel electrophoresis
scFv	=	Single-chain variable fragment
Tet	=	Tetracycline
VH	=	Variable heavy
VL	=	Variable light
UDW	=	Ultrapure deionized water
WB	=	Western blot

CHAPTER 1

INTRODUCTION

1.1 General introduction

Acrylamide (AA), an unsaturated-amide small molecule, is a by-product of food heating processes (due to Maillard reaction) that are commonly present in cooked foods. This agent was known to be toxic to humans (Svensson et al., 2003; Tareke et al., 2000). It is rapidly absorbed after ingestion and distributed in many organs such as thymus, liver, heart, brain and kidneys (Capuano and Fogliano, 2011; Hu et al., 2014). Due to its genotoxicity and carcinogenicity (Xu et al., 2014), acrylamide was classified as a Group 2A carcinogen by the International Agency for Research on Cancer (IARC, 1994) and a Category 2 carcinogen and Category 2 mutagen by the European Union.

Acrylamide contamination in food is first reported by Swedish national food administration using LC/MS/MS method. The most foods often found acrylamide are potato chips, French fries, baked bread, chocolate, and coffee (Rosén and Hellenäs, 2002). Many researchers have confirmed the presence of acrylamide in different processed foods. For Thai foods, acrylamide has been found in curries, commercial and conventional snacks, instant noodle as well as coffee that contain starch and fat as the major components and cooked at high temperature (Komthong et al., 2012). In addition, as reported in the EFSA's scientific opinion on AA in food, the exposure data reported that coffee was to be one of the sources of this toxicant in adult diets. Several methods for acrylamide detection are reported in the literature, including high-performance liquid chromatography (HPLC) (Gökmen et al., 2005), gas chromatography (Shin et al., 2010), gas chromatography coupled with mass spectrometry (GC-MS) (Lee et al., 2007), liquid chromatography coupled with mass spectrometry (LC-MS/MS) (Yang et al., 2012; Y. Zhang et al., 2011), immunoassay (Zhou et al., 2008) electro-chemical- biosensors (Batra et al., 2013), fluorescent method (Hu et al., 2014) and quartz microbalance sensors (Kleefisch et al., 2004). Most of the methods need advanced equipment. This is an important issue because acrylamide

was suspected to cause cancer in human and there is no concern about acrylamide contaminated (Kumar et al., 2018).

Coffee in fact, forms one of the principal dietary sources of acrylamide, where it is normally drunk in large quantities throughout many countries worldwide that includes Thailand. Moreover, it constitutes a major dietary component in a wide range of population groups, mainly ranging from late adolescents to the elderly. Among the various food groups, it is coffee that is most difficult to limit the formation of acrylamide. One of the reasons for this is that the coffee beans are roasted as a whole, and the structure of the coffee beans is very firm, which makes the pre-roasting processes to limit the formation of acrylamide insufficient. The presented review has highlighted that acrylamide is a potential threat to human health as it is a precursor to carcinogenic compounds. Thus, a device for detecting acrylamide in foods is urgently required. In this study the MuscFv specific to acrylamide was selected and tested against acrylamide using ELISA.

1.2 Research objective

The overall objectives were to develop the Enzyme-linked immunosorbent assay (ELISA), that could detect acrylamide substances in coffee.

The specific purposes of this study were as follows:

1. To produce MuscFv-antibody against acrylamide in coffee.
2. To develop Enzyme-linked immunosorbent assay (ELISA), that could detect acrylamide substances in coffee.
3. Murine ScFv specific to acrylamide should detect acrylamide in coffee using developed ELISA.

1.3 Scope and limitations of the study

The produced scFv-antibody against specifically to acrylamide will be develop Enzyme-linked immunosorbent assay (ELISA), that could detect acrylamide substances in spiked in coffee. The ELISA will be test for the LOD, cut off, and validation using standard method (HPLC).

1.4 Expected results

1. Successfully produce scFv- antibody specific to acrylamide.
2. The Enzyme-linked immunosorbent assay (ELISA), that could detect acrylamide substances in spiked coffee.
3. The result of Enzyme-linked immunosorbent assay (ELISA) was affordability, simplicity, ease of handling.



CHAPTER 2

LITERATURE REVIEWS

2.1 Acrylamide

2.1.1 General information

Acrylamide (or acrylic amide, prop-2-enamide) is an α , β -unsaturated carbonyl with a chemical formula $\text{CH}_2=\text{CHC}(\text{O})\text{NH}_2$ (Figure 2.1). It is a white odorless solid, soluble in water and several organic solvents. The molecular weight 71.08 g/mol and a chemical intermediate used in the production and synthesis of polyacrylamides that can be modified to develop nonionic, anionic, or cationic properties for specific uses. These water-soluble polymers can be used as additives for water treatment, enhanced oil recovery, flocculants, papermaking aids, thickeners, soil-conditioning agents, sewage and waste treatment, processing, and permanent-press fabrics (Habermann CE., 2002).

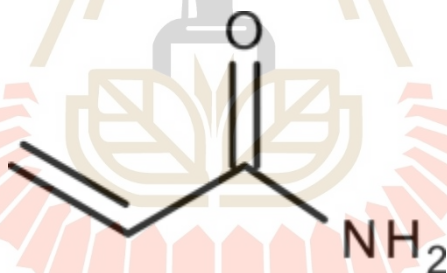


Figure 2.1 Chemical structure of acrylamide.

Acrylamide is formed upon the reaction of asparagine with reducing sugars or from cleavage products call is Maillard reaction (i.e., 2-butanedione, 2 oxopropanal) at temperature higher than 100 C° in low moisture conditions or after prolonged thermal treatment (Mottram et al., 2002; Stadler et al., 2002). Cysteine and methionine in presence of reducing carbonyls and acrolein in presence of ammonia are other precursors of acrylamide. The reaction mechanisms involve 3-amino propionamide as reaction intermediate upon the formation of the Schiff base and the decarboxylation and hydrolysis via Strecker degradation or the direct decomposition of the Schiff base via intramolecular cyclization forming the azomethine Lide that directly decomposes on cleavage of the CeN bond to give acrylamide and 1-amino-2-hex lose

(Granvogl et al., 2006; Yaylayan et al., 2003). Due to the presence of an acryloyl group, acrylamide is highly reactive, and it can polymerize, or form Michael adducts with free amino group, thiols or other nucleophiles.

2.1.2 Maillard Reaction

The Maillard reaction, named after L. C. Maillard, is also known as nonenzymatic browning. It is an extremely complex process, which is which reaction between reducing sugars and proteins by the impact of heat. The Maillard reaction starts with reducing sugar reacting with an amine, creating glycosyl amine. These substances undergo a reaction called Amadori rearrangement to produce a derivate of amino deoxy fructose. The reaction is continuous, and very reactive intermediate substances are formed, which subsequently react in several different ways. Eventually, a furan derivate is gained, and this derivate reacts with other components to polymerize into a dark-colored, insoluble material containing nitrogen. The Maillard reaction also takes place at room temperature but at a much slower rate and occurs at its slowest by low temperatures, low pH, and low water activity (a_w) levels.

Maillard reactions occur particularly when food products are processed at high temperatures. It is a form of non-enzymatic browning commonly associated with the desirable color and aromas of cooked foods including bread, meat, roasted nut, coffee and confectionaries to name a few. It has also been linked to the formation of various compounds exhibiting antioxidant, antimutagenic properties and/ or antibiotic potencies. However, although some chemicals produced by Maillard reactions are involved in the improvement of flavors and the sensory appeal of many foods, others are known to be potentially harmful (mutagens, carcinogens)

Maillard reaction was proposed as the major route for acrylamide formation, there are also some minor routes. Alternatively, to acrylamide formation from asparagine through Maillard reaction, it was shown that asparagine might be converted to acrylamide in the absence of any carbonyl compound (Figure 2.2) The 3-amino-propionamide (3-APA) is the major precursor in this route, which is generated directly from asparagine(Granvogl et al., 2007). Formation of acrylamide through 3-APA proceeds to a lower extent. However, 3-APA might also be generated in foods under enzymatic action on asparagine, and rapidly converted to acrylamide even under aqueous conditions and at relatively low temperatures (Becalski et al., 2011).

Acrolein is also one of the precursors in acrylamide formation and could be formed through oxidative lipid degradation, carbohydrate degradation and Maillard reaction (Stadler and Studer, 2016). As shown in (Figure 2.3), acrolein is oxidized to acrylic acid and then reacts with ammonia (produced from amino acids via Strecker degrade at ion in the presence of carbonyl compounds) yielding acrylamide (Yasuhara *et al.*, 2003). However, since acrolein is highly reactive, it prefers reacting with food components than oxidation to acrylic acid. Acrylic acid could also be formed from thermal decomposition of aspartic acid, carnosine and β -alanine (Stadler *et al.*, 2002; TAEYMANS *et al.*, 2004).

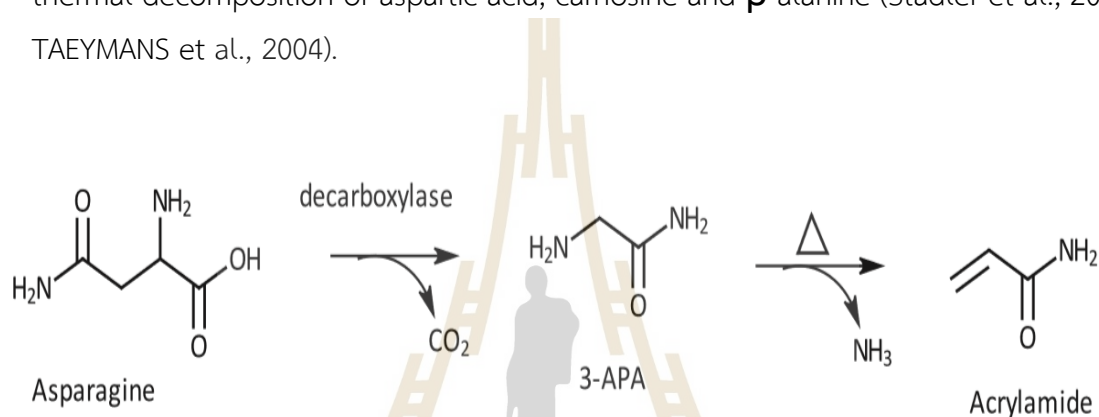


Figure 2.2 Formation of acrylamide through 3-APA.

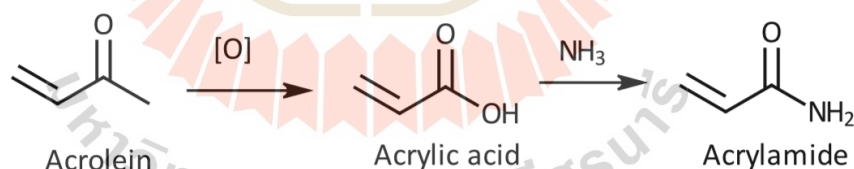


Figure 2.3 Formation of acrylamide from acrolein.(Yasuhara *et al.*, 2003).

Maillard reactions (Geng *et al.*, 2011; Hellwig & Henle, 2014; Lund & Ray, 2017; Thorpe & Baynes, 2003)). subdivided Maillard reaction into three stages as follows:

1. Initial stage: the product remains without any color and without ultraviolet (UV) absorption. Two reactions occur at this stage: sugar-amine condensation and Amadori rearrangement.

2. Intermediate stage: the product's color may change to yellow with UV absorption. This stage will involve sugar degradation and fragmentation, as well as degradation of amino acids.

3. Final stage: the product becomes highly colored, and reactions such as condensation of aldols, condensation of aldehyde-amine and formation of heterocyclic nitrogen compounds will occur.

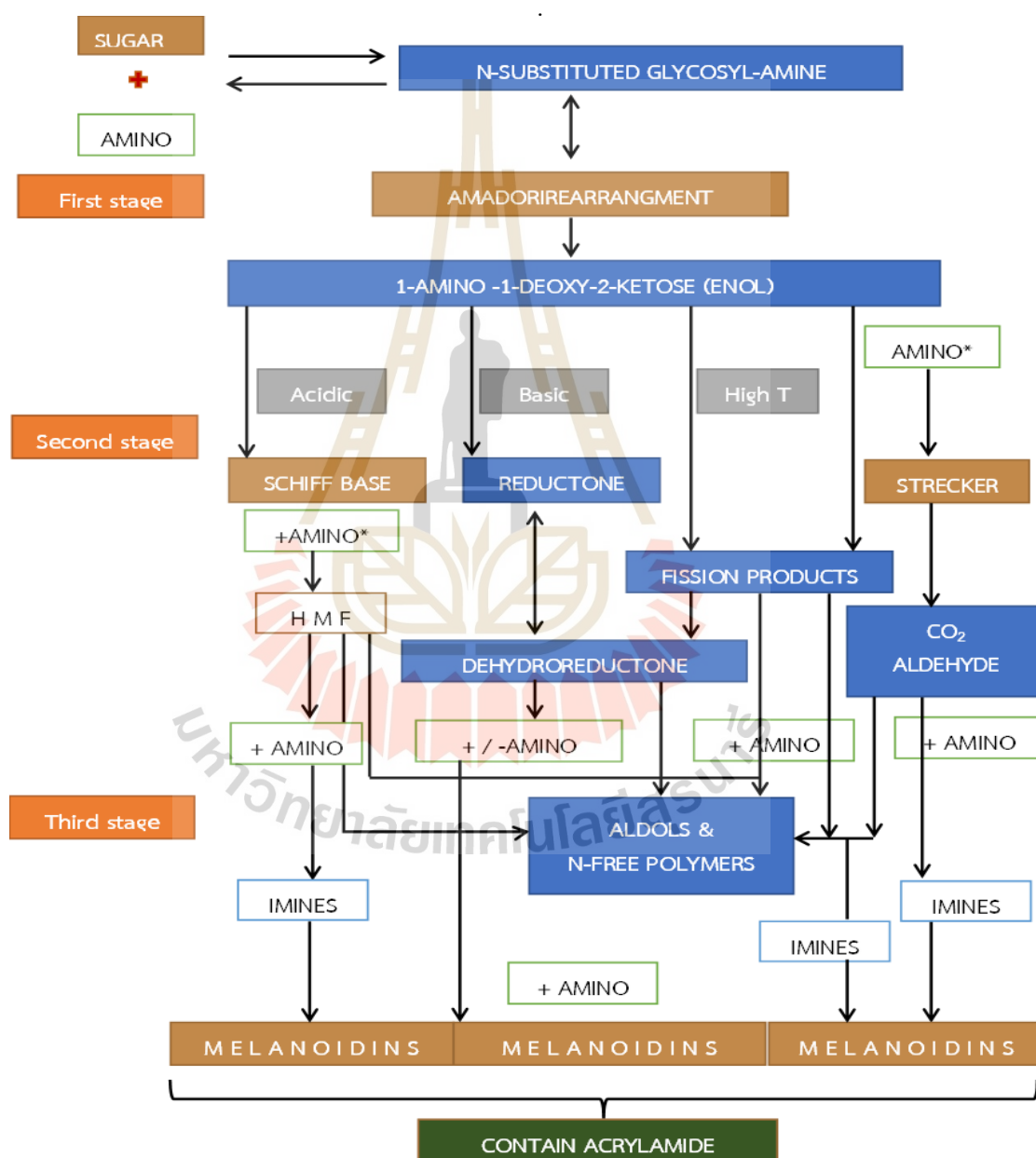


Figure 2.4 Maillard reactions. (Hodge,1953)

The different reactions above-mentioned are described in (Figure 2.4). These three stages are known in literature as Early, Advanced, and Final Maillard reactions, respectively (Mauron J., 1981). Melanoidins are the final products of non-enzymatic browning and should be distinguished from melanin, which are the final products of enzymatic browning. The dark-brown products formed in foods by enzymatic and non-enzymatic reactions are very complex to differentiate and their chemical analysis is difficult since they are relatively intractable.

2.1.3 Metabolism of acrylamide

Once acrylamide is consumed, it is absorbed by the gastrointestinal tract and, via the circulation, is distributed to peripheral tissue. (Schabacker et al., 2004) They observed that acrylamide monomers pass the monolayer of Caco-2 cells (human intestine model) through passive diffusion. Despite the high bioavailability of dietary acrylamide, diet is complex, and interactions between acrylamide and food ingredients are possible due to the high reactivity of acrylamide with peptides. (i.e. acrylamide uptake in humans has been hypothesized to be impaired by a diet rich in proteins) (Carere 2006, Vesper *et al.*, 2007). Several studies concluded that acrylamide does not accumulate in the body; however, it has been detected in several animal tissues (i.e. heart, thyroid, stomach, kidney, liver, and testis) (Pingot et al., 2013; Tareke et al., 2000; Vikström et al., 2012). Concern increased when a group from Germany found acrylamide levels in breast human milk and observed that acrylamide could pass the placenta and reach the developing fetus (Aktaş et al., 2022). Acrylamide has a low molecular weight and is highly water soluble. These properties mean acrylamide is more likely to be biologically active in the body. Acrylamide is metabolized in animals and in humans via at least two main pathways: conjugation with reduced glutathione for elimination, and conversion to a chemically reactive epoxide, glycidamide, in a reaction catalyzed by the cytochrome P450 enzyme complex Cyp2e1 (Tareke et al., 2008).

In animals and in humans, the conversion of acrylamide to glycidamide (2,3-epoxy propionamide) is known to primarily occur via the enzyme Cyp2e1; however, there could be other pathways that contribute to the formation of glycidamide, but these are likely to play only a minimal role. Both in vitro and in vivo studies confirmed that acrylamide is converted to glycidamide by Cyp2e1 in experimental animals and in

humans; nevertheless, rats and mice have higher conversion rates than humans (Barber et al., 2001). Studies in CYP2E1-knockout mice (absence of Cyp2e1) showed that mice did not excrete glycidamide or metabolites derived from glycidamide. Furthermore, some authors observed that in presence of allyl and diallyl sulfide (inhibitors of cytochrome P450 2E1, extracted from garlic) the conversion of acrylamide to glycidamide was attenuated.

Acrylamide reacts very slowly with DNA and has only been observed in in vitro studies; however, glycidamide clearly forms adducts with guanine and adenine. In addition, acrylamide and glycidamide are alkylating agents that can react with plasma albumins, proteins, and the amino acid valine of hemoglobin to form N-(2-carbamoyl ethyl) valine (HbAA) and N-(2-carbamoyl-2-hydroxyethyl) valine (HbGA). These hemoglobin adducts (HbAA and HbGA) are considered valid biomarkers that reflect human internal exposure within the last 120 days (the average lifespan of erythrocytes) (Schabacker et al., 2004; Zödl et al., 2007). Hemoglobin adduct measurements are reproducible with intraclass correlation in the range of 0.77 to 0.80. DNA adducts of acrylamide and glycidamide are not yet developed for use in human epidemiology studies. Both acrylamide and glycidamide can be excreted from the body by conjugating with reduced glutathione-S-transferases (GST). This reaction results in the formation of glutathione conjugates which will be transformed to mercapturic acids (such as N-acetyl-S-(2-carbamoyl-ethyl)-cysteine, or N-acetyl-S-(2-carbamoyl-2-hydroxyethyl)-cysteine) and eliminated in urine. Likewise, glycidamide can also be hydrolyzed by the microsomal epoxide hydrolase (mEH) to glyceramide, a less reactive metabolite that is also excreted in urine (Dybing et al., 2005a; Fennell et al., 2006). The half-life of acrylamide in human organism is 2-7 hours which shows how slowly this substance is being removed from the body (Sörgel et al., 2002). The mechanism of acrylamide is still an incomplete mechanism. As a result, it causes the accumulation of acrylamide in the body to continue for a long time and the amount of acrylamide that accumulates can affect the movement of red blood cells and human hemoglobin ((Bergmark, 1997; Neuhäuser-Klaus & Schmahl, 1989).

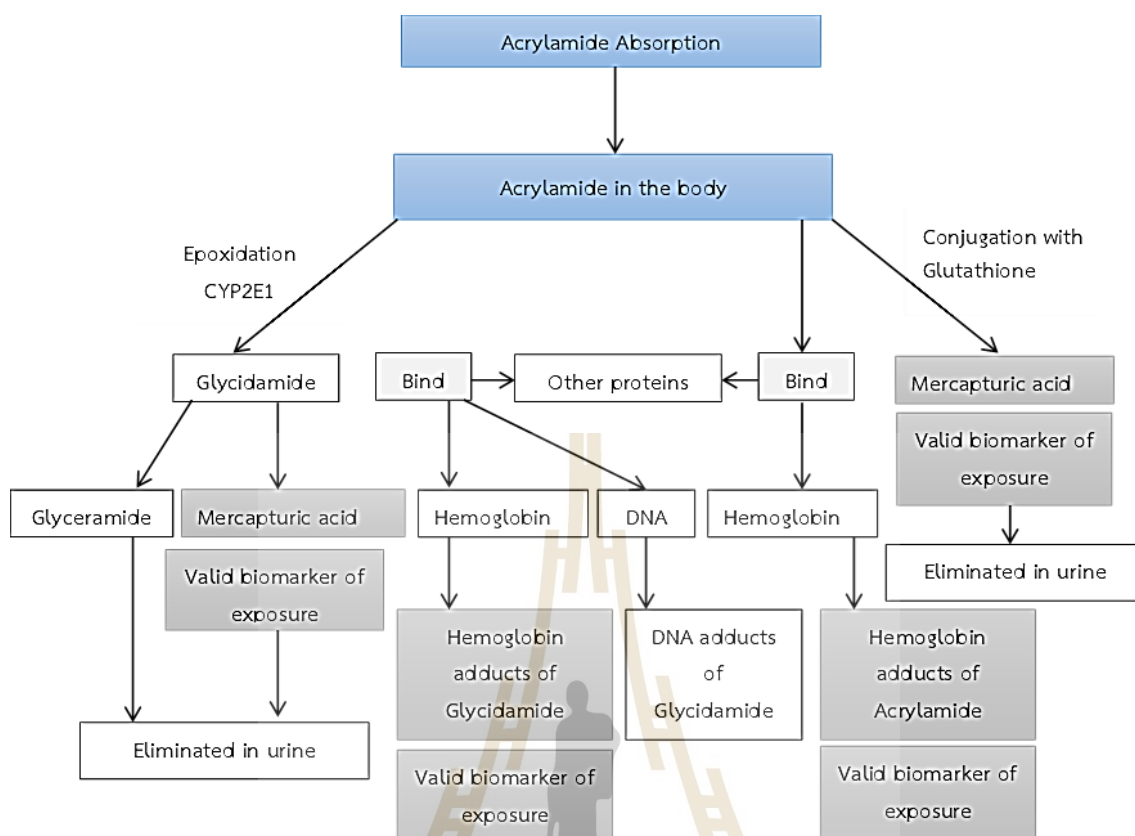


Figure 2.5 Metabolism of acrylamide

2.1.4 Toxicity of acrylamide

Acrylamide has been classified as a Group 2A carcinogen by the International Agency for Research on Cancer (IARC) and a category 2 carcinogen and category 2 mutagen by the European Union; moreover, the EFSA mentions acrylamide formation in foods as one of their major concerns. Several toxicological studies highlighted that acrylamide could bind hemoglobin, can be metabolized in the highly reactive glycidamide epoxide and its concentration in water should be below 0.1 mg/L. When the body receives acute acrylamide compounds will directly affect the central nervous system and peripheral nervous system (Neuhäuser-Klaus & Schmahl, 1989; Tilson HA., 1981) and the intermediate glycerides derived from the decomposition process acrylamide within the cell is also able to capture DNA and destroy the genetic code of the organism (Svensson et al., 2003; Tareke et al., 2000). A report on the toxicity of acrylamide on the reproductive system of mice which directly affects the strength of sperm (Friedman M., 2003) and to be carcinogenic in humans (Bjellaas et al., 2007;

IARC., 1994; Tareke et al., 2000) that results in the induced abnormal chromosome division.

The documented and confirmed potential toxicity of AA to organisms is extensive. Prolonged, low-dose exposure to AA can lead to symptoms such as skin peeling and erythema, numbness of limbs, hyporeflexia, and peripheral neuropathy. Additionally, in animals, extended ingestion of AA may cause ataxia, muscle weakness, and dyskinesia (Pundir et al., 2019a; Zhao et al., 2022). The potential toxicity of AA to the body and its mechanism are presented.

Neurotoxicity: The central nervous system plays a crucial role in the body's oxidative metabolism. Prolonged intake of AA can trigger reactive oxygen species to continually assault cell membrane lipids, proteins, and DNA, leading to damage in vital organs and the onset of diseases like Alzheimer's and Parkinson's disease (Wang et al., 2022). Certain studies have noted that AA intake resulted in elevated levels of oxidative stress-related enzymes such as superoxide dismutase, glutathione peroxidase, and catalase in both peripheral blood and the brain (Hou et al., 2021). Additionally, it prompted the disruption of the structure or function of the peripheral nervous system, leading to diminished or loss of movement and sensation (Reshmitha & Nisha, 2021).

Immunotoxicity: AA can also stimulate the immune system to produce immune responses and activate mitogen-activated protein kinase, nuclear factor- κ B, and other related pathways for defense. Some studies have reported that treating human neuroblastoma cells with AA could activate extracellular signal-regulated protein kinase to induce the death signaling pathway, c-Jun terminal protein kinase, and p38 mitogen-activated protein kinase pathways, and upregulate the expression of proapoptotic proteins, resulting in cell apoptosis (Matoso et al., 2019; Okuno et al., 2006).

Reproductive toxicity: AA has also been proven to exhibit reproductive toxicity. After being catalyzed by the cytochrome P450 enzyme, AA is epoxidized to form glycidamide. Then, AA and GA react with protamine in the testis to produce S-(2-formamido-2-hydroxyethyl) cysteine and S-carboxyethyl cysteine, eventually affecting fertility (Hansen et al., 2010; H. Zhang et al., 2022). AA can damage the reproductive system by damaging normal Sertoli cells in male rats and the function of Leydig cells, as well as induce the abnormal secretion of testosterone and luteinizing hormone,

resulting in abnormal sperm-related gene expression, decreasing the number of sperm to reduce the activity of sperm, and increasing the sperm deformity rate (ALKarim et al., 2015; Yuxin Ma et al., 2011). Further, AA can induce ovarian dysfunction in female Wistar rats by upregulating apoptosis-related genes (Firouzabadi et al., 2022) .

Other Toxicities: AA has the potential to harm various organs including the liver, kidneys, lungs, bladder, and digestive tract, and it may even lead to conditions such as testicular mesothelioma, adrenal cortical adenoma, astrocytoma, and oral tumors (Yuan et al., 2022a). Currently, there are no studies specifically addressing the adverse effects of AA in coffee on human health; however, its toxic effects in food have been well-established through animal experiments or in vitro studies using human cells. An AA toxicity test conducted in rats in early 2005 revealed an LD50 ranging from 107 to 203 mg/kg.bw, confirming AA's low toxicity (Dybing et al., 2005b). Nonetheless, some studies have indicated that AA's detrimental effects on human health primarily manifest as damage to immune function, the nervous system, genetic material, mitochondrial dysfunction, mutation, genotoxicity, and its potential carcinogenicity (Liu et al., 2022; Yuan et al., 2022b). For instance, many GA-induced mutations in human tumors occurred at A base pairs, with AT > TA and AT > GC mutations at specific TP53 codons (Hözl-Armstrong et al., 2020). In essence, DNA adducts offer a plausible mechanistic explanation for the types of mutations and mutational signatures observed following GA treatment, a reactive metabolite of AA [57]. Consequently, European regulations have recommended a maximum AA content of 400 ug/kg in roasted coffee (D.; B. M.; C. J. K.; R. B. L. Benford et al., 2022).

2.2 Conventional antibody

2.2.1 Antibody

The antibody, a glycoprotein originating from B cells, is molecularly categorized as an immunoglobulin protein (Ig). In its inactive state, the antibody adopts a Y-shaped configuration. Its fundamental structure comprises a heterotetrametric consisting of four polypeptide chains: two identical heavy (H) chains and two identical light (L) chains. Each H chain, approximately 50 kDa in size, is linked to an L chain, about 25 kDa, via a disulfide bond. Additionally, the two H chains are connected through disulfide bond(s). The association between H-L and H-H chains is further facilitated by non-covalent interactions, including hydrophobic forces, ionic bonds,

hydrogen bonds, van der Waals forces, and salt linkages. (Figure 2.6)(Davies et al., 1975a).

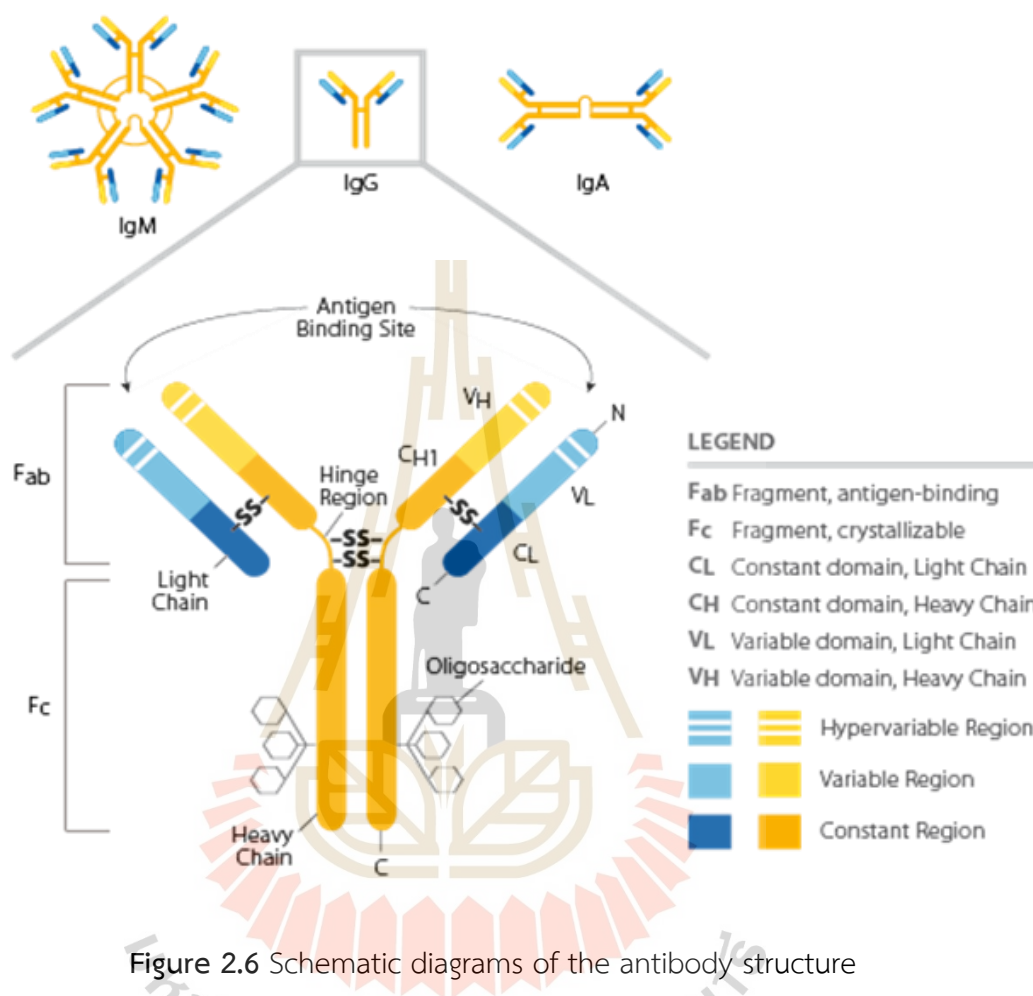


Figure 2.6 Schematic diagrams of the antibody structure

Two types of L chains exist, characterized by variations within them: kappa (κ) and lambda (λ) chains. In humans, κ and λ chains make up 60% and 40% respectively, whereas in mice, κ chains constitute 95% and λ chains 5% (Hieter et al., 1981). Lambda chains comprise $\lambda 1$, $\lambda 2$, $\lambda 3$, and $\lambda 4$ subtypes, whereas κ chains lack subtypes. The C-terminal portions of the H chains differ, classifying into five types: μ , δ , γ , ϵ , and α . Immunoglobulins carrying these types are denoted as IgM, IgD, IgG, IgE, and IgA classes/types, respectively. (Figure 2.7) (Amzel & Poljak, 1979).

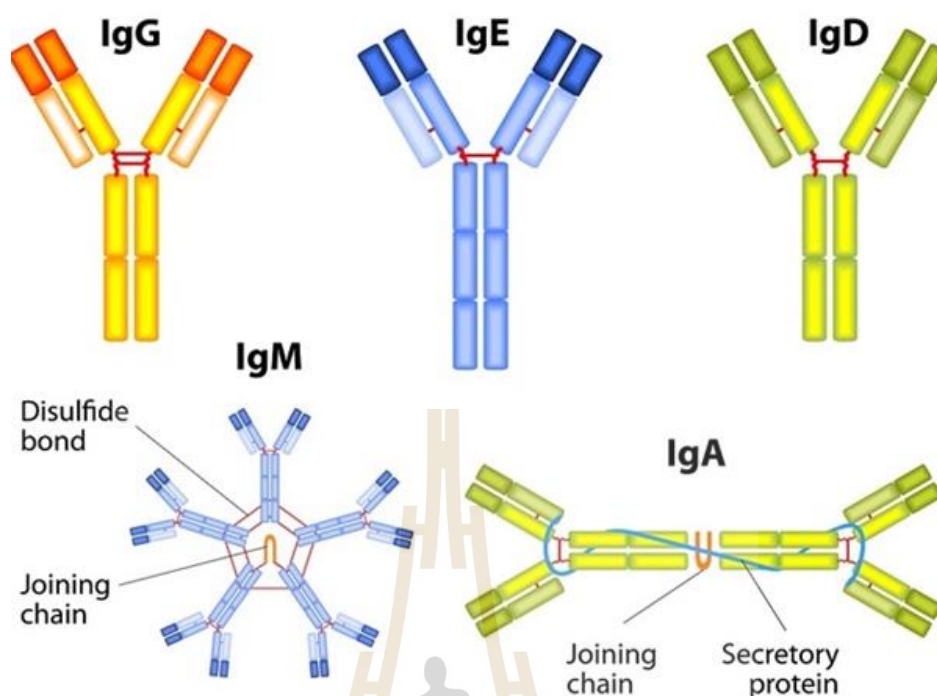


Figure 2.7 Schematic diagrams of all human antibody classes / types: IgM, IgD, IgG, IgE, and IgA

The antibody primary structure can be separated into two Fab and one Fc fragments after papain cleavage or one $F(ab')_2$ fragment and degraded Fc pieces after pepsin cleavage. The Fab and the $F(ab')_2$ consist of 1 and 2 antigen binding site (s), respectively. The function of the Fab and the $F(ab')_2$ is for antigen binding while the Fc region has several activities such as Fc receptor binding and complement fixing (Stura E.A., 1993).

The N-terminal half of L chain and N-terminal quarter of H chain contain high sequence variation which creates diversity of the epitope specificity among different antibodies. The Variable regions of the L and H chains are called variable light chain (VL) and variable heavy chain (VH) domains, respectively. Within each VL and VH domain, there are three hypervariable regions called complementary determining regions (CDRs) which are the sites that interact with the epitope. Each binding site of each antibody contains 3 VL-CDRs and 3 VH-CDRs. The other portions of VL and VH domains are less variable than the CDRs and are called immunoglobulin framework regions (FIRs). There are four FIRs in each VL and VH; from N-terminal, they are FIR1,

FR2, FR3, and FR4, respectively. The FRs serve as Scaffold of the CDRs (Davies et al., 1975b).

The remaining parts of antibody molecule apart from the variable regions (VL and VH) are more constant in terms of amino acid sequences. The constant region can be divided into 2 domain types, called constant light chain (CL) domain and constant heavy chain (CH) domain. Each H chain is composed of three or four CH domains (CH1-CH4) depending on the immunoglobulin isotypes while the L chain contains only one CL. The peptide sequence between the CH1 and CH2 are proline-rich which makes the Y-arm of the antibody flexible. This region is called "Hinge region". Overall, the CDRs of VL and VH formed the antibody binding site or paratope which is located at the tips of the Y-shape arms of the resting antibody molecule. The hyper variable amino acid sequences of the CDRs determine antigenic specificity of each antibody molecule (Amzel & Poljak, 1979)

2.2.2 Antigen-Antibody Binding

The region of an antigen that interacts with an antibody is called an epitope or an immune determinant region. The binding of an antibody to the antigen is dependent on reversible, non-covalent interactions, and the complex is in equilibrium with the free components. The binding pocket of an antibody can accommodate from 6 to 10 amino acids. Small changes in the antigen structure (such as a single amino acid) can affect the strength of the antibody-antigen interaction. The measure of the strength of the binding is called affinity, and it is usually expressed in terms of the concentration of an antibody-antigen complex measured at equilibrium. It typically ranges from micro (10^{-6}) to pico (10^{-12}) molar. High-affinity antibodies can bind more antigen in a shorter period than low-affinity ones, and they form more stable complexes. Hence, high-affinity antibodies are usually preferred in immunochemical techniques (S. rath & Madeleine E. devey, 1988).

Avidity is another parameter used to characterize the antibody-antigen binding reaction. It is the measure of overall stability of the complex, determined by the antibody's affinity for the epitope, the number of binding sites per antibody molecule and the geometric arrangement of the interacting components. Avidity describes all factors involved in the binding reaction, and it determines the success of all immunochemical techniques. Antibodies are usually highly specific for the antigen.

However, some antibodies show cross-reactivity to similar epitopes on other molecules. This makes the immunochemical method less specific but at the same time more applicable to situations where the target is a class of structurally related molecules. Assay specificity and sensitivity are determined by the quality of antibodies used in the method. Polyclonal antibodies are isolated from the serum of immunized animals, usually rabbits, and the serum is a combination of numerous antibodies with different specificities and affinities. Monoclonal antibodies are more homogenous in terms of specificity and affinity because of the production method involving immunization of mice followed by hybridoma technologies (Goding, 1983).

2.2.3 Single-Chain Fragment Variable (scFv)

Fv fragment is the smallest unit of immunoglobulin molecule with function in antigen-binding activities. An antibody in scFv (single chain fragment variable) (Figure 2.8) format consists of variable regions of heavy (VH) and light (VL) chains, which are joined together by a flexible peptide linker that can be easily expressed in functional form in *E.coli*, allowing protein engineering to improve the properties of scFv such as increase of affinity and alteration of specificity (Lake D. F., 1994). The length of the flexible DNA linker used to link both V domains is critical in yielding the correct folding of the polypeptide chain. Previously, it has been estimated that the peptide linker must span 3.5 nm) between the carboxy^o terminus of the variable domain and the amino terminus of the other domain without affecting the ability of the domains to fold and form an intact antigen-binding site (Law, 2021)

In addition to the linker peptides designed de novo, peptide sequences derived from known protein structure have been applied to provide a compatible length and conformational in bridging the variable domains of a scFv without serious steric interference (Bird et al., 1988) Apart from the length of the linker, their amino acid composition also plays an important role in the design of a viable linker peptide. They must have a hydrophilic sequence to avoid intercalation of the peptide within or between the variable domains throughout the protein folding(Feige et al., 2010). Nowadays, the most extensively used designs have sequences comprising stretches of Gly and Ser residues which meant for flexibility and or together with the charged residues such as Glu and Lys interspersed to enhance the solubility (Whitlow et al., 1993).

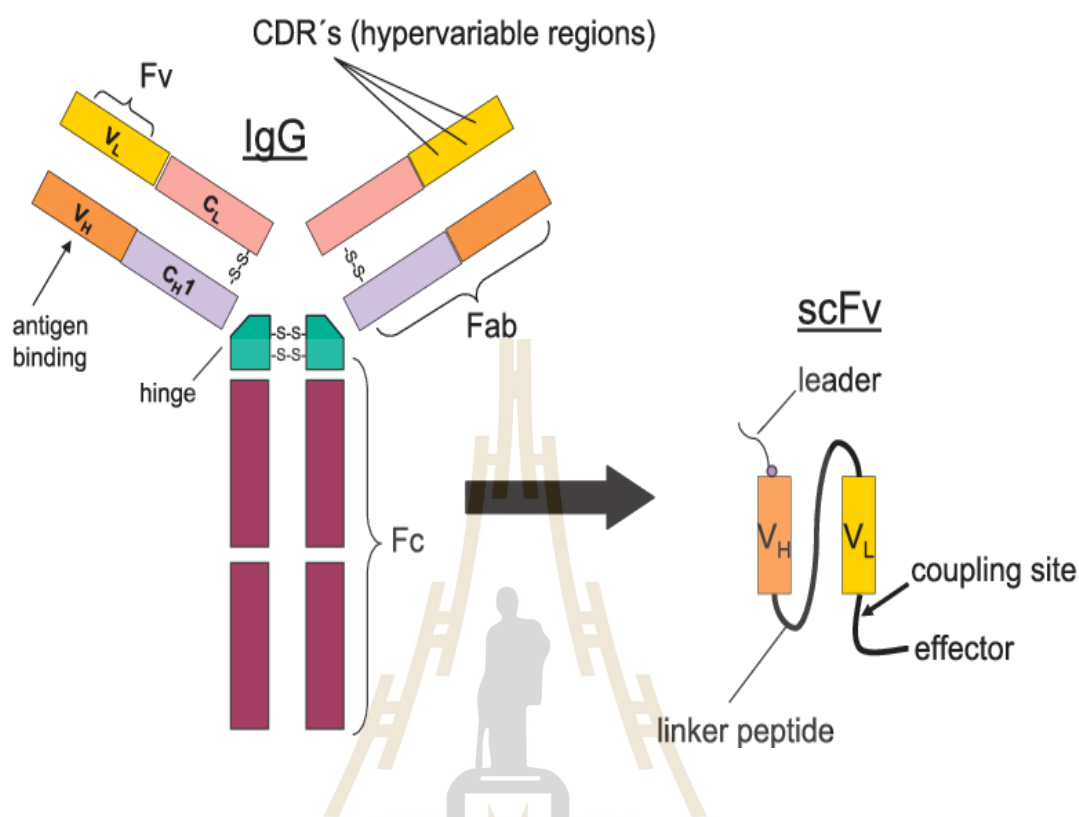


Figure 2.8 Antibody model showing subunit composition and domain distribution along the polypeptide chains. Single-chain fragment variable (scFv) antibody generated by recombinant antibody technology appears in the shaded area.

2.2.4 The Generation of scFv (Single-Chain Fragment Variable) Antibodies

scFv (single chain fragment variable) antibodies have been constructed mainly from hybridoma (Huston, 1988), spleen cells from immunized mice (Finlay & Lugovskoy, 2019), and B lymphocytes from human. scFv is a noncovalent heterodimer comprised of the V_H and V_L domains (Skerra & Plückthun, 1988) in which can then be used in the construction of recombinant scFv antibody. In order to attain them, mRNA is first isolated from hybridoma (or also from the spleen, lymph cells, and bone marrow) followed by reverse transcribed into cDNA to serve as a template for antibody genes amplification (PCR). With this method, large libraries with a diverse range of antibody V_H and V_L genes could be created. One successful approach to recombinant antibody production has been developed by McCafferty and coworkers in which they utilized the phage recombinants that are displaying antibody at their tips together with

the new techniques of affinity selection, called bio-panning step. The work by McCafferty (McCafferty et al., 1990) thus has opened the opportunity for in vitro selection of scFv from large libraries of variable domains circumventing the traditional hybridoma method.

In the scFv construction, the order of the domains can be either VH-linker-VL or VL-linker-VH and both orientations have been applied (Sheikholvaezin et al., 2006). The even though (Luo *et al.*, 1995) have shown that the expression of scFv (single-chain fragment variable) of *Pichia pastoris* system is VL-linker-VH orientation-dependent; most of the scFv are constructed in a VH-linker-VL orientation. One of the most popular methods used is through PCR assembly (Lake D. F., 1994) which was first described by Horton et al. (Horton et al., 1989). In this method, it allows the V domains of antibody to be cloned without any prior information about the nucleic acid as well as amino acid sequence of the antibody (LeBoeuf et al., 1998). Moreover, the V domains of antibody can be combined by in vitro recombination directly after the PCR of VH and VL genes into plasmid or phagemid (Hogrefe et al., 1993). Alternatively, scFv can also be constructed with sequential cloning or combinatorial infection.

Numerous scFv have been constructed against hapten, protein, carbohydrate, receptor, tumor antigen, and viruses (He et al., 2002). All these scFv have good potential for use in many fields such as medical therapies and diagnostic applications.

2.3 Phage display technology

2.3.1 Phage display

Bacteriophage (phage) is a virus that infects and replicates within bacteria and archaea, following the injection of their genome into its cytoplasm. Phage is composed of proteins that encapsulate a DNA or RNA genome and may have relatively simple or elaborate structures (Smith, 1985). (Figure 2.9)

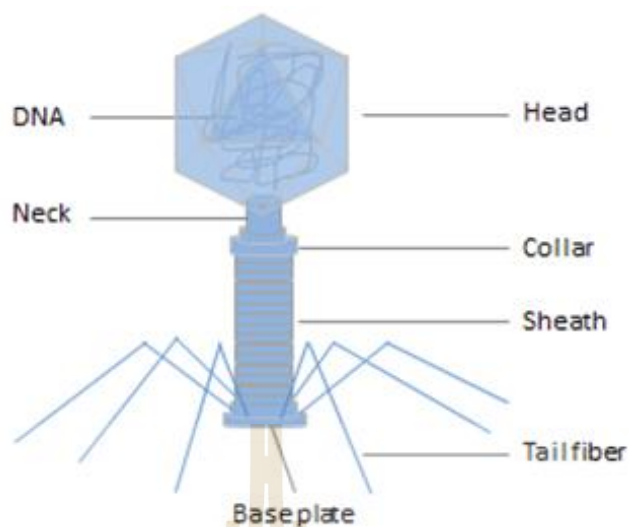


Figure 2.9 Bacteriophage (phage)

2.3.2 Phage display

Phage display was first developed by G. Smith in 1985 (Smith, 1985) as a method of presenting polypeptides on the surface of lysogenic filamentous bacteriophages. In phage display technique, a gene encoding a protein of interest is inserted into a phage coat protein gene, causing the phage to display the protein on the outside and containing the gene for the protein inside, resulting in a connection between genotype and phenotype.

Phage display is generally a new strategy to exhibit peptides on the surface of bacteriophage. For the first time, phage display introduced by George Smith in 1985. As per this system, phages can be expressed the desired (poly) peptides as a component of their surface proteins. In this technique, the (poly) peptide expresses as fusion with one of the surface proteins of the bacteriophage and in this way the desired (poly) peptide is chosen by binding to different target (Smith, 1985). In fact, this method is based on the reaction between the ligand and receptor. Displaying of proteins on the surface of the phages is dependable strategy for choice of uncommon qualities that code proteins with binding activity. Phage display can be set to show different quantities of peptides with substantial differences in polyvalent configuration. The level of display relies on upon the sequence and length of poly (peptides) (Wilson et al., 1998). In the case of small peptides (smaller than 8 residues), hundreds or thousands copies of them can be displayed (Zalewska-Piątek & Piątek, 2021). This

technology is fit for delivering small peptides (1–20 residues) with high binding affinity to any protein (Sidhu et al., 2000). Phage display is based on genetic manipulation of genes of surface proteins of filamentous phages like M13 and fd. Foreign DNA enter into the genome of filamentous phage (for example gene III) and foreign peptide encoded as a fusion protein with a surface coating protein (Pande et al., 2010). Rapid identification and isolation of high specific phage to its own target (through bio panning process) is an advantage of phage display technique. Bio panning causes recognizable proof of individual peptides in the scope of micro molar to nanomolar range (Arap, 2005). In this review we outlined distinctive applications of phage display from the past to present.

2.3.3 *E.coli* filamentous bacteriophages (f1, fd, M13)

The most common bacteriophages used in phage display are *E.coli* filamentous bacteriophages (f1, fd, M13). A filamentous bacteriophage is a type of phage, defined by its filament-like or rod-like shape. Filamentous phages usually contain a genome of single-stranded DNA and infect Gram-negative bacteria. The family of Ff, M13, fd, and f1 are vital phages which have utility in phage display among which M13 phage is the most generally used (Rakonjac et al., 2017).

M13 bacteriophage has a cylindrical shape with a length of 880 nm and a diameter of 6 nm. It encapsulates a single-strand genome that encodes five different capsid proteins which comprise two groups, major coat proteins (pVIII) and minor coat proteins (pVII, pIX, pVI and pIII). (Figure 2.10)

E. coli filamentous bacteriophages are commonly used for phage display. Most antibodies and peptides are displayed at phage proteins pIII (Kim et al., 2019) and pVIII (Hess et al., 2012), which constructed pIII and pVIII display system. Moreover, hybrid phage system enables displaying large proteins with all five M13 coat proteins as N-terminal fusions with pIII, pVIII, pVII and pIX, and as C-terminal fusions with pVI, pIII, and pVIII.

1. pIII is the protein that determines the infectivity of the virion. It consists of 406 amino acid residues and occurs at the phage tip in 3 to 5 copies (Lowman HB & Clackson T., 2004). An advantage of using pIII rather than pVIII is that pIII allows for monovalent display when using a phagemid combined with a helper phage. Moreover,

pIII allows for the insertion of larger protein sequences (>100 amino acids)(Sidhu et al., 2000) and is more tolerant to it than pVIII.

2. pVIII is the main coat protein of Ff phages, which is expressed by gene 8 and occurs in 2700 copies. Therefore, it is used to enhance detection signal when phage displayed antibody associates with antigen. Peptides are usually fused to the N-terminus of pVIII which are usually 6-8 amino acids long copies (Lowman HB & Clackson T., 2004). This makes the use of this protein unfavorable for the discovery of high affinity binding partners. Moreover, modifications of pVIII are made to increase the efficiency of display onto pVIII, and now there has been great progress.

3. pVI has been widely used for the display of cDNA libraries, which is an attractive alternative to the yeast-2-hybrid method for the discovery of interacting proteins and peptides due to its high throughput capability (Lowman HB & Clackson T., 2004). pVI has been used preferentially to pVIII and pIII for the expression of cDNA libraries because one can add the protein of interest in the C-terminus of pVI without greatly affecting pVI's role in phage assembly.

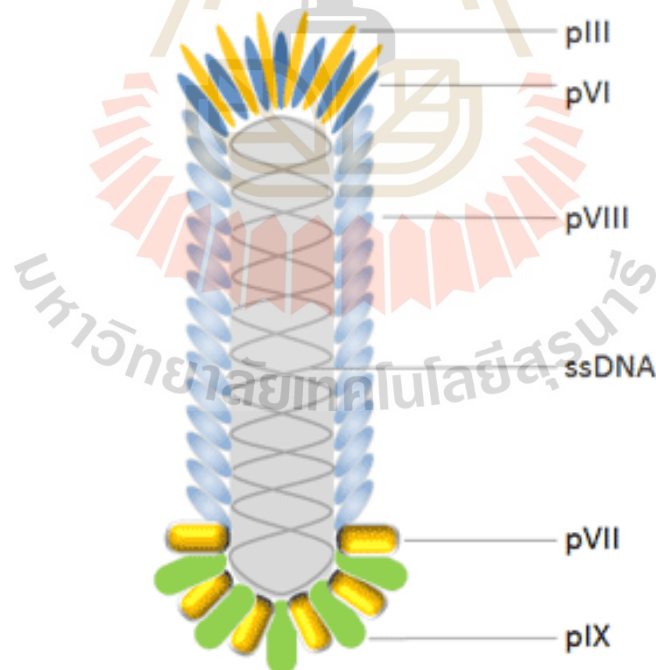


Figure 2.10 *E.coli* filamentous bacteriophages

4. pVII and pIX, located to the phage tip opposite that of pIII, may both complement current phage display systems and be used as alternative scaffolds for display and selection to further improve phage display as the ultimate combinatorial engineering platform.

2.3.4 Phage bio- panning

In general, there are 5 steps for phage display technology as below:

STEP1: Construct phage display library. Recombinant DNA technology is used to incorporate foreign cDNA into viral DNA. Different sets of genes are inserted into the genomes of multiple phages. Spliced into gene for a coat protein, so that the protein will be displayed on the outside of phage particles, and these separate phages will only display one protein, peptide, or antibody. Collections of these phages can comprise libraries, such as antibody phage library, protein phage library, or random phage library.

STEP2: Binding. These libraries are exposed to selected targets and only some phages will interact with targets. The target is for which specific ligands planned to be (Rahbarnia et al., 2017) identified such as immobilized protein, cell surface protein or vascular endothelium.

STEP3: Washing. Unbound phages can be washed away, and only those which showing affinity for the receptors were left.

STEP4: Elution. Recovery of the target bound phage by elution.

STEP5: Amplification. Eluted phages showing specificity are used to infect new host cells for amplification, or direct bacterial infection and amplification of the recovered phage.

Back to step 1, repeated cycle 2-3 times for stepwise selection of best binding sequence. After that, you can Enrichment and purification the phage repertoire by precipitation methods to increasing the phage titer (Rahbarnia et al., 2017) (Figure 2.11).

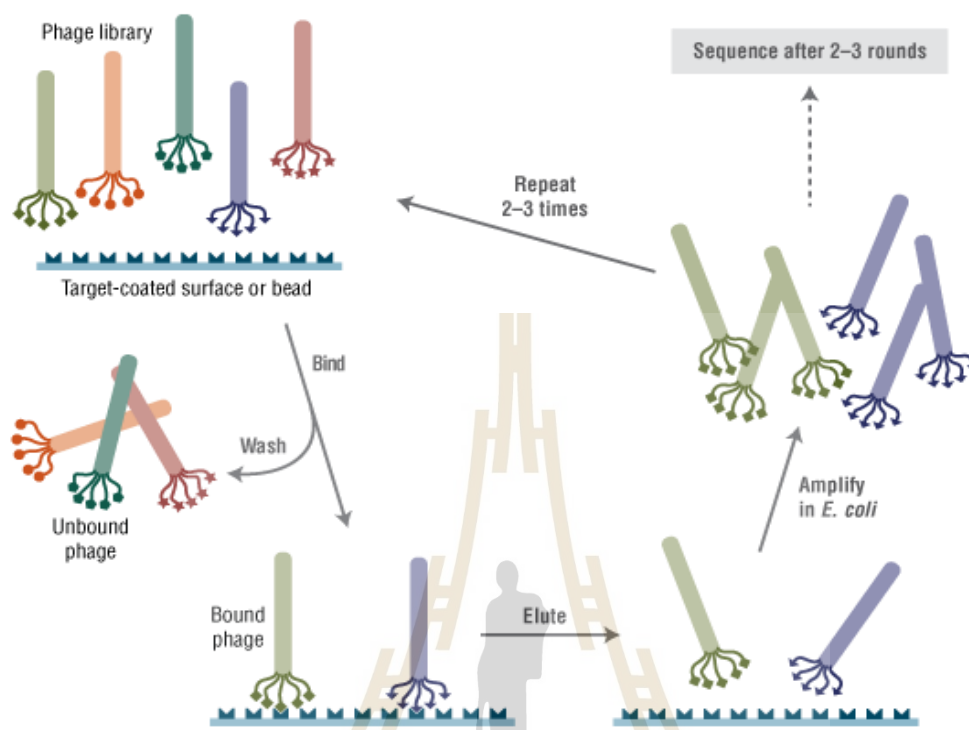


Figure 2.11 steps for phage bio-panning

2.4 Principle of enzyme-linked immunosorbent assay (ELISA)

The enzyme-linked immunosorbent assay (ELISA) is available for specific detection of target analytes based on the recognition reaction between antigen and antibody.

Polystyrene plates with 96 wells are used to conduct the ELISA. The wells, each of which contains a separate serum, are used to incubate the serum. The 96 samples being analyzed comprise positive and negative control serums. The appropriate antigen or antibody coated on the solid surface catches the antibodies or antigens in the serum. By washing the plate with wash buffer, the serum and unbound antibodies or antigens are removed from the surface (Aydin, 2015a).

To detect bound antibodies or antigens, secondary antibodies linked to peroxidase or alkaline phosphatase enzymes are introduced into each well. Following a designated incubation period, excess secondary antibodies are removed by washing.

Once the appropriate substrate is introduced, it interacts with the enzyme, resulting in the development of a color that correlates with the amount of antigens or antibodies in the sample. The optical density of the color is measured at 450 nm, and the intensity indicates the quantity of antigen or antibody detected (Cho et al., 2005).

2.4.1 The Procedure of ELISA

1. To enable the antibody to capture the antigen molecules, assay samples or standard solutions are introduced into the antibody-coated wells and allowed to incubate for a set period.

2. Subsequent to this binding phase, the reaction mixture is discarded, and any excess materials are rinsed out of the wells.

3. Horseradish peroxidase (HRP) enzyme is employed to detect a second antibody that recognizes a distinct epitope on the antigen prior to its introduction into the wells.

4. The second antibody, labeled with an enzyme, binds to the antigen previously bound by the first antibody at the base of the wells. Consequently, the HRP enzyme becomes permanently attached to the well surface. The fixed enzyme concentration correlates directly with the amount of antigen captured.

5. Introducing an enzyme's chromogenic substrate facilitates the measurement of enzyme activity. Tetramethylbenzidine is commonly used in HRP assays. The chromogenic substrate develops into a colored product after incubation for a specified duration. The reaction is halted by adding a stop solution, such as dilute sulfuric acid, and absorbance is subsequently measured using a plate reader.

6. Plotting the concentration of standard solutions generates a standard or calibration curve (P. Tijssen, 1985).

2.4.2 Different ELISA Formats

Several ELISA formats have been developed. Each type has its own advantages and can be used qualitatively to detect the presence of antibody or antigen and quantitatively (Figure 2.12) by establishing standard curve obtained from known concentration of antibody or antigen by serial dilution. Based on this standard graph, concentration of unknown samples can be determined (Stephanie D, 2013)

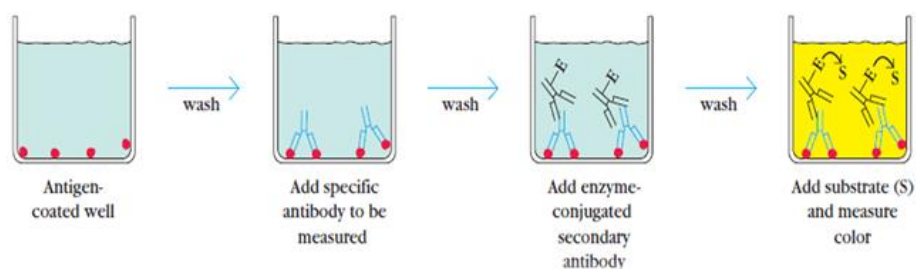


Figure 2.12 Steps of ELISA

1. Indirect ELISA In indirect ELISA, samples to be analyzed for a specific antigen is adhered to the wells of a microtiter plate, followed by a solution of non-reacting protein such as bovine serum albumin (BSA) to block any areas of the wells not coated with the antigen. The primary antibody, which binds specifically to the antigen, is then added, followed by an enzyme-conjugated secondary antibody. A substrate for the enzyme is introduced to quantify the primary antibody through a color change. The concentration of primary antibody present in the serum directly correlates with the intensity of the color. The role of Toll-like receptor activation during cutaneous allergen sensitization using ovalbumin (OVA) in the modulation of allergic asthma has been demonstrated (Haapakoski R, 2013) (Figure 2.13). A main disadvantage of indirect ELISA is that the method of antigen immobilization is not specific. When serum is used as the test antigen, all proteins in the sample may adhere to the wells of a microtiter plate. This limitation, however, can be overcome using a capture antibody unique to the specific test antigen to select it out of the serum, as illustrated in the sandwich ELISA technique.

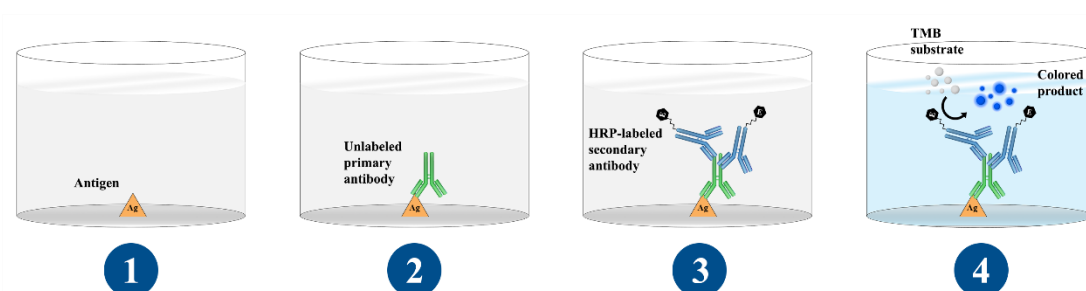


Figure 2.13 Indirect ELISA

2. **Direct ELISA** follows the same principle as discussed above, except that the primary antibody is linked to the detection enzyme (Figure 2.14). Therefore, no secondary antibody is required. This method is very quick but is typically not as sensitive or flexible as the indirect method.

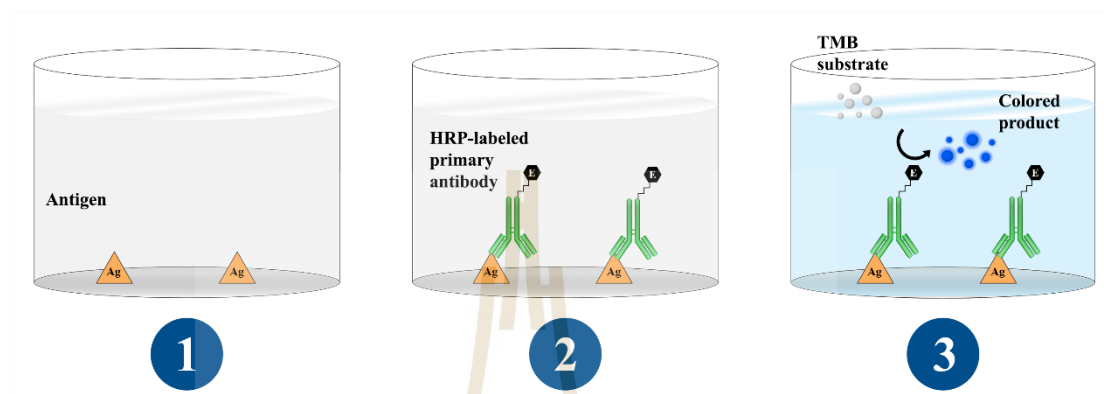


Figure 2.14 Direct ELISA

3. **Sandwich ELISA** In this format the well surface is prepared with a known quantity of bound antibody to capture the desired antigen. Non-specific binding sites are blocked by BSA treatment, and the antigen-containing sample is applied to the plate. A specific primary antibody is then added that “sandwiches” the antigen. Enzyme-linked secondary antibodies are applied that bind to the primary antibody. Unbound antibody–enzyme conjugates are washed off by repeated through washing treatments. All steps are followed very critically and carefully to avoid the chances of cross-contamination. Enzymatic reaction develops the color after addition of substrate that can be quantified later by ELISA plate reader. The technique has been used to analyse the patient sera for the determination of enhanced keratinocyte growth factor (KGF) levels in keloid and scleroderma patients compared to healthy controls to quantify human KGF (Canady et al., 2013) (Figure 2.15). One advantage of using a purified specific antibody to capture antigen is that it eliminates the purification part of specific antigen from a mixture of other antigens, thus simplifying the assay and increasing its specificity and sensitivity.

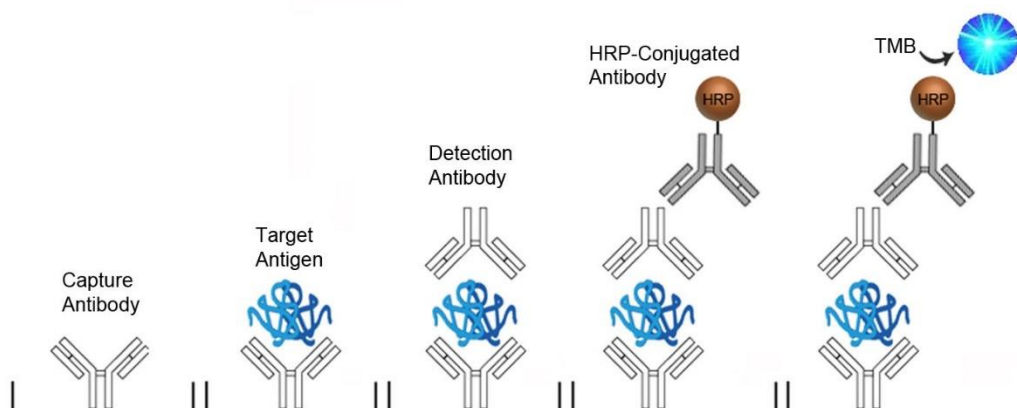


Figure 2.15 Sandwich ELISA

4. Competitive ELISA The key event of competitive ELISA is the process of competitive reaction between the sample antigen and antigen bound to the wells of a microtiter plate with the primary antibody. First, the primary antibody is incubated with the sample antigen and the resulting antibody–antigen complexes are added to wells coated with the same antigen. Unbounded antibodies are washed off after incubation. The more antigens in the sample, the more primary antibody will be bound to the sample antigen. Therefore, there will be a smaller amount of primary antibody available to bind to the antigen coated on the well. Secondary antibody conjugated to an enzyme is added, followed by a substrate to elicit a chromogenic or fluorescent signal. Absence of color indicates the presence of antigen in the sample (Figure 2.16). The main advantage of competition ELISA is its high sensitivity to compositional differences in complex antigen mixtures, even when the specific detecting antibody is present in relatively small amounts. This method can be used to determine the potency of U.S. standardized allergen extracts (Dobrovolskaia et al., 2006) and to measure the total antibodies to the capsular polysaccharide of *Haemophilus influenzae* type b in human sera from vaccinated subjects. Competitive ELISA is often used to detect HIV antibodies in the sera of patients and detection of *Candida albicans* Sap2 in cancer patient serum samples (Bhattacharyya et al., 2013; Wang L et al., 2015).

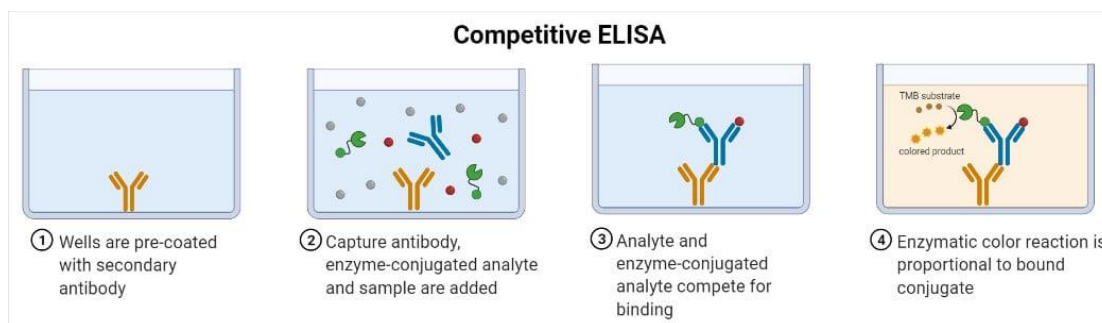


Figure 2.16 Competitive ELISA

5. Multiple and portable ELISA In this technique a multicatcher device with 8 or 12 immunosorbent pins deep in a collected sample. The washings, incubation and chromogens are executed by immersing the pins in microwells with reagents. The important advantage of this technique is ready-to use lab kits are available as relatively inexpensive. It can be used for large population screening and does not require skilled personnel. This makes it an ideal tool for low-resource settings (Balsam et al., 2013). Clinical applications of this type of ELISA include point-of-care detection of infectious diseases, bacterial toxins, oncologic markers and drug screening. Evaluation of a multiplex ELISA for autoantibody profiling in patients with autoimmune connective tissue diseases described (Caro Perez A, 2014).

2.4.3 Application of ELISA

- To determine whether the provided sample contains any unidentified antigens or antibodies. Gestational hormones, Pregnancy hormones, etc.
- In the food sector to look for possible food allergies. Milk, Peanuts, Eggs, etc.
- To assess the serum antibody concentration in viral infections.
- To monitor the progression of endemic instances of various diseases. HIV, Bird flu, Lyme disease, etc (Aga et al., 2003).

2.4.4 Limitations of ELISA

- A time-consuming wash-based assay. Even with the development of automated plate washers, the labor-intensive ELISA test still requires a number of time-consuming wash procedures. There is a lot of variation between the wells, which leads to low agreement between replicates. This could make it challenging to fit the linear

standard curve or could result in your samples having significant error bars, which would muddle the results (Carterette, 2012) .

- Time to completion. The experiment typically takes 4-6 hours to complete because there are numerous wash processes and incubation periods. This excludes the assay plate preparation step, which entails covering the assay plate with a capture antibody overnight (Sidney et al., 2013).

- Need for a sizable sample volume. An ELISA typically uses a 96-well format and needs 100–200 L of material for testing. The high demand for sample volume will limit the number of the capacity to add replicates for more precise, dependable results can be severely constrained by targets that can be quantified from the test sample (Murdock et al., 2013).

- Inability to scale. ELISA is frequently carried out in a conventional 96-well plate format and cannot be scaled via downsizing to boost throughput (Steinegger et al., 2020) .

- Limited dynamic range. The optical density (OD), which is typically 2 logs, limits the linear dynamic range for ELISA, an absorbance-based readout. This requires testing samples to fall within the linear section at various dilutions. Once more, this refers to the quantity of samples needed for testing and the possibility of out-of-range samples necessitating an expensive repeat run of the entire assay (Sylvia et al., 2000).

- A tall backdrop. The potential for excessive background in ELISAs reduces the assay's sensitivity. This could result from contaminated TMB substrate or ineffective cleaning procedures. Cross reactivity, etc. Data loss or falsely negative or positive results can result from high background. Signal Stability (Aydin, 2015b).

- The short signal stability of the ELISA makes readings necessary shortly after adding the stop solution. • It happens frequently that the reaction is not completely halted, and subsequent reads of the plate will show how the data drifts over time.

- Finding weak connections. Weak protein-protein (or antibody-protein) interactions may go undetected in ELISA experiments because of the numerous wash stages(Suriben et al., 2020).

2.5 Formation of acrylamide (AA) in Coffee

2.5.1 Pathway of AA Formation in Coffee

Temperature is the main condition for AA production. Once the temperature exceeds 120 °C, AA is generated. Coffee roasting is performed at a temperature of >150 °C, thereby creating a favorable precondition for AA formation (Schouten et al., 2020, 2021). The three main AA formation pathways in coffee are presented in Figure 2.17.

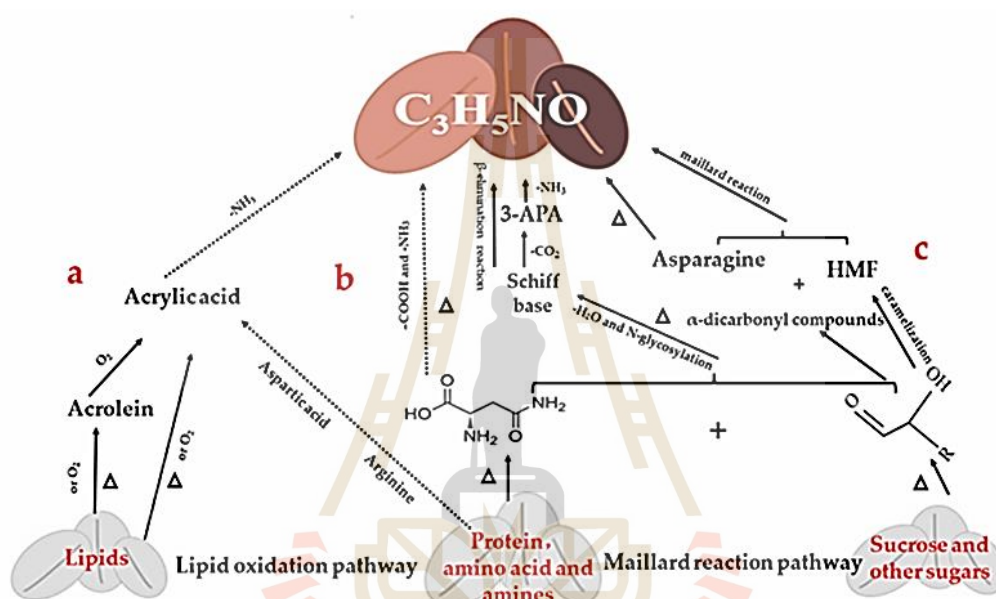


Figure 2.17 Potential pathways of acrylamide formation during coffee processing. (a) Lipid oxidation pathways; (b) Protein and amino acid degradation pathways; (c) Maillard reaction pathway.

Firstly, lipid reactions serve as a significant indicator influencing coffee quality and could potentially lead to AA production (Figure 2.17a). Inadequate treatment during roasting, storage, processing, transportation, and other stages can result in the oxidation and degradation of coffee lipids, thereby generating harmful compounds and impacting cholesterol conversion (Cong et al., 2020; Coreta-Gomes et al., 2020). AA may be formed through a dihydroxylation reaction between acrolein and acrylic acid, which are produced following lipid decomposition, along with existing amino acids or ammonia formed during protein pyrolysis (Cong et al., 2020; Endo et al., 2013). Additionally, acrylic acid can generate AA through its reaction with ammonia.

Fortunately, the formation of AA via acrolein and acrylic acid is restricted due to the low release and capture of free ammonia in coffee and the high processing temperature.

Secondly, the heat-induced reaction of proteins and amino acids can also give rise to AA (Figure 2.17b). Proteins in coffee, particularly aspartic acid, degrade into free amino acids. Subsequently, aspartic acid undergoes decarboxylation and deamination to produce AA under high-temperature conditions (Corrêa et al., 2021; Sáez-Hernández et al., 2022). Given the extremely high temperatures employed during coffee roasting, amino acids also contribute to the formation of melanoidins, which contribute to the dark color of coffee.

The Maillard reaction represents the most prevalent pathway for AA production in coffee through free amino acids and reducing sugars (Figure 2.18c). Asparagine and sucrose (0.30-90 mg/g) in coffee serve as essential precursors in AA formation. Despite sucrose not being a reducing sugar, its decomposition during the initial stages of coffee roasting can directly impact AA synthesis by generating new compounds containing carbonyl groups or decomposing into low-molecular-weight reducing sugars (Alamri et al., 2022; Figueroa Campos et al., 2020). The unstable Schiff base, which arises from the thermal reactions involving dehydration and N-glycation conjugation of asparagine and reducing sugars, quickly rearranges to form 3-amino propanamide (3-APA), followed by a decarboxylation B-elimination reaction to produce AA (Barrios-Rodríguez et al., 2022). Sucrose degradation under low moisture conditions occurs via glycosidic bond cleavage, leading to the formation of glucose and fructofuranosyl cations (Delatour et al., 2020). Dehydration of glucose results in the formation of α -dicarbonyl compounds, which may react with asparagine to yield AA (Hamzalıoğlu & Gökmen, 2020). Upon heating, sugars also form furan compounds in coffee, serving as another precursor for AA formation (Cai et al., 2014; Gökmen et al., 2012). Essentially, under high-temperature conditions, sugar undergoes decarboxylation via the oxazolidine-5-ketone pathway to produce HMF; further deamination, condensation, and hydrolysis result in AA formation (Schouten et al., 2022; Verma & Yadav, 2022). HMF is also generated during the caramelization process through the elimination of three water molecules from glucose (Hamzalıoğlu & Gökmen, 2020).

2.5.2 Control AA Production in Processing Stages

AA production has the potential to arise during every phase of coffee processing. Thus, it necessitates rigorous control employing suitable methods at each stage. Figure 2.18 outlines strategies for suppressing AA formation across various stages, encompassing variety selection, drying, processing, roasting, storage, and brewing.

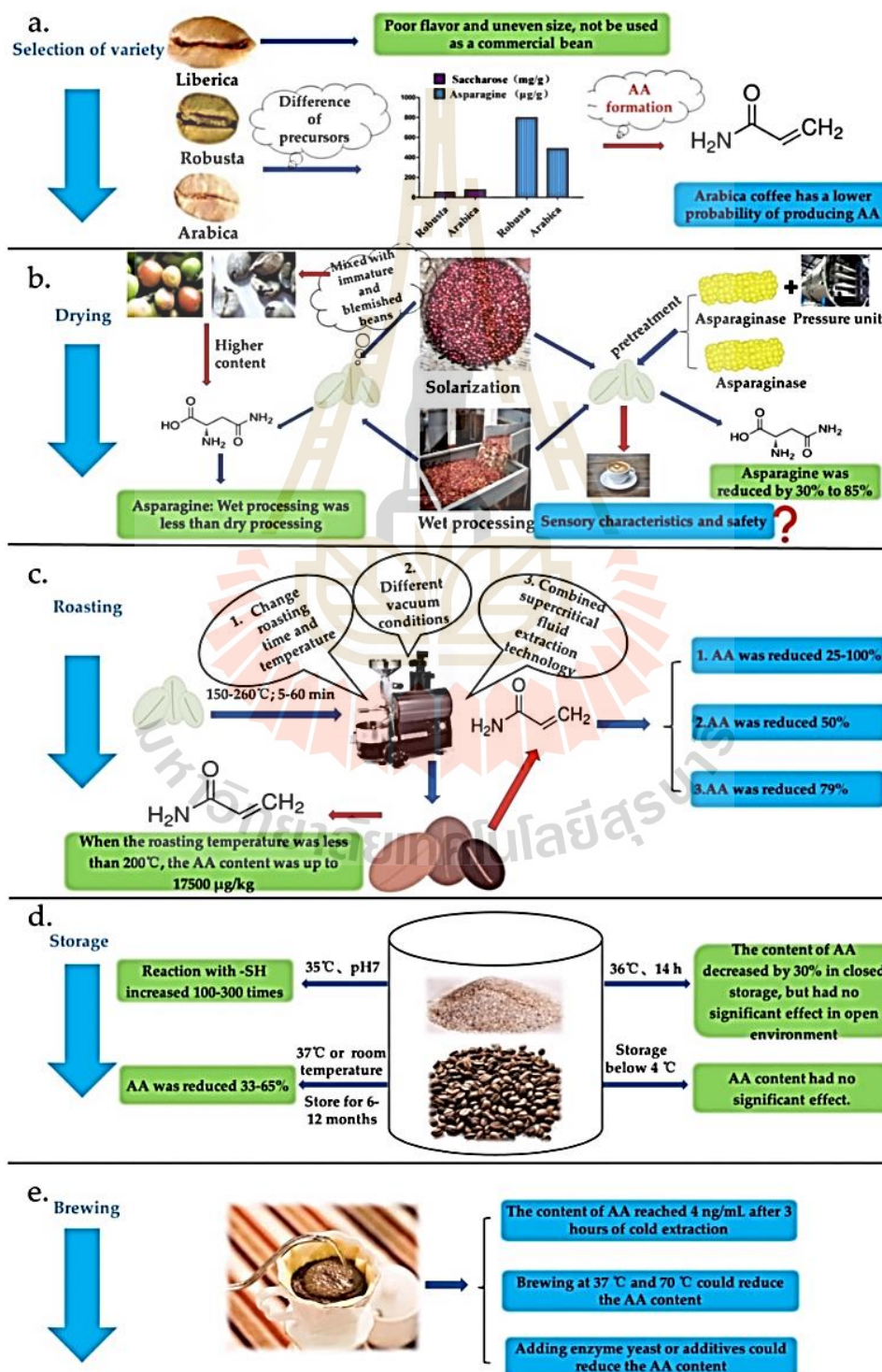


Figure 2.18 A review of studies investigating acrylamide inhibition during coffee processing. (a) Selection of variety; (b) Drying process stage; (c) Roasting stage; (d) Storage stage; (e) Brewing stage.

Controlling the presence of AA in coffee is paramount to ensure its quality and safety. This necessitates meticulous management at every stage of coffee processing. Beginning with the selection of green beans, opting for high-quality options is key. Furthermore, employing the wet processing method can yield lower AA precursor content and facilitate the degradation of precursors through proteases (Rubayiza & Meurens, 2005). Roasting emerges as a crucial stage for AA generation, with control over temperature (220°C) and duration (over 10 minutes) significantly reducing AA content (Caporaso et al., 2022). Introducing pressure during roasting can further aid in diminishing AA levels. The duration of storage and brewing temperature also play vital roles in influencing AA content in coffee beverages (Andrzejewski et al., 2004a). Prolonged storage periods (e.g., 12 months) at 37°C and brewing at lower temperatures (e.g., 4°C) over extended periods (e.g., 3 hours) can minimize the AA dissolved in coffee beverages (Hoenicke & Gatermann, 2005). However, while existing research predominantly focuses on reducing AA production, it is imperative to explore other potentially harmful substances, assess coffee quality, delve into inhibition mechanisms, and advance the practical application of novel technologies to produce high-quality coffee with diminished AA levels in the future.

2.5.3 Detection of acrylamide

Given the toxicity of AA, precise evaluation and reduction of its concentration in coffee are vital to mitigate potential risks to consumer safety. However, direct quantitative analysis is challenging due to the lack of distinct chromophoric groups, such as conjugated double bonds in aromatic rings and conjugated triple bonds. (Akgün & Arıcı, 2019; Xian et al., 2019). As a result, sample pre-treatment is usually necessary. Currently, methods for assessing AA in coffee fall into traditional and novel categories. Traditional detection methods include gas chromatography (GC), gas chromatography-mass spectrometry (GC-MS), high-performance liquid chromatography-mass spectrometry (HPLC-MS), high-performance liquid chromatography-mass spectrometry/mass spectrometry (HPLC-MS/MS), and capillary electrophoresis (CE) (Pundir et al., 2019b). Novel detection techniques encompass enzyme-linked immunosorbent assay (ELISA), biosensors

(electrochemical biosensors, fluorescence sensors), spectroscopy, highly sensitive gas chromatography detectors (high-resolution time-of-flight mass spectrometry, nitrogen-phosphorus detectors, tandem mass spectrometry), inhibition-based spectrophotometry, and machine vision approaches (Asnaashari et al., 2019; Singh et al., 2014). Although there are few studies utilizing these innovative detection methods for AA analysis in coffee, they have been widely applied for food detection purposes.

Traditional methods provide swift, sensitive, and precise analysis, rendering them suitable for detecting ultra-trace amounts of AA in food. However, sample derivatization is required to enhance stability. In a study conducted by Ku Madihah et al. (Madihah et al., 2012), researchers utilized a solid-phase extraction C18 column conditioned with 3 mL of acetone and 3 mL of formic acid to extract AA from coffee powder. Analysis was performed using gas chromatography equipped with a Flame Ionization Detector at a temperature of 260 °C, revealing an AA concentration of 0.23 mg/100 g.

Novel detection techniques not only retain the rapid, sensitive, and precise attributes of traditional methods but also partly address the uncertainty associated with derivatization. By employing a 3-mercaptopbenzoic acid-AA-bovine serum protein (BSA) complex to generate antibodies and utilizing an indirect competition approach for AA detection in food via ELISA, recovery rates of 95-100% can be achieved (Quan et al., 2011a). A quick and reliable technique for evaluating AA content in fried foods involves surface-enhanced Raman spectroscopy, with a detection range of 5-100 ug/kg and detection and quantification limits at 2 ug/kg. Acrylamide recoveries range from 73.4% to 92.8%, demonstrating consistency with the conventional LC-MS/MS method (Cheng et al., 2019).

CHAPTER 3

RESERCH METHODOLOGY

3.1 MuscFv antibody production

3.1.1 Selection of Phage clone displaying murine scFv that bound to AA by bio-panning

3.1.1.1 Immobilization of acrylamide (AA)

Acrylamide standard 0.5 mg in 100 μ L of Carbonate/Bicarbonate buffer pH 9.6 (**Appendix E**) were immobilized on the surface of well of microtiter plate. The microtiter plate was incubated at 37°C overnight. (Bovine serum albumin (BSA) for subtracting the phage libraries.)

3.1.1.2 Phage binding

Construction of the murine scFv (MuscFv) phage display library for bio-panning to produce anti-AA MuscFv used in this study were kindly given by Asst.Prof. Dr.Jeeraphong Thanongsaksrikul from Faculty of Allied Health Sciences, Thammasat University, Thailand. Bio-panning were performed according to protocols (Thanongsaksrikul et al., 2018) Briefly, Preparation of LB – Tetracycline (Tet) Conc. 20 μ g/ μ L and LB – Ampiciline (Amp) Conc. 100 μ g/ μ L (**Appendix C**) and then streak XL – 1 blue *E. coli* bacteria from stock glycerol on LB – Tet and LB – Amp plate and incubate at 37°C overnight. After that incubate single colony of XL – 1 blue *E. coli* in 2 ml LB – Tet culture medium with shaker at 37°C, 250 rpm overnight. Preparation of log phase *E. coli* XL – 1 blue bacteria culture. Incubate 10% bacteria cell suspension by using overnight culture of *E. coli* XL – 1 blue in 3 ml of LB – Tet culture medium and incubate at 37°C, 250 rpm to get log phase. Phage binding the antigen coated 3 wells with PBS 200 μ L 3 times and block with 200 μ L of 3% BSA in PBS into the well and incubate at 37°C in moisture chamber for 1 hr and wash 3 times with PBS – 0.05% Tween20 200 μ L. (**Appendix E**) After washing were added 200 μ L of scFv phage library to the BSA well and incubate at 37°C in a moisture chamber for 1 hr. Then collect 200 μ L of scFv phage library from BSA well to Immobilization AA well and incubate at 37°C in a

moisture chamber for 1 hr. After washing were added 200 μ l of log phase *E. coli* XL – 1 blue into the AA well. Incubate at 37°C in a moisture chamber for 15 mins. The phage infected *E. coli* was collect 200 μ l into the tube 1.5 ml. Repeat steps 9 -11 one more time. Take phage infected *E. coli* for dilution (Undilute, 1:10, 1:100) in LB – Broth. And take 100 μ l of each dilution to spread on LB – Amp plate. (Note, undiluted, 1:10, 1:100) and incubate at 37°C overnight. The remaining portions of the transformed *E. coli* XL – 1 blue were kept in 20% glycerol at -80 °C for further use.

3.1.1.3 Screening for phage transformed *E. coli* clones that carried recombinant phagemids with the inserted murine scFv (MuscFv)-coding sequences

The phage-transformed *E. coli* clones were grown overnight at 37 °C on LB – Amp plate. The *E. coli* colonies that appeared on the plates we randomly and checked for the presence of the murine scFv (MuscFv) against AA by direct colony PCR using sequencing primers that annealed at nucleotide sequences of pelB Primer 5'-ATACCTATTGCCTAC GGCAGC-3' and gIII Primer 5'-TAGCATTCCACAG ACAGCCC-3' in a pSEX81 phagemid vector (Macrogen Oligo, Madrid, Spain). The replica plates of the selected colonies were PCR reaction mixture into PCR tube and make patching on LB-A replica pate. Then resuspend the colony in the reaction mixture and culture replica plate incubate at 37°C overnight. Each PCR reaction mixture was prepared as the following:

Ingredient	Volume (μ L)
Expand High Fidelity buffer without MgCl ₂ (10x)	1.25
2.5 mM each dNTP	0.25
25 mM Mg Cl ₂	1.0
gIII Primer 10 μ M	0.25
pel B primer 10 μ M	0.25
Tag polymerase (5U/ μ l)	0.05
Ultrapure deionized water (UDW)	9.45
Total (μL)	12.5

The PCR thermal cycles were:

1. Initial denaturation	at 95 °C for 30 seconds
2. Thirty cycles of	
a. Denaturation	at 95 °C for 30 seconds
b. Annealing	at 58 °C for 45 seconds
c. Extension	at 72 °C for 1 minutes
3. Final extension	at 72 °C for 3 seconds

3.1.1.4 Agarose gel electrophoresis

The PCR amplified product was verified by agarose gel electrophoresis. One percent agarose gel was prepared by dissolving the agarose powder (QP products, USA) in 1x TAE buffer. The suspension was melted by using a microwave oven. The gel was set and cooled down. Polymerization of the agarose suspension was allowed to occur in a gel casting apparatus (Bio-Rad, Calif A). The sample to be resolved was mixed with 6x DNA loading dye and loaded into a slot made in the cast gel. The DNA was run in 1x TAE buffer at 100 Volts for 30 minutes. After electrophoresis, the gel was placed in 1x TAE buffer containing 10 mg/ml for 5 minutes. The DNA band was revealed by using QUANTUM CX5 Edge – Gel Documentation System (Vilber, Collégien, France. (MuscFv insert size = approx. 900 bp)

3.1.1.5 *MuscFv*-phage recusing from individual *E. coli*

The *MuscFv*-phage was isolated from individual colonies of *E. coli* positive. Each colony was transferred from a replica plate into 2 ml of LB-Amp in a 15 ml tube and incubated overnight at 37°C with shaking at 250 rpm. A 10% cell suspension of each *E. coli* clone was prepared by adding 250 µl of the overnight culture of each clone into 2.5 ml of LB-AGT (LB with a final concentration of glucose 0.1 M, ampicillin 100 µg/ml, and tetracycline 20 µg/ml) in a 15 ml tube. This was then incubated at 37°C with shaking at 250 rpm for approximately 4 hours. When at OD600 nm reached approximately 0.4, each tube (2.5 ml) was infected with 16.03 µl of M13KO7 helper phage at an MOI of 1:20 (M13KO7 phage stock = 1.56 x 10¹² cfu/ml). The tubes were

then incubated at 37°C without shaking for 30 minutes followed by 30 minutes with shaking at 250 rpm. After that, the tubes were centrifuged at 8000 rpm for 10 minutes at room temperature, and the supernatant from each tube was discarded. The bacterial cell pellet was then resuspended in 2.5 ml of LB-AK (LB with a final concentration of ampicillin 100 µg/ml and kanamycin 25 µg/ml) and incubated overnight at 30°C with shaking at 250 rpm. Finally, the tubes were centrifuged again at 8000 rpm for 15 minutes at 4°C, and the supernatant (containing LB-AK with *muscFv*-phage) was collected into new 15 ml tubes.

3.1.1.6 Titration of the rescued *muscFv* phage by plate count method

Inoculate 10% bacterial cell suspension by using overnight culture of normal *E. coli* XL-1 blue cell in 5 ml of pre-warmed LB-Tet culture broth (supplemented with the final concentration of 20 µg/ml) and incubate at 37 °C, 250 rpm for ~ 4 hrs to get log phase (OD₆₀₀ ~ 0.4-0.5). Prepare 20 µl of the individual rescued *muscFv*-phages by 10-fold serially diluted in LB broth (10⁻¹ to 10⁻⁸) and then mix the diluted rescued *muscFv*-phages with 100 µl of the log-phase *E. coli* XL-1 blue (total 120 µl). Incubate the tubes at 37 °C for 1 hr. Plate each dilution onto LB-Amp plates, depositing 10 µl per dot with 5 dots per dilution and incubate the plates at 37 °C overnight. Count the colonies formed on the LB-Amp plates and calculate the titre.

3.1.1.7 Binding assay of the *muscFv*-phage by indirect ELISA

To determine Binding assay of the *muscFv*-phage, the indirect ELISA was performed. Acrylamide standard 0.5 mg in 100 µL of bicarbonate coating buffer (**Appendix E**) was immobilized onto wells of an ELISA plate (Corning, USA). The plate was kept dry coated at 37 °C, Overnight incubation. After removing the unbound proteins, the coated wells were washed three times with PBS-T 0.05% (**Appendix E**). All wells were blocked with 3% BSA in PBS (250 µl /well) and incubate at 37 °C in moisture chamber for 1 hr. After washing, were added acrylamide standard. Incubate with 100 µl of the normalised titre of individual *muscFv* (section 3.1.1.6) phage clones (~ 10⁸ cfu/ml) diluted in PBS-T at 25 °C in moisture chamber for 1 hr. Also add 100 µl of phage diluent for Blank and positive control wells. After washing the wells with PBS-T 0.5% x 5 times (and 2 times with PBS-T 0.05%). All well were added 100 µl of Mouse anti-M13 (GE Healthcare) (1 in 6,000 in antibody diluent; 0.2% BSA in PBS-T) and

incubated at 25 °C in moisture chamber for 1 hr. All well were washed and added 100 µL of goat anti-mouse-immunoglobulin-horseradish peroxidases (HRP) conjugate (Dako,Denmark, EU). (1 in 5000 in antibody diluent) and incubated at 25 °C (RT) in moisture chamber for 1 hr. After washing, the chromogenic substrate, i.e., ABTSTM (KPL, Maryland, USA) was added to each well. Incubated 15mins, 30 mins and 1 hr at RT in dark chamber and measured OD₄₀₅ nm of the content in each well was determined using a microplate reader (Global Genetics).

3.2 Sub-cloning of muscFv antibodies

3.2.1 Sub-cloning of *muscFv*- AA from pSEX81 vector to pOPE101 vector

The inserted gene sequences and protein expression vector backbones were doubly digested with specific restriction enzymes. In pSEX81 (Progen Biotechnik GmbH, Heidelberg, Germany) the recognition sites of the restriction endonucleases *NcoI* and *HindIII* allow the insertion of a VH gene fragment. For insertion of a VL gene fragment the sites of the restriction endonucleases *MluI* and *NotI* (Thanongsaksrikul et al., 2018) Briefly, the *muscfv* coding sequence was directionally cloned into pOPE101 by *NcoI* and *NotI* restriction enzymes (Thermo Scientific, USA). The mixtures for DNA digestions were prepared as followed:

Digestion reaction mixture for pSEX81: *muscfv*

Ingredient	Volume (µL)
10x buffer (µl)	2
DW (µl)	15
pDNA (µg)	1
<i>NotI</i> (fast digest) (µl)	1
<i>NcoI</i> (fast digest) (µl)	1
Total (µl)	20

The expected size scfv~ 755 bps insert (depends on sequence) double digested pSEX-81 ~4.1 kb and cult plasmid ~4883 bps.

Digestion reaction mixture for pOPE101

Ingredient	Volume (μL)
10x buffer (μL)	2
DW (μL)	15
pDNA (μg)	1
<i>NotI</i> (fast digest) (μL)	1
<i>NcoI</i> (fast digest) (μL)	1
Total (μL)	20

The inserted gene sequences and protein expression vector backbones were doubly digested with specific restriction enzymes. In pOPE101 (Progen Biotechnik GmbH, Heidelberg, Germany) the recognition sites of the restriction endonucleases *NcoI* and *HindIII* allow the insertion of a VH gene fragment. For insertion of a VL gene fragment the sites of the restriction endonucleases *MluI* and *NotI* are recommended. The expected double digested pOPE101~3184 kb and cult plasmid ~3970 bps.

The mixtures were incubated at 37 °C for 2 hours and the digested plasmids were verified by 1% agarose gel electrophoresis as section 3.1.1.4. The *muscfv* fragments and digested protein expression vectors were purified from agarose gels by GenePFlow™ Gel/PCR Kit (DFH100, DFH300). (Geneaid, Taipei, Taiwan).

3.2.2 Ligation of DNA sequences coding for *muscfv*-AA in to pOPE101 vector

The purified *muscfv* fragments were ligated into the purified digested protein expression vectors by using T4 DNA ligase (New England BioLabs, Ipswich, UK). The mixtures were prepared as followed:

Ligation reaction

Ingredient	Volume (μL)
pOPE101 vector (50 ng)	2.5
scfv insert (30 ng)	2
DW (μL)	3.5
T4 ligase reaction buffer (10X)	1
T4 DND ligase	1
Total (μL)	10

The mixtures were kept at 4 °C for 16 hours and introduced into chemically competent XL 1 blue *E. coli* by heat shock transformation method.

3.2.3 Preparation of chemically competent XL 1 blue *E. coli*

an overnight culture of XL 1 blue *E. coli* was prepared by inoculating one isolated colony of the bacteria into 2 mL of Luria-Bertani (LB) broth (**Appendix C**) and incubated at 37 °C with shaking at 250 rpm for 16 hours. 100 μL of the overnight culture were inoculated into 10 mL of fresh LB broth and incubated at 37°C with shaking at 250 rpm until OD₆₀₀ nm reached 0.4-0.5. The culture was kept in an ice-bath for 1 hour and centrifuged at 4500 x g, 4°C for 15 minutes to collect the cell pellet. The pellet was resuspended in 5 mL of ice-cold 100 mM MgCl₂ solution and centrifuged at 4500 x g, 4°C for 15 minutes. After discarding the supernatant, the cell pellet was resuspended in 1 mL of ice-cold 100 mM CaCl₂ solution and kept in ice-bath for at least 1 hour. The chemically competent *E. coli* cells were freshly used, or they could be kept at -80°C until use later. For keeping at -80°C, the competent cell suspension was added with 20% final concentration of glycerol.

3.2.4 Transformation and screening for XL 1 blue *E. coli* transformants.

The ligation mixtures from section 3.1.1.9 were introduced into XL 1 blue *E. coli* competent cells by heat shock method. Briefly, ligation was mixed with 100 μL of competent cell suspension and kept in an ice-bath for 20 minutes. The mixture was heated at 42°C for 2 minutes in a water-bath and immediately moved to

an ice-bath for 5 minutes. The preparation was added into 900 μL of LB broth and incubated at 37°C with shaking at 250 rpm for 1 hour. The culture was spread onto LB agar plates containing 100 μg ampicillin/mL (LB-Amp), and Isopropyl β -D-1-thiogalactopyranoside (IPTG) (**Appendix C**). The agar plates were incubated at 37°C for 16 hours. White colonies of the transformed *E. coli* transformants were randomly picked to screen for positive the colonies which carrying recombinant plasmid containing *muscFv* coding sequence means of colony PCR. Replica plates for individual colonies were made on agar plates for subsequent use. The PCR reaction using pelB primer and pOPE101 sequencing primer mixture prepared as the following:

Ingredient	Volume (μL)
Expand High Fidelity buffer without MgCl_2 (10x)	1.25
2.5 mM each dNTP	0.25
25 mM Mg Cl_2	1.0
gIII Primer 10 μM	0.25
pel B primer 10 μM	0.25
Tag polymerase (5U/ μL)	0.05
Ultrapure deionized water (UDW)	9.45
Total (μL)	12.5

Thermal cycles of the PCR are shown below. The PCR amplified products were verified by agarose gel electrophoresis as section 3.1.1.4

1. Initial denaturation	at 95 °C for 30 seconds
2. Thirty cycles of	
a. Denaturation	at 95 °C for 30 seconds
b. Annealing	at 58 °C for 45 seconds
c. Extension	at 72 °C for 1 minutes
3. Final extension	at 72 °C for 3 seconds

The insertion of the *muscfy* coding sequence was verified by DNA sequencing and bioinformatic analysis (Integrated DNA Technologies, Inc., USA). The sequencing data were compared with the parental clone in pSEX81.

3.3 Expression and purification of anti-AA MuscFv antibodies

3.3.1 Small scale expression of the anti-AA MuscFv antibodies

The transformed XL 1 blue *E. coli* clones were tested for their ability to express the recombinant proteins anti-AA MuscFv antibody in small bacterial culture scale. Bacterial colonies that carrying the respective recombinant plasmids as detected by colony PCR were inoculated into 5 mL of LB-A broth and incubated at 37°C with shaking at 250 rpm for 16 hours. Individual overnight cultures (1%) were inoculated into 10 mL of fresh LB-A broth and incubated at 37°C with shaking at 250 rpm until OD₆₀₀ nm were 0.4-0.5. Each culture was added with 0.1 mM IPTG and incubated at 37°C with shaking at 250 rpm for 5 hours. After centrifugation at 4,500 x g, for 15 minutes, each cell pellet was resuspended in 1 mL phosphate-buffered saline, pH 7.4 (PBS) and sonicated at 0.5 cycle, 40% amplitude for 2 minutes in an ice-bath. The bacterial homogenate was centrifuged at 12,000 x g, 49°C for 15 minutes. The supernatant was collected (native/soluble *E. coli* fraction); the cell pellet was resuspended in 200 µL of 10% SDS and boiled for 5 minutes (denaturing/insoluble fraction). Both native/soluble and denaturing/insoluble fractions were analyzed by sodium dodecyl sulfate-polyacrylamide gel electrophoresis (SDS-PAGE) and Western blot analysis (WB) (Appendix). The transformed *E. coli* clones that could express the recombinant proteins were used further in large-scale production of the respective proteins.

3.3.2 Large-scale expression of anti-AA MuscFv antibodies

An overnight culture 4 mL of the transformed *E. coli* clone that could express the anti-AA MuscFv antibodies from 3.1.1.12.1 were inoculated into 400 mL of LB-Amp broth and incubated at 37°C with shaking at 250 rpm until OD₆₀₀ nm were 0.4-0.5. The culture was induced with 0.5 mM IPTG and kept at 20°C with shaking 5 hours. One mL of the culture was collected and checked for the anti-AA MuscFv antibodies expression by SDS-PAGE and WB (Appendix F).

3.3.3 Purification of anti-AA MuscFv antibodies

The purified to affinity chromatography on Ni-NTA Resin Nickel IMAC Resin for 6X His Tagged protein purification using native condition. (A Geno Technology, Inc., USA). The IPTG-induced bacterial pellet was resuspended in 10:1 (v/w) of Buffer C (**Appendix D**) and sonicated at 0.5 cycle, 40% amplitude for 5 minutes using sonicator (Ultrasonic Processors, Cole-Parmer Instrument Company, USA). The homogenate was centrifuged at 12,000 x g, 40C for 30 minutes. The supernatant was collected for purification. The Ni-NTA™ agarose beads were equilibrated with 5 times bed bead volume of Buffer C. After discarding the supernatant, the bacterial lysate containing recombinant anti-AA MuscFv antibodies was added to mix with the beads. After incubation, the agarose beads were packed into a column and the unbound fraction was collected. After washing, the bound protein was eluted with elution buffer (Imidazole dilution: concentration: 10 mM, 50 mM, 75 mM, 100 mM, 500 mM) (**Appendix D**) (5 fractions were collected). The beads were washed with 1 M imidazole in Buffer C to elute out all proteins. After washing with UDW, the beads were kept in 20% ethanol at 4°C for reuse. All fractions were analyzed SDS-PAGE and Western blot analysis (WB) for the presence of the anti-AA MuscFv antibodies. The fractions containing the target protein were pooled and refolded in PBS. The purified anti-AA MuscFv antibodies test ELISA binding to acrylamide compared with BSA for cross-reactivity.

3.4 Protein determination and characterization

3.4.1 Sodium dodecyl sulfate-polyacrylamide gel electrophoresis

Sodium dodecyl sulfate-polyacrylamide gel electrophoresis (SDS-PAGE) was used to separate proteins in electric field according to their molecular masses system, the proteins were denatured by heating in buffer containing SDS and reducing agent, β -mercaptoethanol. The denatured proteins bound by SDS became negatively charge and these proteins migrated in electric field and were separated in accordance with the protein sizes.

3.4.1.1 Protein separation

The polyacrylamide gel was cast according to the manufacturer's instruction (Bio-Rad, California, USA). Twelve percent resolving and 4% stacking gel were prepared in 1.5 M Tris-HCl, pH 8.8 and 0.5 M Tris-HCl, pH 6.8, respectively (**Appendix F**). Proteins were prepared by denaturing with 6x sample buffer containing SDS and heated for 5 minutes. Individual denatured proteins, as well as PageRuler® pre-stained protein ladder (Thermo Fisher Scientific, Waltham, MA, USA) were added into slots made on the stacking gel. Electrophoresis was run in electrode buffer by applying electricity of 20 mA per gel. The electrophoresis continued until the dye front reached the lower edge of the resolving gel. After removing the gel containing separated proteins from the cassette, the gel was stained with Coomassie Brilliant Blue G-250 dye (CBB) (Affymetrix, Santa Clara, CA 95051, USA) or transblotted onto a nitrocellulose membrane (NC) for WB.

3.4.1.2 Western blot analysis (WB)

The separated proteins in SDS-PAGE gel were transblotted onto NC by transblot apparatus (Bio-Rad, California, USA). The transblotting was run in a transfer buffer (**Appendix F**) by applying electricity of 100 Volts for 1 hr. The blotted NC was blocked with 3% BSA in TBS-T buffer, pH 7.5 at 25 °C for 1 hr. After washing with TBS-T buffer, the blocked membrane was probed with either antibody specific to the epitope tag on the target protein (e.g., 6xHis tag or E-tag) or primary antibody to the protein antigen and kept at 25°C for 1 hr. After washing, the membrane was incubated with enzyme-conjugated secondary antibody against the primary antibody isotype and the antigen-antibody reactive bands were revealed by adding appropriate chromogenic substrate (BCIP/NBT substrate).

3.4.2 Characterization and Homology modeling and intermolecular docking

3.4.2.1 Computerized simulations

The anti-AA MuscFv were selected and analyzed for nucleotide sequence using pelB (5'-ATACCTATTGCCTACGGCAGC-3') and pOPE101 (5' -TAGATCTTCTTCTG-AGATCAGC -3') primers as section 3.1.1.4 (Integrated DNA Technologies, Inc., USA). The anti-AA MuscFv a representative *muscFv* sequence, DNA encoding from selected anti-

AA MuscFv antibodies the sequence was complement determining regions (CDRs) and immunoglobulin framework regions (FRs) of muscfv sequences from selected MuscFv display phages were determined (IMGT/V-QUEST tool of the International ImMunoGeneTics Information System (IMGT®)). CDRs and immunoglobulin FRs from anti-AA MuscFv were also aligned using Bio-Edit and ClustalW2 program. Checked the position of VH, VL and Linker according to the vector pOPE101 for validation of protein structure and translated to amino acid via website <https://web.expasy.org/translate/>. Anti-AA MuscFv submitted sequence of each protein to modeled using the website AlphaFold2.ipynb - Colaboratory (google.com) waiting till you get the result and chose the best match model of each protein (antigen and antibody (scFv)) to submit for docking. Meanwhile, we searched for acrylamide 3D structure modeled pdb files <https://www.rcsb.-org/>. Predict the 3D model of the docking results were obtained according to their binding affinities by using AutoDock Vina. PyMOL and Discovery Studio were used for the largest docking clusters of the interactive residues with the lowest local energy were selected.

3.5 Production of ELISA detect AA in coffee

3.5.1 Determination of the cutoff value of Anti-AA MuscFv antibody by indirect ELISA

To establish the cutoff value of the indirect ELISA, 10-fold dilutions of the AA standard were used. Each dilution was tested in triplicate. The OD₄₀₅ nm value plus three times the standard deviation (SD) was used as the cutoff. All experimental samples were considered positive if the OD₄₀₅ nm value was higher than this cutoff value. Briefly, the indirect ELISA was performed 10-fold dilutions of the AA standard in 100 µL of bicarbonate coating buffer (**Appendix E**) was immobilized onto wells of an ELISA plate (Corning, USA) were added BSA as control antigens of wells and kept at 37°C until dry. After washing with PBST, all wells were blocked with 250 µL of 3% BSA in PBS at 37°C for 1 hour. After removing the blocking reagent by washing, purified anti-AA MuscFv antibodies were added to wells and kept at 25°C for 1 hour. The wells were washed with PBST and incubated with mouse monoclonal anti-c-Myc (Affinity Bioscience) diluted 1:3,000 in PBST for 1 hour, washed, and 100 µL of horse-radish-peroxidase-conjugated goat anti-mouse (diluted 1:5000 in PBST) was added. After 1 hour at 25°C, the secondary antibody was removed by washing before added ABTS

(2,2'-Azinobis[3-ethylbenzothiazoline-6-sulfonic acid] -diammonium salt) chromogenic substrate (KPL, Maryland, USA). was added to each well. Incubated 15 mins, 30 mins and 1 hour at RT in dark chamber and measured OD₄₀₅ nm of the content in each well was determined using a microplate reader (Global Genetics). against blank controls (defend as wells to which PBS were added instead of anti-AA MuscFv antibodies).

3.5.2 Validation of AA standard and anti-AA MuscFv antibody

Checker board titration was used to determine the lowest amount of acrylamide detected (LOD) and the lowest amount of Anti-AA MuscFv antibody used in the ELISA. The AA standard was diluted in coating buffer; 0, 0.1, 0.2, 0.4, 0.5, 0.6, 0.8, and 1 mg/mL and coated in each ELISA well. Triplicate wells of each concentration were performed by ELISA as protocol previously described above as section 3.1.1.14.1

3.5.3 Determination of Anti-AA MuscFv specific to acrylamide in coffee

The validity of Anti-AA MuscFv specific to acrylamide in coffee was conducted by using 2 brands of dark roasted coffee beans: designated coffee A and coffee B. The spike (0.1, 0.3, 0.5, and 0.7 mg/mL) and non-spike with AA standard in coffee was determined by ELISA as protocol previously described above as section 3.1.1.14.1. Furthermore, the presence of acrylamide in coffee was also confirmed by High-performance liquid chromatography (HPLC).

3.6 Other of related experiments

In addition, the researcher has other studies and experiments to develop the test for acrylamide in coffee using the principle of immunochromatographic strip test.

3.6.1 Production of polyclonal antibody against acrylamide

Rabbit immunization and sample collection in this study was approved by the Animal Care Committee for Scientific Purposes, Suranaree University of Technology. (SUT-IACUC-009/2019). To obtain antibody that would bind to acrylamide, polyclonal antibody will be produced. A total of 2 female New Zealand white rabbits were separated into two groups. A total concentration of 0.01 mg/kg of acrylamide mixed with alum adjuvant were used for the primary intradermal inoculation. Two weeks after the primary inoculation, the boosts were repeated five more times at two-week

intervals. Five or ten milliliters of whole blood samples were collected prior to the primary inoculation for use as negative control and 10 days after the 2nd, 4th and 6th boosts. The antibody titer against acrylamide will be determined using ELISA. Rabbits were returned to the Animal Experiment Center, Suranaree University of Technology at the end of the study.

3.6.2 Preparation of Glutathione S-transferase conjugation AA standard

The culture PGEX 5X-3 GST *E. coli* was streaked onto LB agar plates containing 100 ug ampicillin/mL (LB-Amp), and Isopropyl β -D-1-thiogalactopyranoside (IPTG) (Appendix C). The agar plates were incubated at 37°C for 16 hours. White colonies for use the future experiments. Preparation of chemically competent DH5-Alpha *E. coli* according (section 3.2.3,3.2.4). After competent cell, were transformation for PGEX 5X-3 GST *E. coli* transformants. White colonies of the transformed *E. coli* transformants were randomly picked to screen for positive the colonies by PCR. After confirming PCR, were expression and purification of GST by SDS-PAGE and WB (**Appendix F**) and then were check binding are Anti-GST, mAb anti- AA and anti- AA form rabbit No.1 by dot blot assay.

3.6.3 Production of AuNPs conjugation MuscFv- anti AA

Gold nanoparticle conjugation and anti-AA conjugation of MuscFv- anti AA to colloid gold nanoparticles (AuNPs) with diameters of approximately 40 nm was performed using bioassay works-based conjugation. After optimizing pH, 0.5 ml samples of AuNPs were added to microtubes in 10 vials. Solutions in vials were then adjusted to pH 5.4, 6.6, 7.3, 7.8, 8.2, 8.4, 8.8, 9.2, 9.6, or 10.1 and 7 μ l aliquots of anti-AA were added to each vial. Solutions were then mixed gently using a pipette and were incubated at room temperature for 30 min. Vials showing a darkening purple color, black precipitate, or both in some vials were discarded. 50 μ l aliquots of BSA were added to the vials that did not show precipitation to stop the reactions. The resulting mixtures containing AuNPs-conjugated MuscFv-anti AA were kept at room temperature overnight (16 h) and were then used to assemble strip tests (Tam et al., 2017; Thobhani et al., 2010).

3.6.4 Preparation of immunochromatographic strip test for AA detection

Immunochromatographic strip tests were assembled from sample pads, conjugated pads, test zones, control zones, and absorbent pads. Sample pads were prepared from nitrocellulose membranes dipped in 0.01M PBS (pH 7.4) containing 5% BSA and 0.05% Tween 20 and were then dried at 60°C for 2 h. Conjugated pads were made of fiber glass spiked with MuscFv- anti AA conjugate colloid gold nanoparticles (AuNP). Test zones were prepared by spiking nitrocellulose membrane with 1 mg/ml of mAb anti- acrylamide and control zones spiked with anti-Myc Mouse mAb were dried at 37°C for 2 h. Finally, immunochromatographic strip test detection was performed by placing 100 μ l of AA standard solution 1 mg/ml for positive on sample pads and then incubating for 15 min (Anfossi et al., 2008).



CHAPTER 4

RESULTS AND DISCUSSION

4.1 MuscFv antibody production

4.1.1 Screening of Phage clone displaying MuscFv that bound to AA

Phage bio-panning will be performed to select scFv specific to acrylamide. Mouse scFv phage-displayed library which will be kindly given by Assoc.Prof. Dr.Jeeraphong Thanongsaksrikul from Faculty of Allied Health Sciences, Thammasat University, Thailand. After bio-panning, the *E. coli* colonies containing recombinant phagemid *muscfv* vector were individually picked for direct colony PCR. The *E. coli* clones which carried the plasmid with the *muscfv* inserts gave 15 clones (65.2%) were positive PCR amplicon at the associate sizes (Figures 4.1-4.3).



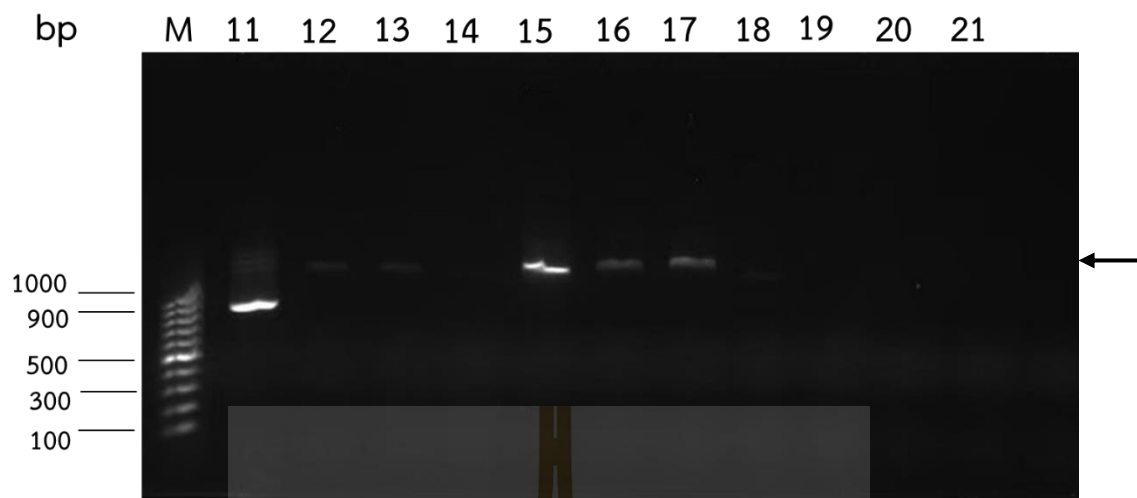
Figures 4.1 PCR amplicon of the phagemid *muscfv* sequence.

Lane M, GeneRuler™ 100 bp DNA ladder

Lanes 1-10, *muscfv* amplicons from *E. coli* clones 1-10 (~750-900 bp) (arrow)

Lane 11, Negative control (without DNA template)

Numbers at the left are DNA sizes in bp



Figures 4.2 PCR amplicon of the phagemid *muscfv* sequence. (Continued)

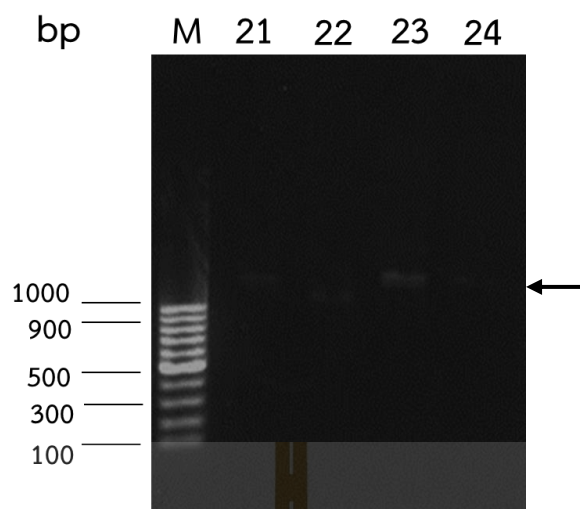
Lane M, GeneRuler™ 100 bp DNA ladder

Lanes 11-20, *muscfv* amplicons from *E. coli* clones 11-20 (~750-900 bp) (arrow)

Lane 21, Negative control (without DNA template)

Numbers at the left are DNA sizes in bp

มหาวิทยาลัยเทคโนโลยีสุรนารี



Figures 4.3 PCR amplicon of the phagemid *muscfv* sequence. (Continued)

Lane M, GeneRuler™ 100 bp DNA ladder

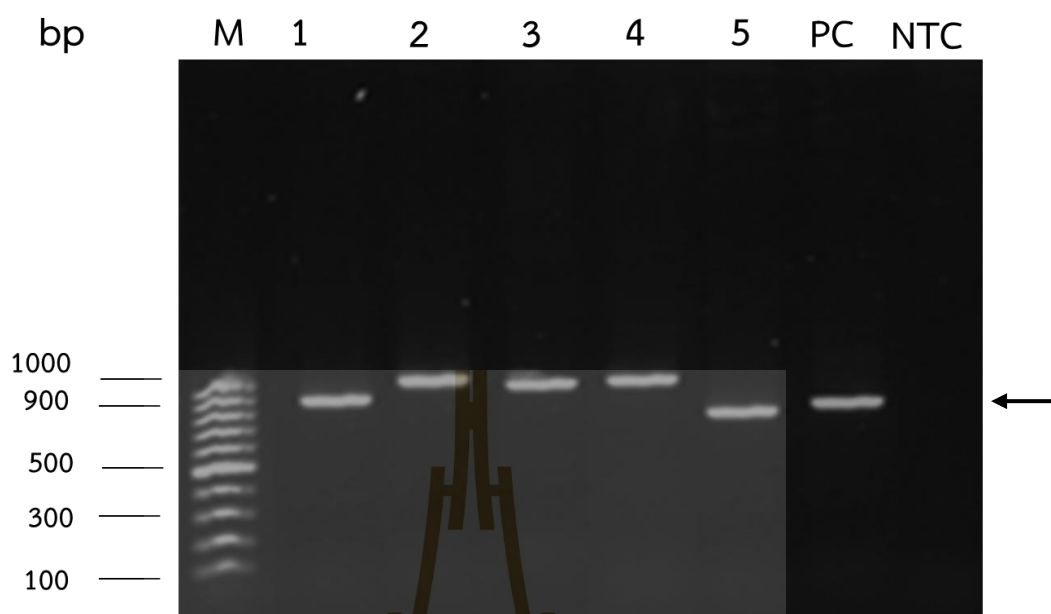
Lanes 21-23, *muscfv* amplicons from *E. coli* clones 21-23 (~750-900 bp) (arrow)

Lane 24, Negative control (without DNA template)

Numbers at the left are DNA sizes in bp

4.1.2 Selection for phage transformed *E. coli* clones that carried recombinant phagemids with the inserted murine scFv (MuscFv)-coding sequences

Identification of positive phage clones checked for the presence of the murine scFv (MuscFv) against AA by PCR using sequencing primers that annealed at nucleotide sequences of pelB Primer 5'-ATACCTATTGCCTAC GGCAGC-3' and gIII Primer 5'-TAGCATTCCACAG ACAGCCC-3' in a pSEX81 phagemid vector (Macrogen Oligo, Madrid, Spain). The positive clones which carried the plasmid with the *muscfv* inserts gave PCR amplicon at the expected sizes. In total positive clone, five clones (21.7%) was giving positive PCR band at associate size; ~750 -900 bp as shown in **(Figures 4.4)**.



Figures 4.4 PCR amplicon of *muscfv* (~750 -900 bp) (arrow) in picked pSEX81-transformed *E. coli* derived from phage bio-panning.

Lane M, GeneRuler™ 100 bp DNA ladder

Lanes 1-5, pSEX81: *muscfv* amplicons from *E. coli* clones 1-5

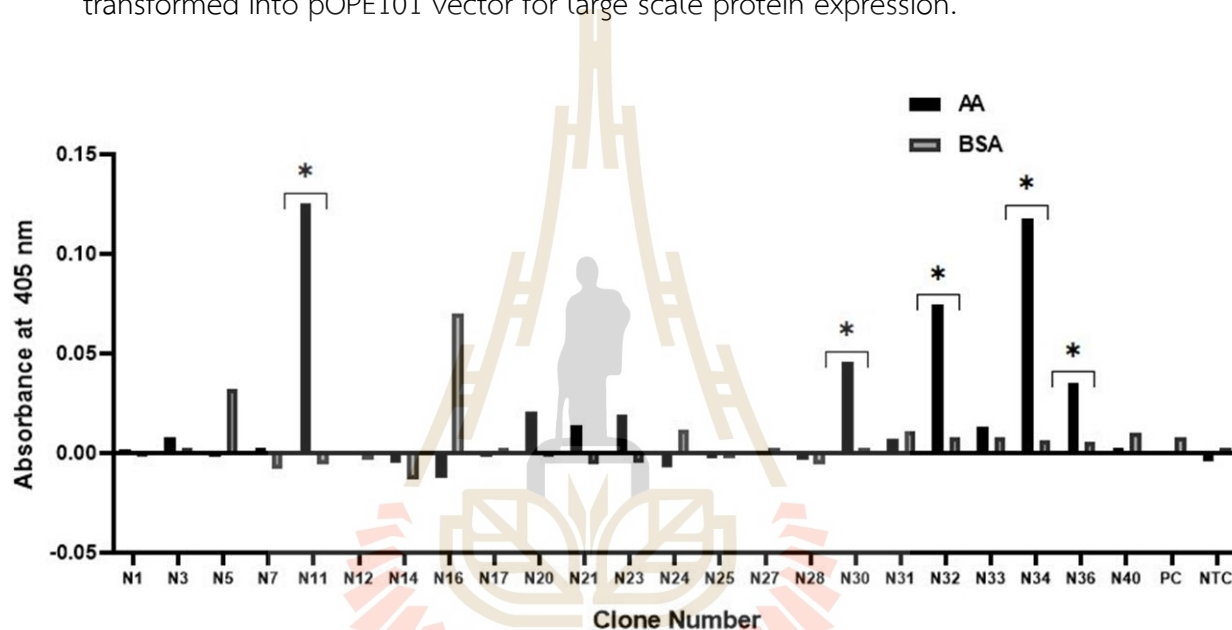
Lane 6, Positive control (with *muscfv*)

Lane 7, Negative control (without DNA template)

Numbers at the left are DNA sizes in bp

4.1.3 Binding of the *muscFv*-AA phage by indirect ELISA

The clones *muscFv*-phage were tested for their ability to bind to the AA by indirect ELISA. 5 clones specific acrylamide binding was N11, N30, N32, and N36 respectively gave positive ELISA result, i.e., the lysates of these clones gave ELISA signals $OD_{405\text{ nm}}$ higher than 0.05 to the immobilized AA and the signals were two times above the signals of the same lysates to the BSA which was used as control antigen (Figure 4.5). According to sequencing result, clone number 11 was chosen for further transformed into pOPE101 vector for large scale protein expression.



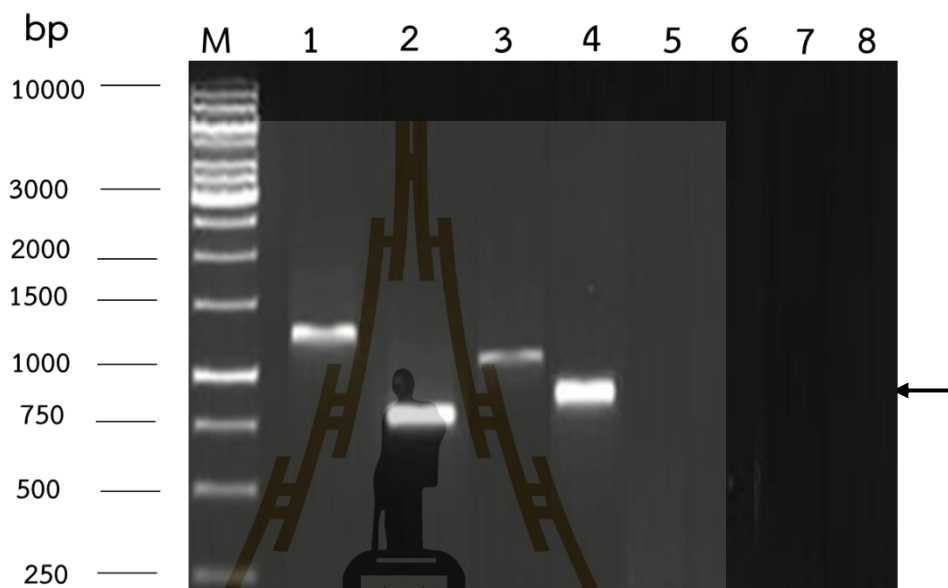
Figures 4.5 Results of indirect ELISA for determining binding of *muscFv*-AA phage. In lysate of 23 randomly selected scFv phagemid, there were 5 indirect ELISA positive clones (i.e., clones N11, N30, N32, N34, N36) that gave ELISA signal above the AA immobilized (background binding) and more than two times above $OD_{405\text{ nm}}$ that the same *muscFv*-AA phage bound to BSA as an antigen control.

4.2 Sub-cloning of *muscFv* antibodies

4.2.1 Sub-cloning of *muscFv*- AA phage from pSEX81 vector to pOPE101 vector

Clone number 11 was selection for phage transformed *E. coli* clones that carried recombinant phagemids with the inserted murine scFv (*MuscFv*)-coding sequences. clones number 11 were doubly digested with specific restriction enzymes.

Then DNA ligation and transformation for sub-clone into pOPE101 vector for large scale recombinant protein expression and purification. Colony directed PCR screening showed four positive PCR amplicon (N11.1, N11.2, N11.3 and N11.4) from 7 colonies screening (71.4%) (**Figures 4.6**).



Figures 4.6 PCR amplicon of pOPE10: *muscfv* (~750 -900 bp) (arrow) in picked pOPE101 -transformed *E. coli* derived from Sub-cloning.

Lane M, GeneRuler™ 100 bp DNA ladder

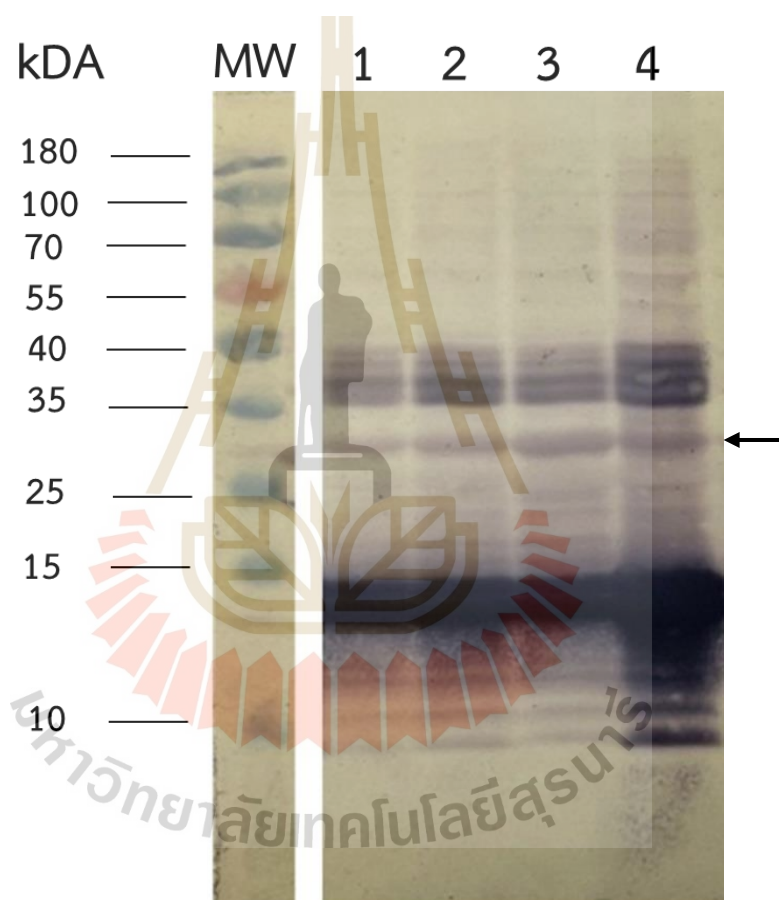
Lanes 1-7, pOPE101: *muscfv* amplicons from *E. coli* clones 1-7

Lane 8, Negative control (without DNA template)

Numbers at the left are DNA sizes in bp

4.3 Expression and purification of anti-AA MuscFv antibodies

E. coli clones which were positive for pOPE101 with *MuscFv* were checked for their ability to express the antibody protein by growing them under the IPTG induced condition. There were 4 positive clones (clones N11.1, N11.2, N11.3 and N11.4) (71.4 %) that expressed soluble anti-AA MuscFv antibodies of all 4 clones showed the positive band at the associate molecular mass (~25-30 kDa) as determined by WB (Figures 4.7).



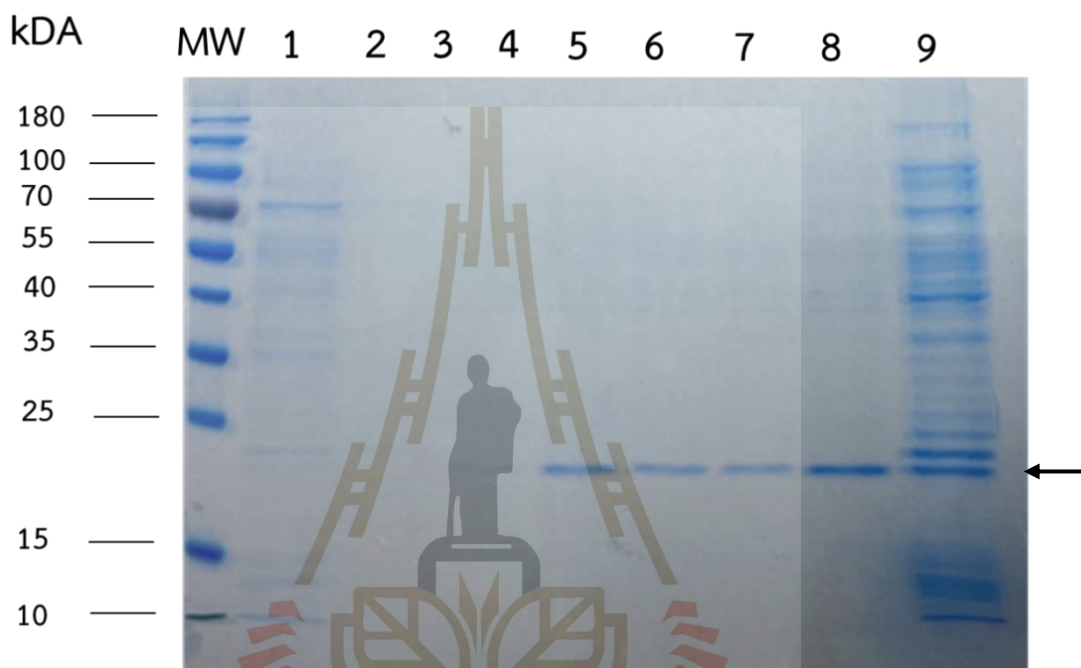
Figures 4.7 anti-AA MuscFv antibodies (~25-30 kDa; arrow) expressed by *E. coli* inserted murine scFv (*MuscFv*) clones as determined by WB

Lane MW, Pre-stained standard protein marker

Lane 1-4, clones N11.1, N11.2, N11.3 and N11.4 expressed soluble anti-AA MuscFv antibodies

Numbers at the left are protein masses in kDa

Purified anti-AA MuscFv antibodies bound specifically to acrylamide. Clone number 11.1 (MscFv-N11.1) was selected for protein expression. After large-scale expression, the bacteria were purified by using the Ni-NTA affinity resin under native condition. The purified proteins were checked by SDS-PAGE and Coomassie staining of the purified MuscFv-N11.1 protein (~25-30 kDa) as shown in (Figures 4.8)



Figures 4.8 Purified anti-AA MuscFv antibodies

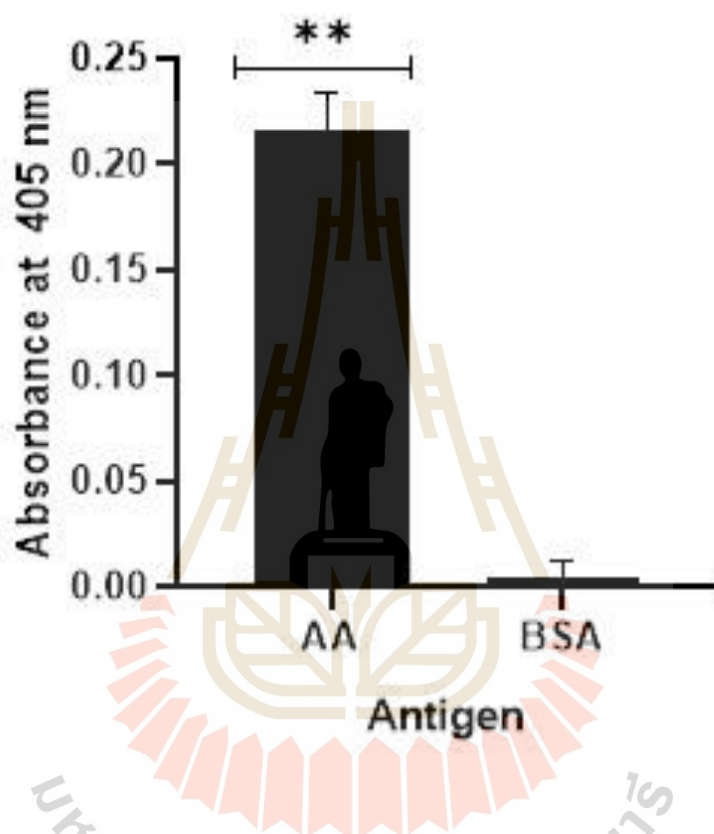
Lane M, Pre-stained standard protein marker

Lane 1-8, SDS-PAGE- Purified anti-AA MuscFv antibodies after CBB staining (~25-30 kDa; arrow)

Lane 9, SDS-PAGE- soluble anti-AA MuscFv antibodies

Numbers at the left are protein masses in kDa

The binding activity of purified MuscFv-N11.1 was verified via indirect ELISA. Coated AA and BSA wells were incubated sequentially with MuscFv-N11.1, mouse monoclonal anti-c-My, HRP-conjugated goat anti-mouse IgG and ABTS substrate, respectively. The absorbance OD at 405 nm. shown in **(Figures 4.9)**. The result showed that MuscFv-N11.1 could bind specifically to AA ($P < 0.001$) when compared to BSA.



Figures 4.9 The ELISA binding result of MuscFv-N11.1 showed statistically significant specific binding of MuscFv to acrylamide when compared with BSA ($P < 0.001$).

4.4 Characterization and Homology modeling and intermolecular docking

4.4.1 Complementary determining regions (CDRs) and immunoglobulin framework regions (FRs) of the MuscFv-N11.1

Complementary determining regions (CDRs) and immunoglobulin framework regions (FRs) of the MuscFv-N11.1 bound AA were determined [IMGT website (<http://imgt.cines.fr>)]. The deduced amino acid sequences of the MuscFv-N11.1

E. coli clones were found to be complete sequences of antigen-binding domains of antibodies (**Appendix G**). The deduced amino acid (aa) sequence of MuscFv-N11.1 was shown including the VH and VL domains joined by a (Glu4 Gly1 Phe1 Ser1) linker, the complementary determining region 1-3 (CDR1-3) (**Figure 4.10**).

MAQVTLKESGPGILQPSQTL SLTCSFSGFSLNTSGMGVSW IRQPSGKGLEWLAHIYWD DDDKRY NPSLKSRLTI	73
VH-CDR1	VH-CDR2
SKDTSRNQLFLKITSVDTADTATYYCARTGDYDYDDRFAYWGQGLTVTVSAAKTTPPKLEEGEFSEARVDIVIT	147
VH-CDR3	Linker
QDELSNPVTSGESVSISCRSSKSLLYKDGKTYLNWF LQRPQGQSPQLLIYLMSTR ASGVSDRFSGSGSGTDFTLEIS	223
VL-CDR1	VL-CDR2
RVKAEDVGVVYCOOLVEYPRTFEGGGTKLEIK	254
VL-CDR3	

Figure 4.10 The deduced amino acid (aa) sequence of MuscFv-N11.1 was shown including the VH and VL domains joined by a (Glu4 Gly1 Phe1 Ser1) linker, the complementary determining region 1-3 (CDR1-3).

4.4.2 Computerized simulations to determine the presumptive epitopes of the MuscFv-N11.1 bound AA

The deduced amino acids sequences of MuscFv-N11.1 were submitted the sequence of each protein to be modeled using the website (<https://colab.research.google.com/github/sokrypton/ColabFold/blob/main/AlphaFold2.ipynb>). The submit to online software for protein modeling and intermolecular molecular docking. This should be indicated that MuscFv-N11.1 was successfully constructed. The molecular docking model of MuscFv-N11.1 was performed. Ribbon display model showing MuscFv-N11.1 in blue, green, gray and red. Superimposed picture of the 3D structures of MuscFv-N11.1 and acrylamide structures as shown in figure 4.11A. MuscFv-N11.1 used D-58, D-60 and Y-105 of VH domain to interact with acrylamide via hydrogen bond (energy rang -12.89 kcal/mol) as shown (**Figure 4.11**).

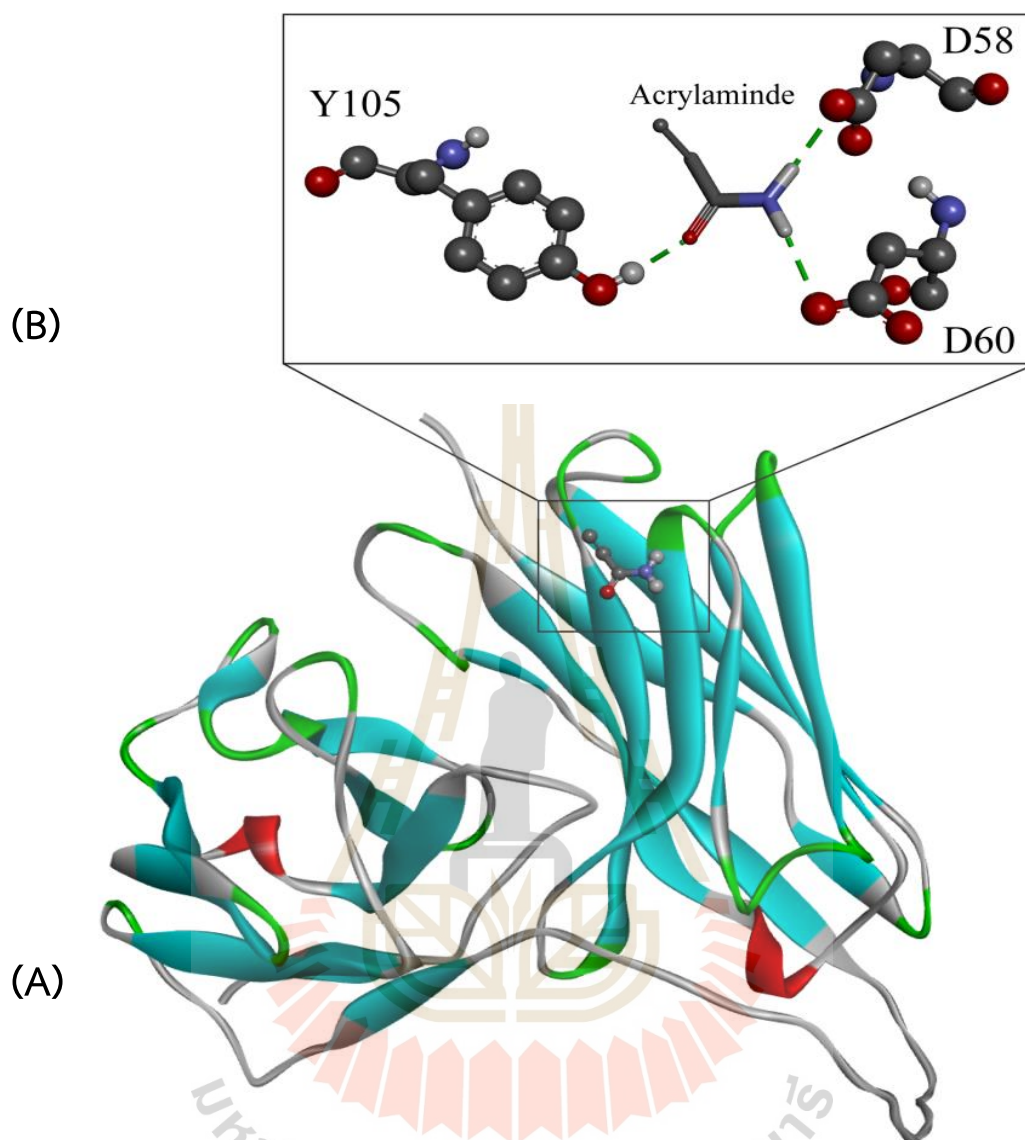


Figure 4.11 Molecular docking model of MuscFv-N11.1 interacts with acrylamide. (A) Ribbon display model showed MuscFv-N11.1. (B) Close-up view of MuscFv-N11.1 and acrylamide, used D-58, D-60 and Y-105 of VH domain to interact with acrylamide via hydrogen bond

Docking results were obtained according to their binding affinities by using AutoDock Vina. PyMOL. Discovery Studio 2021 was used for the largest docking clusters of the interactive residues, and those with the lowest local energy were selected (energy rang -12.89 kcal/mol) as data shown.

Scoring function: vina
 Rigid receptor: test_aa069_unrelaxed_rank_1_model_1.pdbqt
 Ligand: AA_ligand.pdbqt
 Center: X 0.5865 Y 0.2357 Z 0.5062
 Size: X 49.748560524 Y 54.4270596695 Z 57.1724798393
 Grid space: 0.375
 Exhaustiveness: 8
 CPU: 0
 Verbosity: 1

Computing Vina grid ... done.

Performing docking (random seed: -141415395) ...

0% 10 20 30 40 50 60 70 80 90 100%

|---|---|---|---|---|---|---|---|

mode	affinity (kcal/mol)	dist from best rmsd l.b.	best mode rmsd u.b.
------	------------------------	-----------------------------	------------------------

1	-12.89	0	0
2	-10.97	3.011	12.52
3	-10.79	3.713	12.20
4	-10.69	3.913	12.36
5	-9.832	2.538	12.66
6	-9.464	2.916	12.33
7	-9.204	1.45	2.027
8	-9.217	1.596	2.685
9	-8.723	3.876	12.67

4.5 Production of ELISA detect AA

4.5.1 Validation of AA standard and MuscFv-N11.1 antibody

Checker broad titration was used to determine the lowest amount of acrylamide detected (LOD) and the lowest amount of MuscFv-N11.1 used in the ELISA. The AA standard was diluted in coating buffer; 0, 0.1, 0.2, 0.4, 0.5, 0.6, 0.8, and 1 mg/mL and coated in each ELISA well. A concentration of 0.5 mg/mL was found to be the lowest concentration that could be detected and gave similar OD_{405 nm} as the concentration 0.6 and 0.8 mg/mL, respectively. Whereas the lowest amount of Anti-AA muscFv antibody was 0.8 mg/mL (Figure 4.12). Triplicate wells of each concentration of MuscFv-N11.1 were performed.

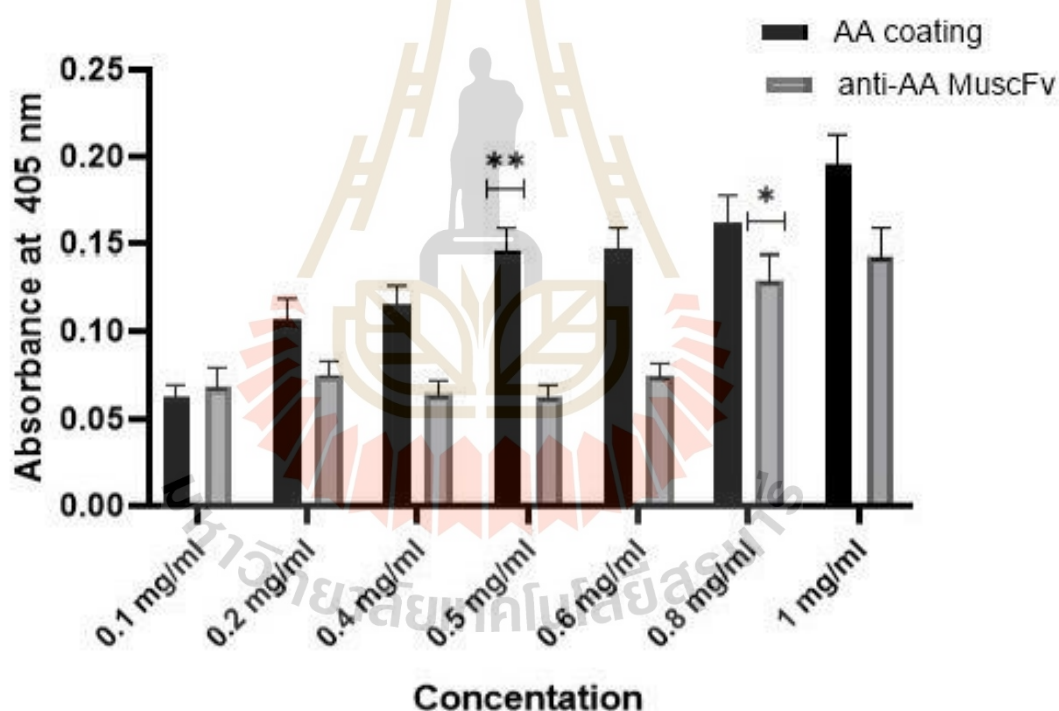
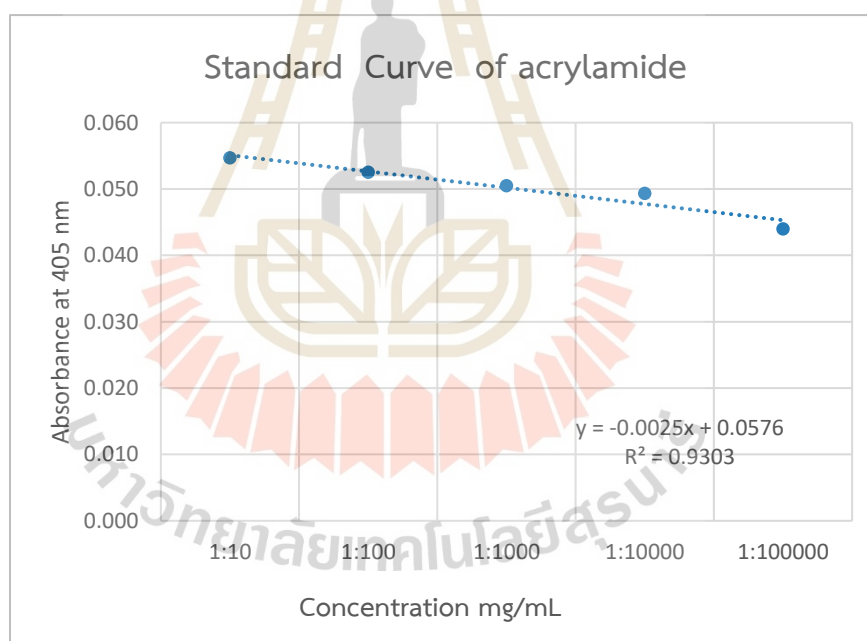


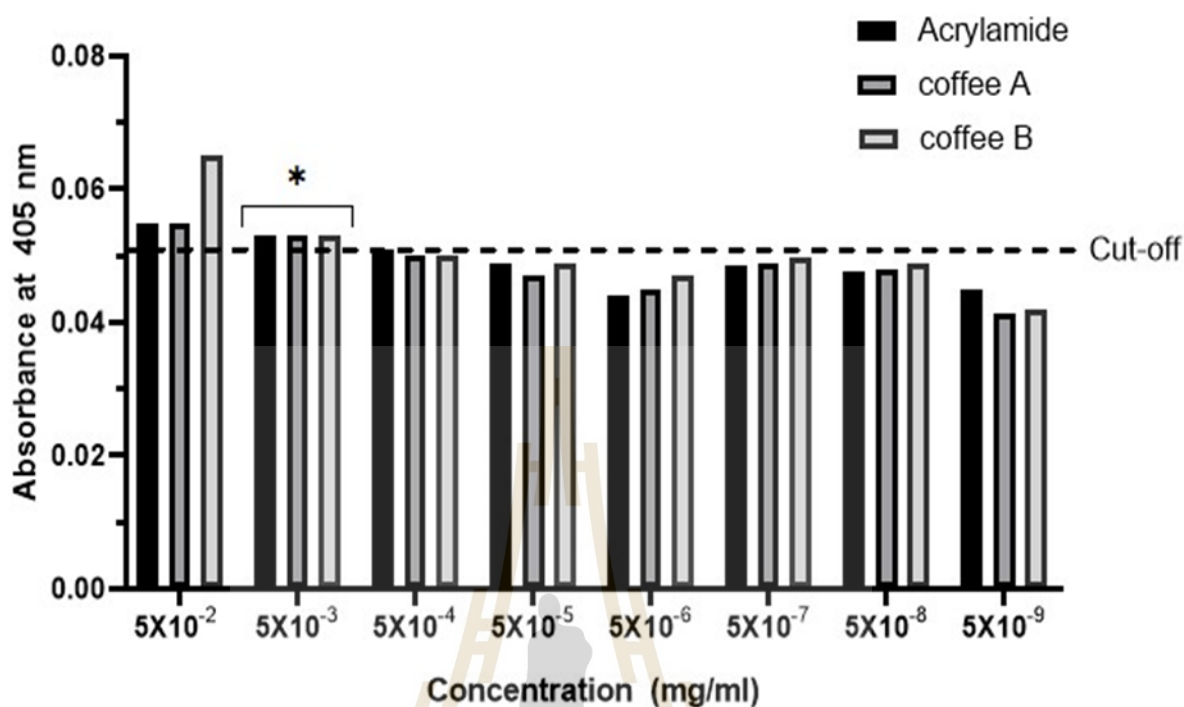
Figure 4.12 Checker broad titration results showed the lowest amount of acrylamide (LOD) was 0.5 mg/ml (black bar) (**) and gave similar OD₄₀₅ concentrations of 0.6 and 0.8 mg/ml, respectively. The lowest amount of anti-AA MuscFv antibody that could be used in ELISA was 0.8 mg/ml (grey bar) (*). Each experiment was performed in triplicate. Values were presented as the means \pm SD.

4.5.2 Determination of the cutoff value of MuscFv-N11.1 by indirect ELISA

After the acrylamide standard's test linearity plot. (Figures 4.13). A illustrates the linear correlation between concentration and area under the peak was found to be linear across the measured concentration range, with an $R^2 = 0.9303$. To establish the cutoff value of the ELISA, the AA standard was 10-folded diluted and analyzed. The mean of the $OD_{405 \text{ nm}}$ values for these samples, as detected by the indirect ELISA, was 0.0510, with a standard deviation of 0.0003, which was calculated using the formula: mean of the negative sample values plus three standard deviations (SDs) (Deshpande,1996) For a 99% confidence interval, the cutoff was defined as follows: mean of the negative serum $OD_{405 \text{ nm}}$ values plus three standard deviations = $0.0510 + 3 \times 0.0003 = 0.0519$. The sensitivity of this in house ELISA was 0.005 mg/ml. as shown in (Figures 4.14).



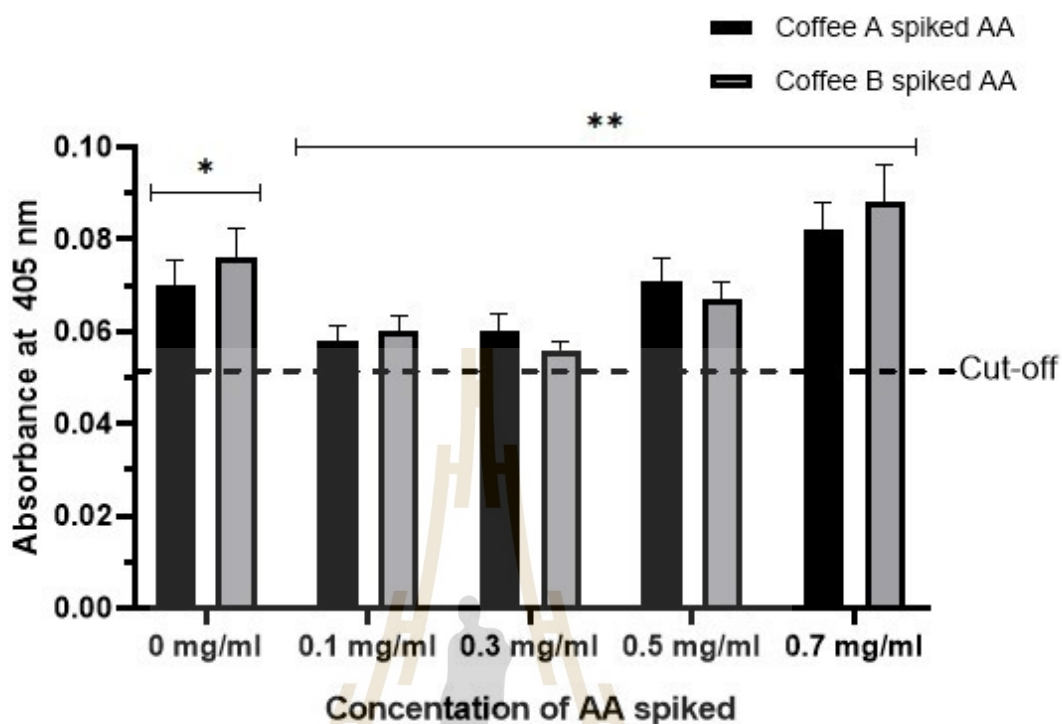
Figures 4.13 Acrylamide standard test linearity plot correlation between concentration and area, with an $R^2 = 0.9303$.



Figures 4.14 The cutoff value of MuscFv-N11.1 specific to acrylamide was performed by the ELISA, the result cutoff value = 0.0519. The sensitivity of this in house ELISA was 0.005 mg/ml (*) (5×10^{-3} mg/ml).

4.5.3 Determination of MuscFv-N11.1 specific to acrylamide in coffee

The determination of MuscFv-N11.1 specific for acrylamide in coffee was performed using ELISA by dark roasted coffee beans containing 2 coffee brands, coffee A and coffee B were spiked with AA standard at concentrations of 0.1, 0.3, 0.5, and 0.7 mg/ml. It was found MuscFv-N11.1 could detect acrylamide in coffee spiked with AA standard. Meanwhile, coffee A and coffee B 0 mg/ml served as the negative controls (NC) were able to detect acrylamide in coffee A and coffee B at similar concentrations (0.5 and 0.7 mg/ml) (**Figures 4.15**). This determination produced a clear gradation of the trend graph in test and control zones.

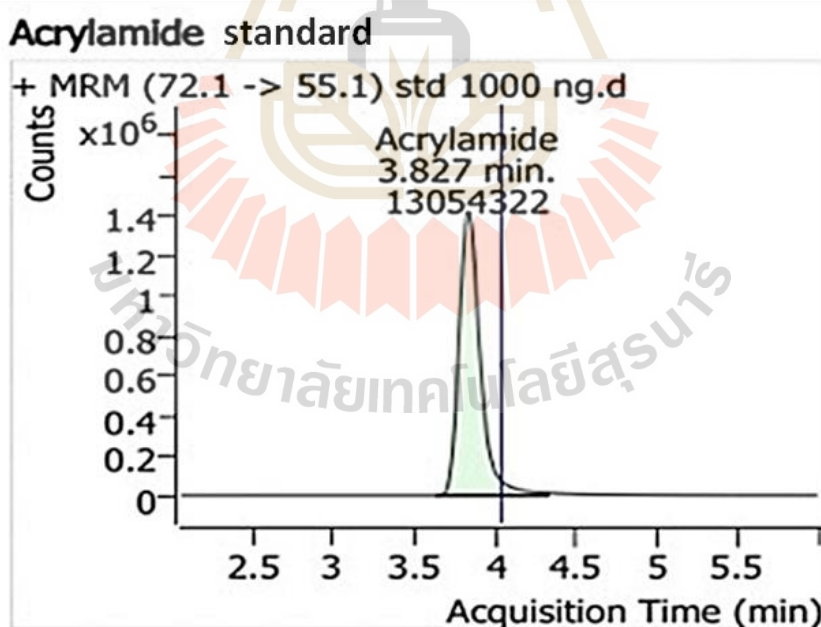


Figures 4.15 The determination of MuscFv-N11.1 specific to acrylamide in coffee was performed using the dark roasted coffee beans containing 2 coffee brands, coffee A (black) and coffee B (grey) spiked with AA standard at concentrations of 0, 0.1, 0.3, 0.5, and 0.7 mg/mL. Furthermore, the non-spiked AA also showed positive results for acrylamide presentation.

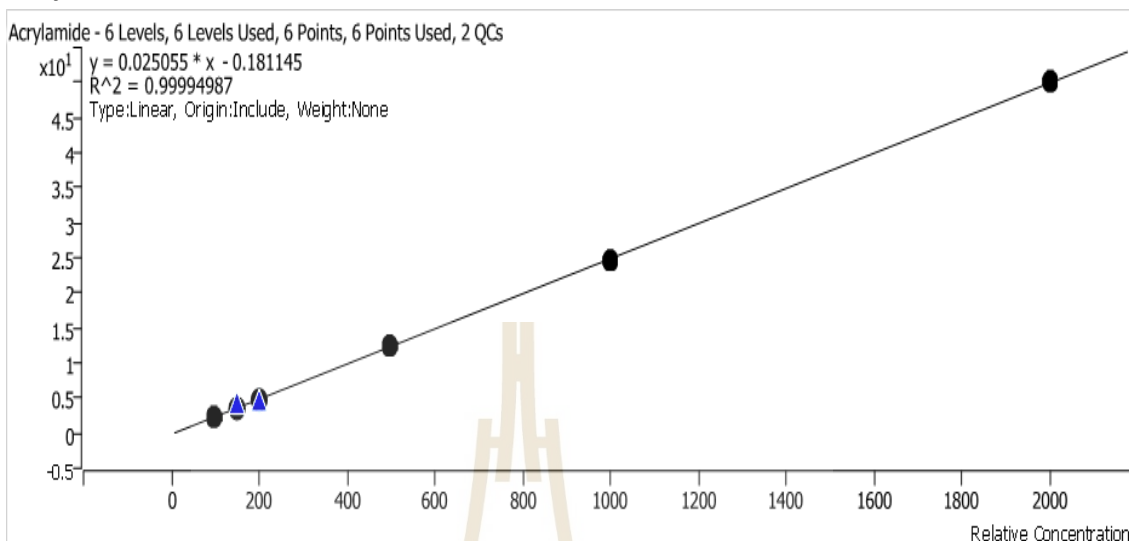
The chromatograms obtained from calibration standard of acrylamide 1000 µg/ml, showing the transition m/z 72.1 > 55.5 and Retention time; RT (RT: 3.827 min) (**Figures 4.16**). The linearity and range tests of the analysis represent the regression equations in the linearity test, such values indicate the ability of the test result to be directly proportional to the AA concentration within a specified range. When injecting 6 levels of AA standard solution in the range of 100-2,000 µg/ml, the relationship between concentration and sub-peak area was linear throughout the tested concentration range, with $y = 0.025055x - 0.181145$, $R^2 = 0.99994987$ indicating that analysis suitability (**Figures 4.17**).

The verified by High-performance liquid chromatography (HPLC) (APPENDIX A). The chromatograms of coffee A1 and coffee B1 were spiked with AA standard at concentrations 0.5 mg/ml showed acrylamide peak and interference corresponding to the calibration standard of acrylamide (RT: 3.840 min), (RT: 3.854 min) respectively (Figures 4.18-4.19). For chromatograms of coffee A2 and coffee B2 were non-spiked with AA standard found that peak acrylamide and interference similar (RT: 3.854 min), (RT: 3.854 min) respectively (Figures 4.20-4.21). Both coffee A and B spiked with AA standard and non-spiked with AA standard cloud detected acrylamide in the dark roasted coffee beans corresponding to an acrylamide standard.

The comparison between the ELISA assay using MuscFv-N11.1 and HPLC methods for the detection of acrylamide in coffee consisting of two coffee brands, coffee A and coffee B were spiked with the AA standard and non-spiked with the AA standard, was performed at similar concentrations of 0.5 mg/ml. The result shows acrylamide could be detected by both methods. Therefore, the conclusion that MuscFv-N11.1 can detect acrylamide in dark roasted coffee beans.

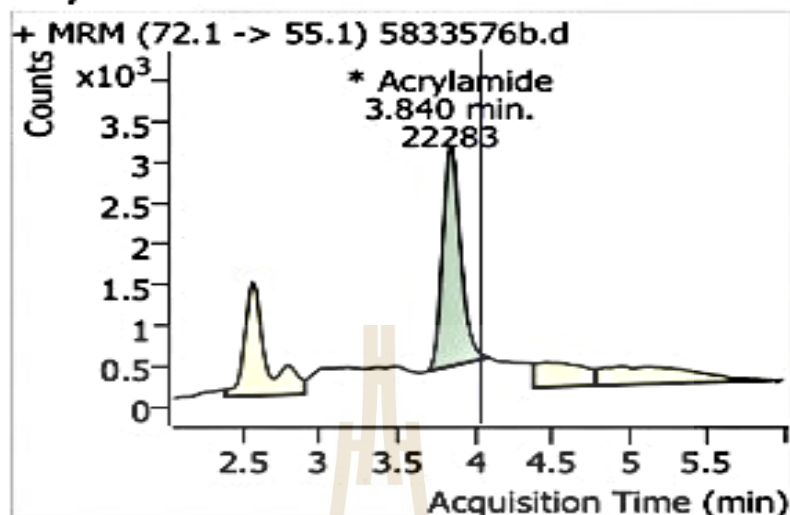


Figures 4.16 Chromatograms of acrylamide standard 1000 ng/ml, (RT: 3.827 min)

Acrylamide %RSE = 2.9

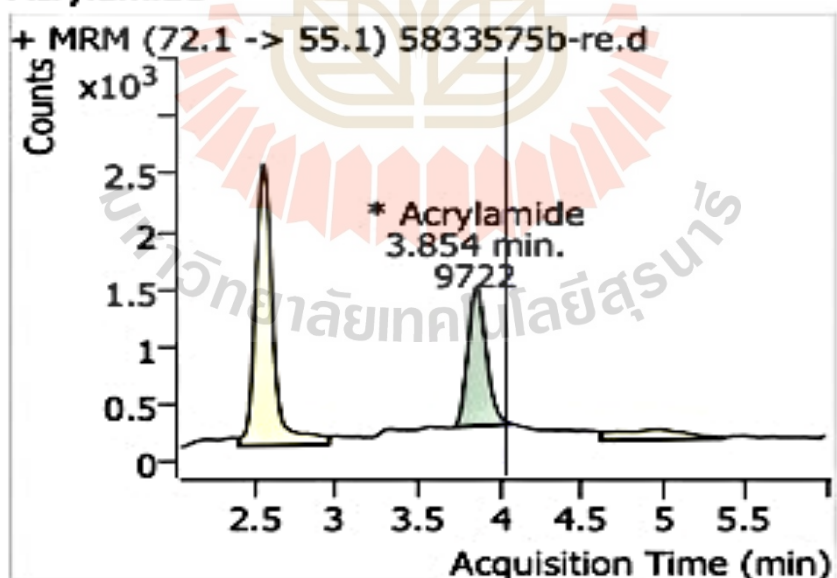
Figures 41.17 Linearity plot for acrylamide standard. For AA standard solution 6 point in the range of 100-2,000 ng/ml, found that the relationship between concentration and sub-peak area was linear throughout the tested concentration range, with $y = 0.025055 * x - 0.181145$ $R^2 = 0.99994987$.

Coffee A 1 Spiked AA Acrylamide



Figures 4.18 Chromatograms of coffee A1 spiked with AA standard at concentrations 0.5 mg/ml showed an acrylamide (RT: 3.840 min) and interference

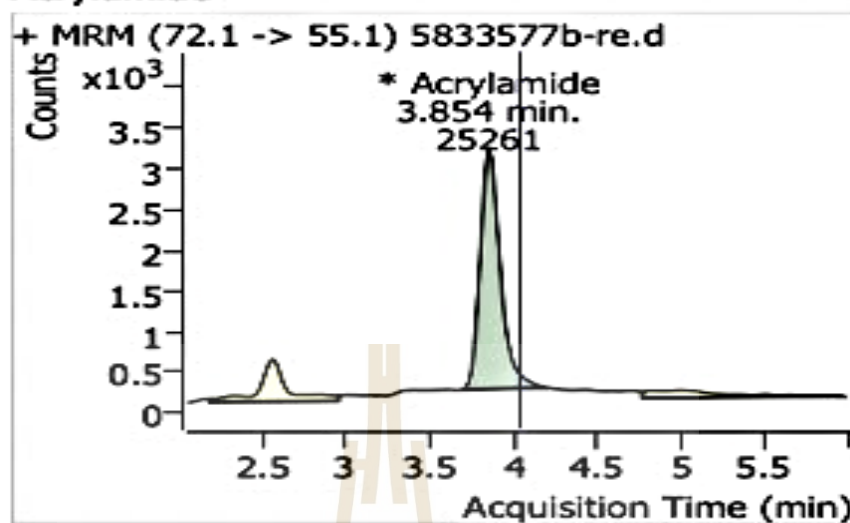
Coffee A 2 Non-spiked AA Acrylamide



Figures 4.19 Chromatograms of coffee A2 non-spiked with AA standard found that an acrylamide (RT: 3.854 min) and interference.

Coffee B 1 Spiked AA

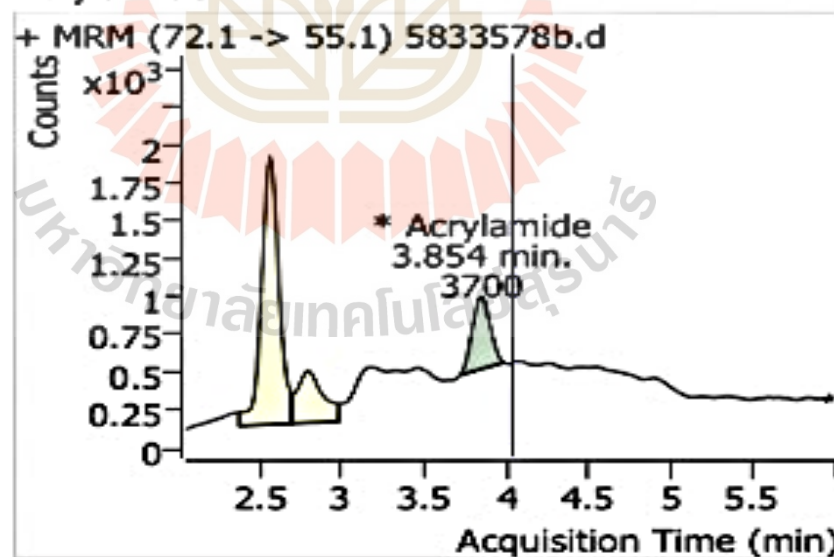
Acrylamide



Figures 4.20 Chromatograms of coffee B1 spiked with AA standard at concentrations of 0.5 mg/ml show acrylamide (RT: 3.854 min) and interference.

Coffee B 2 Non-spiked AA

Acrylamide

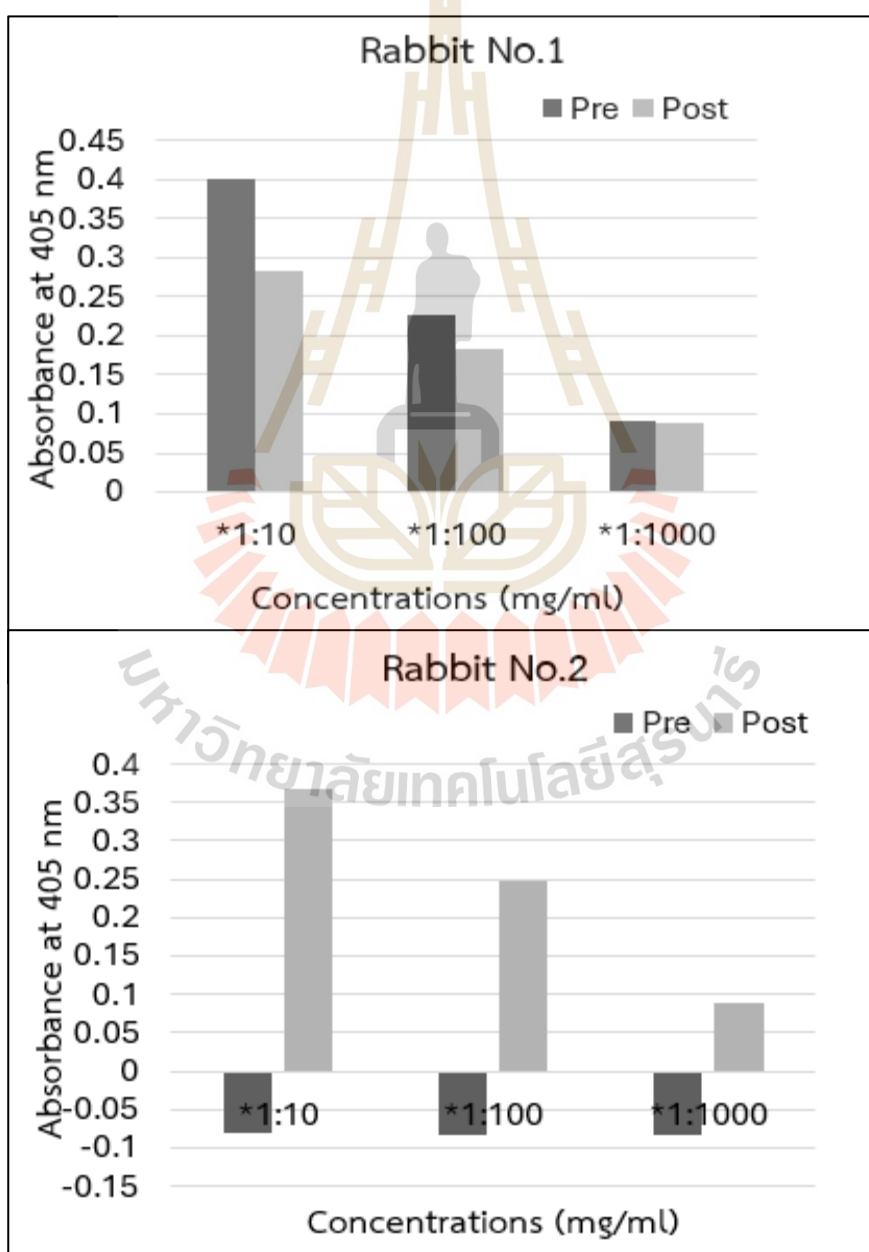


Figures 4.21 Chromatograms of coffee B2 non-spiked with AA standard found that an acrylamide (RT: 3.854 min) showed interference.

4.6 The result of related experiments

4.6.1 Production of polyclonal antibody against acrylamide



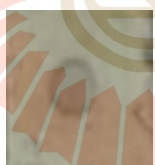

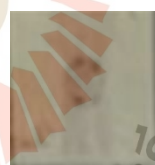
The polyclonal antibody was produced of New Zealand white rabbits two groups. Blood serum samples were checked by broad titration using ELISA. The results showed the lowest amount of polyclonal antibody against acrylamide in rabbit No.1 and rabbit No.2 (Figures 4.22). Due to the very low antibody levels, acrylamide remains undetectable for further experimentation. Consequently, its absence may lead to errors in strip test development.



Figures 4.22 Checker board titration results showed the lowest amount of polyclonal antibody against acrylamide in rabbit No.1 and rabbit No.2. Each experiment was performed in triplicate. Values were presented as the means \pm SD.

4.6.2 Preparation of Glutathione S-transferase conjugation AA standard

Glutathione S-transferase conjugation AA standards were checking binding are Anti-GST, mAb anti- AA and anti- AA form rabbit No.1 by dot blot assay. Each experiment was performed in duplicate. The result showed all antibody binding to GST. The results showed all antibody binding, because acrylamide has a small structure, GST conjugates may obscure its entire structure, potentially leading to false positive results. When used in strip production, acrylamide in coffee cannot be detected.

Anti-GST	mAb Anti- AA	Anti- AA rabbit No.1
		
		

Figures 4.23 Glutathione S-transferase conjugation AA standards were checking binding anti-GST, mAb anti- AA and anti- AA form rabbit No.1 by dot blot assay.

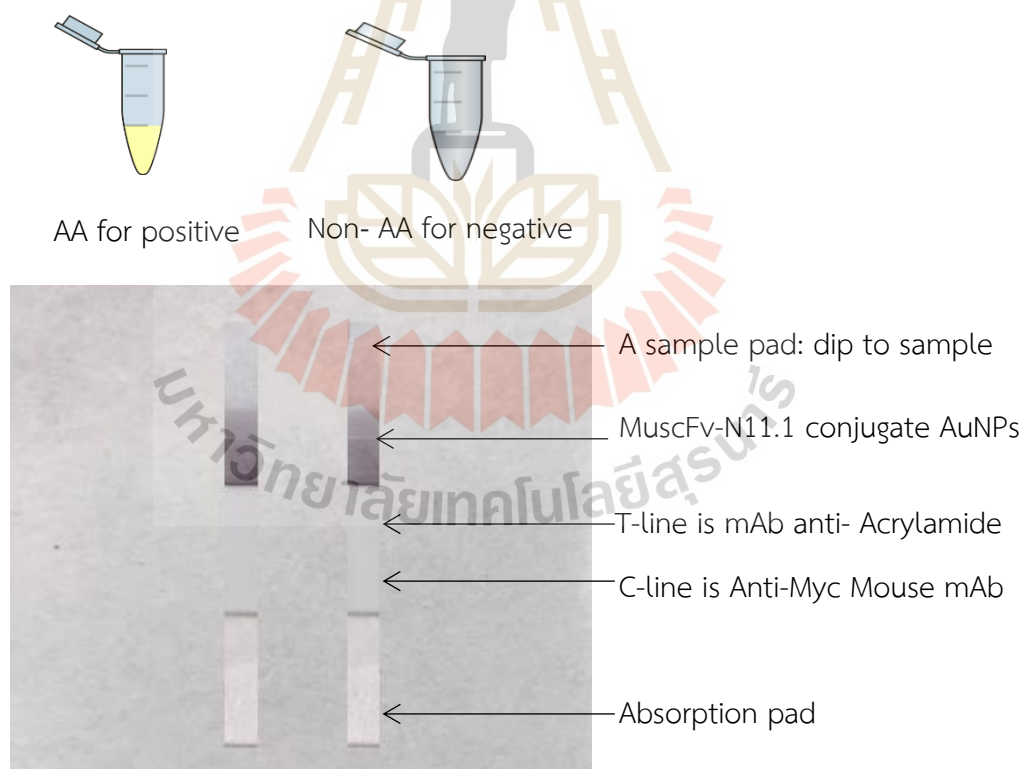
4.6.3 Production of AuNPs conjugation MuscFv- anti AA

The result of application of AuNPs– MuscFv- N11.1 conjugates as probes in immunochromatographic strip tests not allowed detection of AA in coffee samples (data not shown). The size of the AuNPs will affect the sensitivity of the gold nanoparticle immunochromatographic strip. In this study, were not verified with a transmission electron microscope (TEM). However, the availability of strip dependent on pH, which must be optimized for conjugation. In addition, pH controls are required

to avoid nanoparticle aggregation. Thus, antibody molecules are not sufficiently adsorbed onto the surfaces of nanoparticles.

4.6.4 Preparation of immunochromatographic strip test for AA detection

Immunochromatographic strip tests were assembled from sample pads, conjugated pads were made of fiber glass spiked with MuscFv- anti AA conjugate colloid gold nanoparticles (AuNP). Test zones were spiking nitrocellulose membrane of mAb anti- acrylamide and control zones spiked with anti-Myc Mouse mAb and absorbent pads. The sample pads are dipped into an acrylamide (AA) solution for the positive group, whereas the control group employs a solution that does not contain acrylamide and then incubating for 15 min. The results indicate the absence of bands in both groups. In this experiment, several trials should be conducted to determine the optimal amount of spiked antibody applied to the test line, control line, and sample flows, which will facilitate the development of a colored band through binding.



Figures 4.24 The results from the immunochromatographic strip tests showed the absences of bands in both groups.

4.7 Discussion

An acrylamide belongs to a group of toxins that is harmful to human and animal health, due to both acute and chronic effects, including neurotoxicity, genotoxicity, carcinogenicity, reproductive toxicity, hepatotoxicity, and immunotoxicity (Rifai & Saleh, 2020). The presence of acrylamide was found predominantly in heat-treated carbohydrate-rich foods, such as potatoes, biscuits, cereals, and coffee; announced by the Swedish National Food Administration in April 2002 (Taeymans et al., 2004). The European Food Safety Authority (EFSA) has determined an estimated dosage range within which the substance is likely to cause potential health effects. Acrylamide has been estimated to range from 425 for average adult consumers down to 50 for high consuming toddlers. In coffee determined it to 400 $\mu\text{g}/\text{kg}$ for roasted coffee and not more than 850 $\mu\text{g}/\text{kg}$ for instant coffee (D. Benford et al., 2022). Among a variety of established methodologies for analyzing acrylamide, namely high-performance liquid chromatography (HPLC) (Gökmen et al., 2005), gas chromatography coupled with mass spectrometry (GC-MS) (Lee et al., 2007; Shin et al., 2010) and immunoassay (Zhou et al., 2008) etc. were described. The immunological methods are among the most rapid, simplest, cheapest, and most suitable for on-lab screening.

ELISA, a rapid method based on the recognition of antigen-antibody binding with high specificity and affinity, utilizes optical detection of colored products catalyzed by enzyme labels. Due to its specificity and affinity, coupled with efficient enzymatic catalysis, ELISA methods offer optimal recovery and adaptability for detecting AA in various food samples, including Chocolate products, Cocoa powder, Nuts, French fries, roast potatoes, potato crisps/chips, biscuits, baked, and toasted (Rifai & Saleh, 2020). They advantage such as affordability, simplicity, ease of handling, and portability, proving particularly effective in identifying AA in thermally processed foods (Quan et al., 2011b). ELISA also demonstrates good sensitivity, selectivity, high-throughput capabilities, and compatibility with other technologies like biotin-avidin amplification and chemiluminescence, thus attracting increased attention for AA detection in foods (Liang et al., 2022). However, the multiple washing and incubation steps in ELISA extend the detection process, making it more suitable for primary screening of food products with excessively high AA concentrations during processing

or on the market. In comparison, standard methods like LC-MS/MS and GC-MS provide rapid detection, meeting the needs of food industries, regulatory bodies, and consumers (Desmarchelier et al., 2020). Nevertheless, they require further refinement to enhance accuracy, sensitivity, repeatability, reproducibility, multi-step, and portability for achieving online and real-time detection of trace amounts of AA (Aykas et al., 2022).

In this study, mouse variable heavy and light chain formed of MuscFv-N11.1 was selected from *muscfv*-phage library. The *muscfv*-phage library size utilized in this experiment with substantial antibody sequence diversity, which was comparable to the other non-immune libraries previously reported (Thanongsaksrikul et al., 2010, 2018; Thattanon et al., 2020). Similarly, a related study using immunized phage display library a specific nanobody termed Nb-7E against an acrylamide derivative xanthyl acrylamide (XAA) was isolated from an immunized phage display library and confirmed to be able to detect acrylamide (Liang et al., 2022). MuscFv-N11.1 was found to be specific to acrylamide by using established ELISA. The result confirmed by HPLC that both bands of coffee have acrylamide. The chromatograms showed acrylamide peak and interference corresponding to an acrylamide calibration standard with a retention time of 3.8 min. Similarly, a study in-depth study of acrylamide formation in coffee during roasting: role of sucrose decomposition and lipid oxidation using determination of acrylamide in coffee by liquid chromatography - tandem mass spectrometry. Acrylamide peak showed retention time of 2-3.1 min (Kocadağlı et al., 2012). Corresponding to study determination of acrylamide after its extraction from potato chips was acrylamide spiked in chips sample and analyzed using ultrasound-assisted liquid-liquid extraction (UA-LLE) technique / HPLC-UV showed acrylamide peak at retention time of 4.15 min (Ghalebi et al., 2019). Computerized docking models showed that MuscFv-N11.1 used VH domain (D-58, D-60 and Y-105) to interact with acrylamide via hydrogen bond. The binding efficacy of MuscFv-N11.1 to acrylamide was less than 0.005 mg/mL.

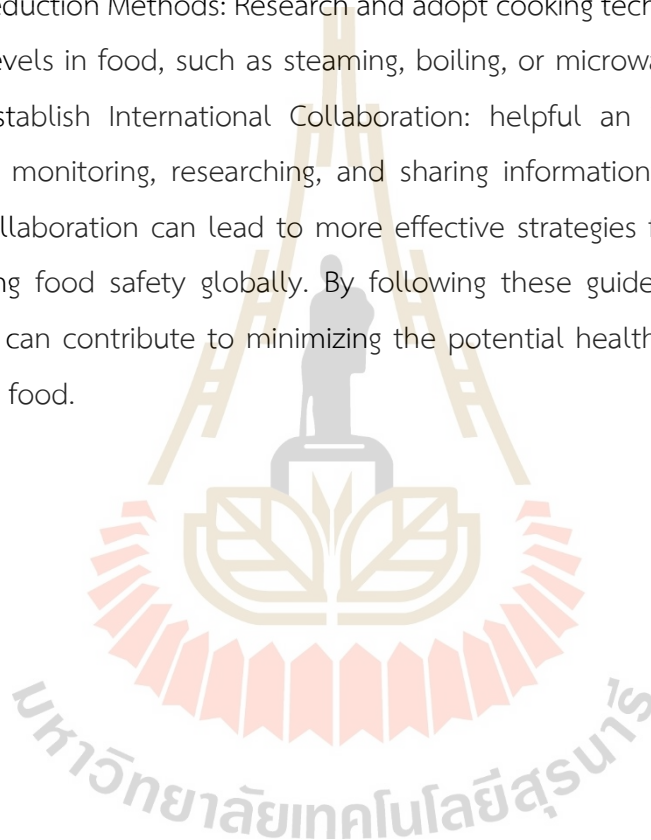
This work could involve future applications aimed at determining the amount of acrylamide intake that may potentially cause cancer in humans. Since acrylamide has a carcinogenic potency in rats that is similar to that of other carcinogens in food,

the intake levels for acrylamide are likely to be higher. For humans, the relative potencies of cancer-causing agents in food are not known. Only limited human population data are available for acrylamide and these provide no evidence of cancer risk from occupational exposure. All such studies have limited power to detect small increases in tumor incidence. The consultation recognized the presence of acrylamide in food as a major concern in humans based on the ability to induce cancer and heritable mutations in laboratory animals.

The FAO/WHO announced exposure assessment based on the available data, food is estimated to make a significant contribution to total exposure of the general public to acrylamide. Average intakes for the general population were estimated to be in the range of 0.3 to 0.8 microgram of acrylamide intake per kilogram of body weight per day. Within a population, it is anticipated that children will generally have intakes that are two to three times those of adults when expressed on a body weight basis. Dietary intakes of acrylamide by some consumers may be several times higher than the average. Developing and other countries with insufficient information for determining population level dietary exposures to acrylamide should consider generating interim information relevant to their own circumstances. This could include analyzing total diet study samples, where they are available, for acrylamide, as the basis for estimating per capita dietary intake estimate; determining levels of acrylamide in a limited range of staple foods prepared in ways that reflect common domestic practice for future policy. In the case, limit allowable amounts of acrylamide in food. If it is shown that acrylamide has harmful effects on humans, the policy will assist food. If efforts to reduce or eliminate acrylamides are not successful, the FDA may require warning labels on foods. Such labels would inform consumers of the risks of acrylamide and could dissuade consumers from purchasing foods with high acrylamide level.

However, acrylamide has been found in certain foods that have been cooked and processed at high temperatures, and the levels of acrylamide increase with the time of heating. Advice to minimize the risks associated with acrylamide in food. Firstly, avoid excessive cooking: reduce cooking methods that promote the formation of acrylamide, such as frying, baking, and roasting at high temperatures for prolonged

periods. In coffee it was demonstrated that roasting process had the most significant effect on acrylamide levels in natural coffee, however there were no relationships found with coffee species. Due to the high acrylamide levels demonstrated in coffee substitutes, recommended amounts should be defined and manufacturers should be obliged to reduce such levels in these products. Second, choose healthy eating practices: choose to use a balanced diet rich in fruits, vegetables, whole grains, and lean proteins, which can help mitigate potential risks associated with acrylamide. Investigate Reduction Methods: Research and adopt cooking techniques that can lower acrylamide levels in food, such as steaming, boiling, or microwaving instead of frying or baking. Establish International Collaboration: helpful an international network dedicated to monitoring, researching, and sharing information about acrylamide in food. This collaboration can lead to more effective strategies for reducing exposure and enhancing food safety globally. By following these guidelines, individuals and organizations can contribute to minimizing the potential health risks associated with acrylamide in food.



CHAPTER 5

CONCLUSION AND RECOMMENDATION

5.1 Conclusion

Single-chain fragment variable (scFv) antibody format is preferred than intact antibodies due to its smaller size and less possibility of developing anti-mouse antibody response. In general, monoclonal antibody especially scFv antibody for diagnostic purposes can bind to a variety of antigens such as haptens, proteins, and whole pathogens, and they can as well be used in the enzyme-linked immunosorbent assay (ELISA). Besides, it is possible to be designed as bispecific antibody to work as immunotoxin. It thus makes scFv the best candidate for medical, diagnostic and research applications. This study aims to produce MuscFv-antibody against and develop Enzyme-linked immunosorbent assay (ELISA), that could detect acrylamide substances in coffee. The materials, methods, and results of the summarized as the followings

For the discovery of novel antibodies, the first identification of phage clone displaying MuscFv that bound to AA. After bio-panning, 23 clones of the *E. coli* colony containing recombinant phagemid *muscfv* vector were individually picked for direct colony PCR. The *E. coli* clones which carried the plasmid with the *muscfv* inserts gave 15 clone (65.2%) were positive PCR amplicon at the associate sizes ~750 -900 bp. The selection for phage transformed *E. coli* clones that carried recombinant phagemids with the inserted murine scFv (*MuscFv*)-coding sequences. Identification of positive phage clones checked for the presence of the murine scFv (*MuscFv*) against AA by PCR using sequencing specific primers. The result of positive clone, five clones (21.7%) giving positive PCR band at associate sizes ~750 -900 bp. Moreover, the results of indirect ELISA for determining binding of *muscfv*-AA phage. In lysate of 23 randomly selected scFv phagemid, there were indirect ELISA positive clones (i.e., clones N11, N30, N32, N36) that gave ELISA signal and were selected clone for further experiment.

For the MuscFv construct design process sub-cloning of *muscfv*- AA phage from pSEX81 vector to pOPE101 vector. Clone number 11 was selection for phage transformed *E. coli* clones that carried recombinant phagemids with the inserted murine scFv (*MuscFv*)-coding sequences. clones number 11 were doubly digested with

specific restriction enzymes. Then DNA ligation and transformation for sub-clone into pOPE101 vector for large scale recombinant protein expression and purification. Colony directed PCR screening showed four positive PCR amplicon (N11.1, N11.2, N11.3 and N11.4) from 7 colonies screening (71.4%). To obtain the MuscFv antibody, expression and purification of anti-AA MuscFv. The *E. coli* clones which were positive for pOPE101 with *MuscFv* were checked for their ability to express the antibody protein. There were 4 positive clones (clones N11.1, N11.2, N11.3 and N11.4) (71.4 %) that expressed soluble anti-AA MuscFv antibodies of all 4 clones showed the positive band at the expected molecular mass (~25-30 kDa) as determined by WB. The purified anti-AA MuscFv antibodies are bound specifically to acrylamide. Clone number 11.1 (MscFv-N11.1) was selected for protein expression. After large- scale expression, the bacteria were purified by using the Ni-NTA affinity resin under native condition. The purified proteins were checked by SDS-PAGE and Coomassie staining of the purified MuscFv-N11.1 protein (~25-30 kDa). The ELISA binding check MuscFv-N11.1 VS BSA. The result found MuscFv-N11.1 showed statistically significant specific binding of MuscFv to acrylamide when compared with BSA ($P < 0.001$).

For characterization and Homology modeling and intermolecular docking. Firstly, determination of complementary determining regions (CDRs) and immunoglobulin framework regions (FRs) of the MuscFv-N11.1. The deduced amino acid sequences of the MuscFv-N11.1 *E. coli* clones were found to be complete sequences of antigen-binding domains of antibodies. The deduced amino acid (aa) sequence of MuscFv-N11.1 was shown including the VH and VL domains joined by a (Glu4 Gly1 Phe1 Ser1) linker, the complementary determining region 1-3 (CDR1-3). The molecular docking model of MuscFv-N11.1 was performed. Ribbon display model showing MuscFv-N11.1 in blue, green, gray and red. MuscFv-N11.1 used D-58, D-60 and Y-105 of VH domain to interact with acrylamide via hydrogen bond (energy range -12.89 kcal/mol).

For validation of AA standard and MuscFv-N11.1 antibody. The checker board titration was used to determine the lowest amount of acrylamide detected (limit of detection: LOD) and the lowest amount of MuscFv-N11.1 used in the ELISA. A concentration of 0.5 mg/mL was found to be the lowest concentration that could be detected and gave similar OD_{405} nm as the concentration 0.6 and 0.8 mg/mL, respectively. Whereas the lowest amount of Anti-AA muscFv antibody was 0.8 mg/mL. Acrylamide standard test linearity plot correlation between concentration and area,

with an $R^2 = 0.9303$. To establish the cutoff value of the ELISA, the AA standard was 10-folded diluted and analyzed. The mean of the OD_{405} nm values for these samples, as detected by the indirect ELISA, the result cutoff value = 0.0519. The sensitivity of this in house ELISA was 0.005 mg/ml (5×10^{-3} mg/ml).

For determination of MuscFv-N11.1 specific to acrylamide in coffee was performed using the dark roasted coffee beans containing 2 coffee brands, coffee A (black) and coffee B (grey) spiked with AA standard at concentrations of 0, 0.1, 0.3, 0.5, and 0.7 mg/mL. The result of non-spike AA also showed positive results for acrylamide presentation. In addition, the verified by High-performance liquid chromatography (HPLC). Chromatograms of acrylamide standard 1000 ng/ml, AA-spiked coffee A and B and non-AA-spiked; All could detect acrylamide in these 2 brands of coffee. Coffee contains many other chemicals that may be beneficial to your health. Cutting it out isn't necessary. Coffee hasn't been shown to increase your risk of cancer. In fact, it has been linked to a reduced risk of some types of cancers, such as liver cancer (Larsson & Wolk, 2007). Completely avoiding acrylamide is impossible. However, you can make a few changes to reduce your acrylamide intake. Instant coffee contains up to twice as much acrylamide as regular coffee, but this amount is still lower than the amount considered to be harmful (Andrzejewski et al., 2004b).

Conclusion of this study, the selection of antibodies against acrylamide from muscFv phage-displayed library was performed in order to select used by acrylamide standard: AA used as antigen for bio-panning were expressed and purified to be specific for acrylamide contaminated in food. Anti-AA MuscFv against acrylamide was produced, and an indirect ELISA was developed for the determination of coffee. The application to samples from coffee indicated that ELISA may be used for the estimation of total acrylamide concentrations. The method has shown satisfactory results in terms of specificity and accuracy, which were confirmed by high-performance liquid chromatography (HPLC).

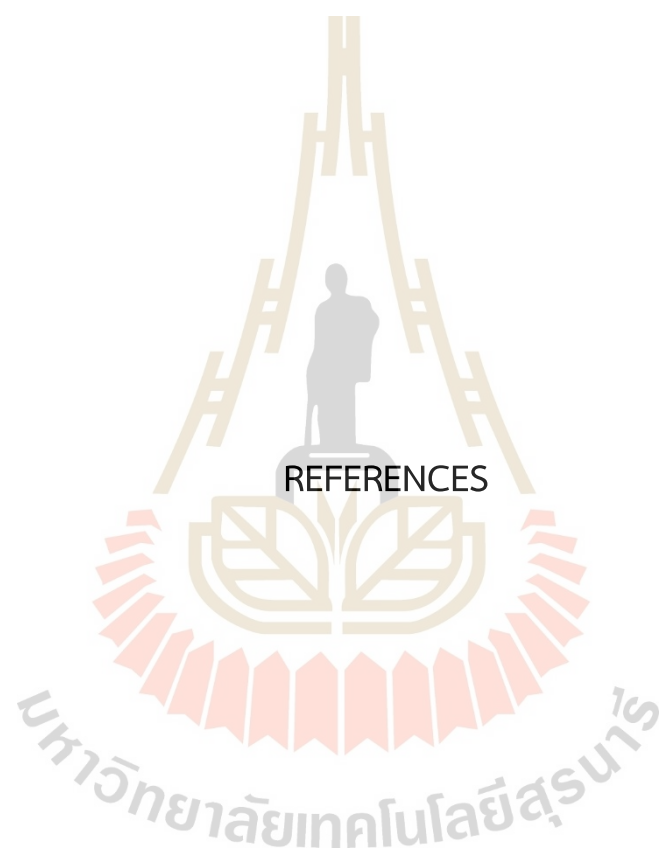
5.2 Recommendation

The current study represents an initial effort to produce Muscfv antibodies specific to acrylamide using phage bio-panning successfully.

Future studies should progress towards developing an immunochromatographic strip test that would allow sensitive, specific, rapid and simultaneous detection of all food. However, given acrylamide's small molecular size, efforts should concentrate on enlarging it to aid in test kit development.

In the future, there should be a study to determine the amount of acrylamide intake that can potentially cause cancer in humans.





REFERENCES

REFERENCES

- Aga, D. S., Goldfish, R., & Kulshrestha, P. (2003). Application of ELISA in determining the fate of tetracyclines in land-applied livestock wastes. *The Analyst*, *128*(6), 658. <https://doi.org/10.1039/b301630g>
- Akgün, B., & Arıcı, M. (2019). Evaluation of acrylamide and selected parameters in some Turkish coffee brands from the Turkish market. *Food Additives & Contaminants: Part A*, *36*(4), 548–560. <https://doi.org/10.1080/19440049.2019.1586454>
- Aktaş, I. G., Hamzalıoğlu, A., Kocadağlı, T., & Gökmen, V. (2022). Dietary exposure to acrylamide: A critical appraisal on the conversion of disregarded intermediates into acrylamide and possible reactions during digestion. *Current Research in Food Science*, *5*, 1118–1126. <https://doi.org/10.1016/j.crfs.2022.07.004>
- Alamri, E., Rozan, M., & Bayomy, H. (2022). A study of chemical Composition, Antioxidants, and volatile compounds in roasted Arabic coffee. *Saudi Journal of Biological Sciences*, *29*(5), 3133–3139. <https://doi.org/10.1016/j.sjbs.2022.03.025>
- AlKarim, S., ElAssouli, S., Ali, S., Ayuob, N., & ElAssouli, Z. (2015). Effects of low dose acrylamide on the rat reproductive organs structure, fertility and gene integrity. *Asian Pacific Journal of Reproduction*, *4*(3), 179–187. <https://doi.org/10.1016/j.apjr.2015.05.001>
- Amzel, L. M., & Poljak, R. J. (1979). Three-Dimensional Structure of Immunoglobulins. *Annual Review of Biochemistry*, *48*(1), 961–997. <https://doi.org/10.1146/annurev.bi.48.070179.004525>
- Andrzejewski, D., Roach, J. A. G., Gay, M. L., & Musser, S. M. (2004a). Analysis of Coffee for the Presence of Acrylamide by LC-MS/MS. *Journal of Agricultural and Food Chemistry*, *52*(7), 1996–2002. <https://doi.org/10.1021/jf0349634>
- Andrzejewski, D., Roach, J. A. G., Gay, M. L., & Musser, S. M. (2004b). Analysis of Coffee for the Presence of Acrylamide by LC-MS/MS. *Journal of Agricultural and Food Chemistry*, *52*(7), 1996–2002. <https://doi.org/10.1021/jf0349634>
- Anfossi, L., Calderara, M., Baggiani, C., Giovannoli, C., Arletti, E., & Giraudi, G. (2008). Development and Application of Solvent-free Extraction for the Detection of

- Aflatoxin M₁ in Dairy Products by Enzyme Immunoassay. *Journal of Agricultural and Food Chemistry*, 56(6), 1852–1857. <https://doi.org/10.1021/jf073133d>
- Arap, M. A. (2005). Phage display technology: applications and innovations. *Genetics and Molecular Biology*, 28(1), 1–9. <https://doi.org/10.1590/S1415-47572005000100001>
- Asnaashari, M., Kenari, R. E., Farahmandfar, R., Abnous, K., & Taghdisi, S. M. (2019). An electrochemical biosensor based on hemoglobin-oligonucleotides-modified electrode for detection of acrylamide in potato fries. *Food Chemistry*, 271, 54–61. <https://doi.org/10.1016/j.foodchem.2018.07.150>
- Aydin, S. (2015a). A short history, principles, and types of ELISA, and our laboratory experience with peptide/protein analyses using ELISA. *Peptides*, 72, 4–15. <https://doi.org/10.1016/j.peptides.2015.04.012>
- Aydin, S. (2015b). A short history, principles, and types of ELISA, and our laboratory experience with peptide/protein analyses using ELISA. *Peptides*, 72, 4–15. <https://doi.org/10.1016/j.peptides.2015.04.012>
- Aykas, D. P., Urtubia, A., Wong, K., Ren, L., López-Lira, C., & Rodriguez-Saona, L. E. (2022). Screening of Acrylamide of Par-Fried Frozen French Fries Using Portable FT-IR Spectroscopy. *Molecules*, 27(4), 1161. <https://doi.org/10.3390/molecules27041161>
- Balsam J, et al. (2013). Low cost technologies for medical diagnostics in low-resource settings. *Expert Opin Med Diagn*, 7(3)(PMID 23480559), 243–255. <https://doi.org/doi:10.1517/17530059.2013.767796>.
- Barber, D. S., Hunt, J., LoPachin, R. M., & Ehrich, M. (2001). Determination of acrylamide and glycidamide in rat plasma by reversed-phase high performance liquid chromatography. *Journal of Chromatography B: Biomedical Sciences and Applications*, 758(2), 289–293. [https://doi.org/10.1016/S0378-4347\(01\)00191-8](https://doi.org/10.1016/S0378-4347(01)00191-8)
- Barrios-Rodríguez, Y. F., Gutiérrez-Guzmán, N., Pedreschi, F., & Mariotti-Celis, M. S. (2022). Rational design of technologies for the mitigation of neo-formed contaminants in roasted coffee. *Trends in Food Science & Technology*, 120, 223–235. <https://doi.org/10.1016/j.tifs.2021.12.034>
- Batra, B., Lata, S., Sharma, M., & Pundir, C. S. (2013). An acrylamide biosensor based on immobilization of hemoglobin onto multiwalled carbon nanotube/copper

- nanoparticles/polyaniline hybrid film. *Analytical Biochemistry*, 433(2), 210–217.
<https://doi.org/10.1016/j.ab.2012.10.026>
- Becalski, A., Brady, B., Feng, S., Gauthier, B. R., & Zhao, T. (2011). Formation of acrylamide at temperatures lower than 100°C: the case of prunes and a model study. *Food Additives & Contaminants: Part A*, 28(6), 726–730.
<https://doi.org/10.1080/19440049.2010.535217>
- Benford, D. ; B. M. ; C. J. K. ; R. B. L., D.; Bignam, M.; Chipman, & J.K.; Ramos Bordajandi, L. (2022). Assessment of the genotoxicity of acrylamide. *EFSA J*, 20, e07293. <https://doi.org/doi:10.2903/j.efsa.2022.7293>.
- Benford, D., Bignami, M., Chipman, J. K., & Ramos Bordajandi, L. (2022). Assessment of the genotoxicity of acrylamide. *EFSA Journal*, 20(5).
<https://doi.org/10.2903/j.efsa.2022.7293>
- Bergmark, E. (1997). Hemoglobin Adducts of Acrylamide and Acrylonitrile in Laboratory Workers, Smokers and Nonsmokers. *Chemical Research in Toxicology*, 10(1), 78–84. <https://doi.org/10.1021/tx960113p>
- Bhattacharyya S, K. S. D. M. (2013). Anti-Toxoplasma gondii antibody detection in serum and urine samples by enzyme-linked immunosorbent assay in HIV-infected patients. *Indian J Pathol Microbiol*, 56(1), 20–23. <https://doi.org/doi:10.4103/0377-4929.116143>.
- Bird, R. E., Hardman, K. D., Jacobson, J. W., Johnson, S., Kaufman, B. M., Lee, S.-M., Lee, T., Pope, S. H., Riordan, G. S., & Whitlow, M. (1988). Single-Chain Antigen-Binding Proteins. *Science*, 242(4877), 423–426.
<https://doi.org/10.1126/science.3140379>
- Bjellaas, T., Ølstørn, H. B. A., Becher, G., Alexander, J., Knutsen, S. H., & Paulsen, J. E. (2007). Urinary Metabolites as Biomarkers of Acrylamide Exposure in Mice Following Dietary Crisp Bread Administration or Subcutaneous Injection. *Toxicological Sciences*, 100(2), 374–380. <https://doi.org/10.1093/toxsci/kfm234>
- Cai, Y., Zhang, Z., Jiang, S., Yu, M., Huang, C., Qiu, R., Zou, Y., Zhang, Q., Ou, S., Zhou, H., Wang, Y., Bai, W., & Li, Y. (2014). Chlorogenic acid increased acrylamide formation through promotion of HMF formation and 3-aminopropionamide deamination. *Journal of Hazardous Materials*, 268, 1–5.
<https://doi.org/10.1016/j.jhazmat.2013.12.067>

- Canady J, A. S. K. S. B. A. (2013). Increased KGF expression promotes fibroblast activation in a double paracrine manner resulting in cutaneous fibrosis. *J Invest Dermatol*, 133(3), 647–657. <https://doi.org/doi:10.1038/jid.2012.389>.
- Caporaso, N., Whitworth, M. B., & Fisk, I. D. (2022). Prediction of coffee aroma from single roasted coffee beans by hyperspectral imaging. *Food Chemistry*, 371, 131159. <https://doi.org/10.1016/j.foodchem.2021.131159>
- Capuano, E., & Fogliano, V. (2011). Acrylamide and 5-hydroxymethylfurfural (HMF): A review on metabolism, toxicity, occurrence in food and mitigation strategies. *LWT - Food Science and Technology*, 44(4), 793–810. <https://doi.org/10.1016/j.lwt.2010.11.002>
- Caro Perez A, et al. (2014). Evaluation of a multiplex ELISA for autoantibody profiling in patients with autoimmune connective tissue diseases. *Autoimmune Dis*, PMID 24527209, 896787. <https://doi.org/doi:10.1155/2014/896787>.
- Carterette, B. A. (2012). Multiple testing in statistical analysis of systems-based information retrieval experiments. *ACM Transactions on Information Systems*, 30(1), 1–34. <https://doi.org/10.1145/2094072.2094076>
- Cheng, J., Zhang, S., Wang, S., Wang, P., Su, X.-O., & Xie, J. (2019). Rapid and sensitive detection of acrylamide in fried food using dispersive solid-phase extraction combined with surface-enhanced Raman spectroscopy. *Food Chemistry*, 276, 157–163. <https://doi.org/10.1016/j.foodchem.2018.10.004>
- Cho, J.-H., Paek, E.-H., Cho, I.-H., & Paek, S.-H. (2005). An Enzyme Immunoanalytical System Based on Sequential Cross-Flow Chromatography. *Analytical Chemistry*, 77(13), 4091–4097. <https://doi.org/10.1021/ac048270d>
- Cong, S., Dong, W., Zhao, J., Hu, R., Long, Y., & Chi, X. (2020). Characterization of the Lipid Oxidation Process of Robusta Green Coffee Beans and Shelf Life Prediction during Accelerated Storage. *Molecules*, 25(5), 1157. <https://doi.org/10.3390/molecules25051157>
- Coreta-Gomes, F. M., Lopes, G. R., Passos, C. P., Vaz, I. M., Machado, F., Geraldês, C. F. G. C., Moreno, M. J., Nyström, L., & Coimbra, M. A. (2020). In Vitro Hypocholesterolemic Effect of Coffee Compounds. *Nutrients*, 12(2), 437. <https://doi.org/10.3390/nu12020437>

- Corrêa, C. L. O., das Mercedes Penha, E., dos Anjos, M. R., Pacheco, S., Freitas-Silva, O., Luna, A. S., & Gottschalk, L. M. F. (2021). Use of asparaginase for acrylamide mitigation in coffee and its influence on the content of caffeine, chlorogenic acid, and caffeic acid. *Food Chemistry*, *338*, 128045. <https://doi.org/10.1016/j.foodchem.2020.128045>
- Davies, D. R., Padlan, E. A., & Segal, D. M. (1975a). Three-Dimensional Structure of Immunoglobulins. *Annual Review of Biochemistry*, *44*(1), 639–667. <https://doi.org/10.1146/annurev.bi.44.070175.003231>
- Davies, D. R., Padlan, E. A., & Segal, D. M. (1975b). Three-Dimensional Structure of Immunoglobulins. *Annual Review of Biochemistry*, *44*(1), 639–667. <https://doi.org/10.1146/annurev.bi.44.070175.003231>
- Delatour, T., Huertas-Pérez, J. F., Dubois, M., Theurillat, X., Desmarchelier, A., Ernest, M., & Stadler, R. H. (2020). Thermal degradation of 2-furoic acid and furfuryl alcohol as pathways in the formation of furan and 2-methylfuran in food. *Food Chemistry*, *303*, 125406. <https://doi.org/10.1016/j.foodchem.2019.125406>
- Desmarchelier, A., Hamel, J., & Delatour, T. (2020). Sources of overestimation in the analysis of acrylamide in coffee by liquid chromatography mass spectrometry. *Journal of Chromatography A*, *1610*, 460566. <https://doi.org/10.1016/j.chroma.2019.460566>
- Dobrovolskaia E, G. A. S. J. et al. (2006). Competition enzyme-linked immunosorbant assay (ELISA) can be a sensitive method for the specific detection of small quantities of allergen in a complex mixture. *Clin Exp Allergy*, *36*(4)(525–30). <https://doi.org/doi:10.1111/j.1365-2222.2006.02466.x>
- Dybing, E., Farmer, P. B., Andersen, M., Fennell, T. R., Lalljie, S. P. D., Müller, D. J. G., Olin, S., Petersen, B. J., Schlatter, J., Scholz, G., Scimeca, J. A., Slimani, N., Törnqvist, M., Tuijelaars, S., & Verger, P. (2005a). Human exposure and internal dose assessments of acrylamide in food. *Food and Chemical Toxicology*, *43*(3), 365–410. <https://doi.org/10.1016/j.fct.2004.11.004>
- Dybing, E., Farmer, P. B., Andersen, M., Fennell, T. R., Lalljie, S. P. D., Müller, D. J. G., Olin, S., Petersen, B. J., Schlatter, J., Scholz, G., Scimeca, J. A., Slimani, N., Törnqvist, M., Tuijelaars, S., & Verger, P. (2005b). Human exposure and internal

- dose assessments of acrylamide in food. *Food and Chemical Toxicology*, 43(3), 365–410. <https://doi.org/10.1016/j.fct.2004.11.004>
- Endo, Y., Hayashi, C., T.; Takayose, K.; Yamaoka, M.; Tsuno, & T.; Nakajima, S. (2013). Linolenic acid as the main source of acrolein formed during heating of vegetable oils. *J. Am. Oil Chem. Soc*, 90, 959–964. <https://doi.org/doi.10.1007/s11746-013-2242-z>
- Feige, M. J., Hendershot, L. M., & Buchner, J. (2010). How antibodies fold. *Trends in Biochemical Sciences*, 35(4), 189–198. <https://doi.org/10.1016/j.tibs.2009.11.005>
- Fennell, T. R., Sumner, S. C. J., Snyder, R. W., Burgess, J., & Friedman, M. A. (2006). Kinetics of Elimination of Urinary Metabolites of Acrylamide in Humans. *Toxicological Sciences*, 93(2), 256–267. <https://doi.org/10.1093/toxsci/kfl069>
- Figuroa Campos, G. A., Sagu, S. T., Saravia Celis, P., & Rawel, H. M. (2020). Comparison of Batch and Continuous Wet-Processing of Coffee: Changes in the Main Compounds in Beans, By-Products and Wastewater. *Foods*, 9(8), 1135. <https://doi.org/10.3390/foods9081135>
- Finlay, W. J. J., & Lugovskoy, A. A. (2019). De novo discovery of antibody drugs – great promise demands scrutiny. *MAbs*, 11(5), 809–811. <https://doi.org/10.1080/19420862.2019.1622926>
- Firouzabadi, A. M., Imani, M., Zakizadeh, F., Ghaderi, N., Zare, F., Yadegari, M., Pouretezari, M., & Fesahat, F. (2022). Evaluating effect of acrylamide and ascorbic acid on oxidative stress and apoptosis in ovarian tissue of wistar rat. *Toxicology Reports*, 9, 1580–1585. <https://doi.org/10.1016/j.toxrep.2022.07.015>
- Friedman M. (2003). Chemistry, biochemistry, and safety of acrylamide. biochemistry, and safety of acrylamide. *J Agric Food Chem*, Jul 30;51(16)(doi: 10.1021/jf030204+), 4504-26.
- Geng, Z., Wang, P., & Liu, A. (2011). Determination of Acrylamide in Starch-Based Foods by HPLC with Pre-Column Ultraviolet Derivatization. *Journal of Chromatographic Science*, 49(10), 818–824. <https://doi.org/10.1093/chrscl/49.10.818>
- Ghalebi, M., Hamidi, S., & Nemati, M. (2019). High-Performance Liquid Chromatography Determination of Acrylamide after Its Extraction from Potato

- Chips. *Pharmaceutical Sciences*, 25(4), 338–344.
<https://doi.org/10.15171/PS.2019.42>
- Goding, J. W. (1983). *Monoclonal Antibodies: Principles and Practicc. Academic Press, Sydnycy. ISBN 0-12-287023-9*
- Gökmen, V., Kocadağlı, T., Göncüoğlu, N., & Mogol, B. A. (2012). Model studies on the role of 5-hydroxymethyl-2-furfural in acrylamide formation from asparagine. *Food Chemistry*, 132(1), 168–174.
<https://doi.org/10.1016/j.foodchem.2011.10.048>
- Gökmen, V., Şenyuva, H. Z., Acar, J., & Sarioğlu, K. (2005). Determination of acrylamide in potato chips and crisps by high-performance liquid chromatography. *Journal of Chromatography A*, 1088(1–2), 193–199.
<https://doi.org/10.1016/j.chroma.2004.10.094>
- Granvogel, M., Bugan, S., & Schieberle, P. (2006). Formation of Amines and Aldehydes from Parent Amino Acids during Thermal Processing of Cocoa and Model Systems: New Insights into Pathways of the Strecker Reaction. *Journal of Agricultural and Food Chemistry*, 54(5), 1730–1739.
<https://doi.org/10.1021/jf0525939>
- Granvogel, M., Wieser, H., Koehler, P., Von Tucher, S., & Schieberle, P. (2007). Influence of Sulfur Fertilization on the Amounts of Free Amino Acids in Wheat. Correlation with Baking Properties as well as with 3-Aminopropionamide and Acrylamide Generation during Baking. *Journal of Agricultural and Food Chemistry*, 55(10), 4271–4277. <https://doi.org/10.1021/jf070262l>
- Haapakoski R, K. P. F. N. S. T. L. S. W. H. L. A. A. H. et al. (2013). Toll-like receptor activation during cutaneous allergen sensitization blocks development of asthma through IFN-gamma-dependent mechanisms. *J Invest Dermatol*, 133(4), 964–972. <https://doi.org/doi: 10.1038/jid.2012.356>.
- Habermann CE. (2002). Acrylamide. In: *Kirk-Othmer Encyclopedia of Chemical Technology*. <https://doi.org/10.1002/0471238961.0103182508010205.a01>
- Hamzalıoğlu, A., & Gökmen, V. (2020). 5-Hydroxymethylfurfural accumulation plays a critical role on acrylamide formation in coffee during roasting as confirmed by multiresponse kinetic modelling. *Food Chemistry*, 318, 126467.
<https://doi.org/10.1016/j.foodchem.2020.126467>

- Hansen, S. H., Olsen, A. K., Søderlund, E. J., & Brunborg, G. (2010). In vitro investigations of glycidamide-induced DNA lesions in mouse male germ cells and in mouse and human lymphocytes. *Mutation Research/Genetic Toxicology and Environmental Mutagenesis*, *696*(1), 55–61.
<https://doi.org/10.1016/j.mrgentox.2009.12.012>
- He, J., Zhou, G., Liu, K.-D., & Qin, X.-Y. (2002). Construction and Preliminary Screening of a Human Phage Single-Chain Antibody Library Associated with Gastric Cancer. *Journal of Surgical Research*, *102*(2), 150–155.
<https://doi.org/10.1006/jsre.2001.6298>
- Hellwig, M., & Henle, T. (2014). Baking, Ageing, Diabetes: A Short History of the Maillard Reaction. *Angewandte Chemie International Edition*, *53*(39), 10316–10329. <https://doi.org/10.1002/anie.201308808>
- Hess, G. T., Cragolini, J. J., Popp, M. W., Allen, M. A., Dougan, S. K., Spooner, E., Ploegh, H. L., Belcher, A. M., & Guimaraes, C. P. (2012). M13 Bacteriophage Display Framework That Allows Sortase-Mediated Modification of Surface-Accessible Phage Proteins. *Bioconjugate Chemistry*, *23*(7), 1478–1487.
<https://doi.org/10.1021/bc300130z>
- Hieter, P. A., Hollis, G. F., Korsmeyer, S. J., Waldmann, T. A., & Leder, P. (1981). Clustered arrangement of immunoglobulin λ constant region genes in man. *Nature*, *294*(5841), 536–540. <https://doi.org/10.1038/294536a0>
- Hoenicke, K., & Gatermann, R. (2005). Studies on the Stability of Acrylamide in Food During Storage. *Journal of AOAC INTERNATIONAL*, *88*(1), 268–273.
<https://doi.org/10.1093/jaoac/88.1.268>
- Hogrefe, H. H., Amberg, J. R., Hay, B. N., Sorge, J. A., & Shopes, B. (1993). Cloning in a bacteriophage lambda vector for the display of binding proteins on filamentous phage. *Gene*, *137*(1), 85–91. [https://doi.org/10.1016/0378-1119\(93\)90255-2](https://doi.org/10.1016/0378-1119(93)90255-2)
- Hözl-Armstrong, L., Kucab, J. E., Moody, S., Zwart, E. P., Loutkotová, L., Duffy, V., Luijten, M., Gamboa da Costa, G., Stratton, M. R., Phillips, D. H., & Arlt, V. M. (2020). Mutagenicity of acrylamide and glycidamide in human TP53 knock-in (Hupki) mouse embryo fibroblasts. *Archives of Toxicology*, *94*(12), 4173–4196.
<https://doi.org/10.1007/s00204-020-02878-0>

- Horton, R. M., Hunt, H. D., Ho, S. N., Pullen, J. K., & Pease, L. R. (1989). Engineering hybrid genes without the use of restriction enzymes: gene splicing by overlap extension. *Gene*, 77(1), 61–68. [https://doi.org/10.1016/0378-1119\(89\)90359-4](https://doi.org/10.1016/0378-1119(89)90359-4)
- Hou, L., Liu, S., Zhao, C., Fan, L., Hu, H., & Yin, S. (2021). The combination of T-2 toxin and acrylamide synergistically induces hepatotoxicity and nephrotoxicity via the activation of oxidative stress and the mitochondrial pathway. *Toxicol*, 189, 65–72. <https://doi.org/10.1016/j.toxicol.2020.11.007>
- Hu, Q., Xu, X., Li, Z., Zhang, Y., Wang, J., Fu, Y., & Li, Y. (2014). Detection of acrylamide in potato chips using a fluorescent sensing method based on acrylamide polymerization-induced distance increase between quantum dots. *Biosensors and Bioelectronics*, 54, 64–71. <https://doi.org/10.1016/j.bios.2013.10.046>
- Huston JS, L. D. M.-H. M. T. M. N. J. M. M. R. R. B. R. H. E. C. R. et al. (1988). Protein engineering of antibody binding sites: recovery of specific activity in an anti-digoxin single-chain Fv analogue produced in *Escherichia coli*. . *Proc Natl Acad Sci U S A.*, 85(16), 5879–5883. <https://doi.org/doi: 10.1073/pnas.85.16.5879>.
- IARC . (1994). International Agency for Research on Cancer Monographs. *Lyon, France*.
- Kim, B., Kim, E., Yoo, Y.-J., Bae, H.-W., Chung, I.-Y., & Cho, Y.-H. (2019). Phage-Derived Antibacterials: Harnessing the Simplicity, Plasticity, and Diversity of Phages. *Viruses*, 11(3), 268. <https://doi.org/10.3390/v11030268>
- Kleefisch, G., Kreutz, C., Bargon, J., Silva, G., & Schalley, C. (2004). Quartz Microbalance Sensor for the Detection of Acrylamide. *Sensors*, 4(9), 136–146. <https://doi.org/10.3390/s40900136>
- Kocadağlı, T., Göncüoğlu, N., Hamzalıoğlu, A., & Gökmen, V. (2012). In depth study of acrylamide formation in coffee during roasting: role of sucrose decomposition and lipid oxidation. *Food & Function*, 3(9), 970. <https://doi.org/10.1039/c2fo30038a>
- Komthong, P., Suriyaphan, O., & Charoenpanich, J. (2012). Determination of acrylamide in Thai-conventional snacks from Nong Mon market, Chonburi using GC-MS technique. *Food Additives and Contaminants: Part B*, 5(1), 20–28. <https://doi.org/10.1080/19393210.2012.656145>

- Kumar, J., Das, S., & Teoh, S. L. (2018). Dietary Acrylamide and the Risks of Developing Cancer: Facts to Ponder. *Frontiers in Nutrition*, 5.
<https://doi.org/10.3389/fnut.2018.00014>
- Lake D. F., S. S. F. , W. E. , B. R. M. , E. A. B. and M. J. (1994). Autoantibodies to the α / β T-cell receptors in human immunodeficiency virus infection: dysregulation and mimicry. *Proc. Natl. Acad. Sei, USA* 91, 10849–10853. <https://doi.org/doi:10.1073/pnas.91.23.10849>.
- Larsson, S. C., & Wolk, A. (2007). Coffee Consumption and Risk of Liver Cancer: A Meta-Analysis. *Gastroenterology*, 132(5), 1740–1745.
<https://doi.org/10.1053/j.gastro.2007.03.044>
- Law, M. (2021). Antibody Responses in Hepatitis C Infection. *Cold Spring Harbor Perspectives in Medicine*, 11(3), a036962.
<https://doi.org/10.1101/cshperspect.a036962>
- LeBoeuf, R. D., Ban, E. M. H., Green, M. M., Stone, A. S., Propst, S. M., Blalock, J. E., & Tauber, J. D. (1998). Molecular Cloning, Sequence Analysis, Expression, and Tissue Distribution of Suppressin, a Novel Suppressor of Cell Cycle Entry. *Journal of Biological Chemistry*, 273(1), 361–368. <https://doi.org/10.1074/jbc.273.1.361>
- Lee, M.-R., Chang, L.-Y., & Dou, J. (2007). Determination of acrylamide in food by solid-phase microextraction coupled to gas chromatography–positive chemical ionization tandem mass spectrometry. *Analytica Chimica Acta*, 582(1), 19–23.
<https://doi.org/10.1016/j.aca.2006.08.042>
- Liang, Y., Zeng, Y., Luo, L., Xu, Z., Shen, Y., Wang, H., & Hammock, B. D. (2022). Detection of Acrylamide in Foodstuffs by Nanobody-Based Immunoassays. *Journal of Agricultural and Food Chemistry*, 70(29), 9179–9186.
<https://doi.org/10.1021/acs.jafc.2c01872>
- Liu, Y., Wang, Y., Zhang, X., Jiao, Y., Duan, L., Dai, L., & Yan, H. (2022). Chronic acrylamide exposure resulted in dopaminergic neuron loss, neuroinflammation and motor impairment in rats. *Toxicology and Applied Pharmacology*, 451, 116190. <https://doi.org/10.1016/j.taap.2022.116190>
- Lowman HB, C. T., & Clackson T. (2004). Phage display: a practical approach. *Oxford: Oxford University Press*, 10–11. <https://doi.org/10.1093/bfcp/3.4.391>

- Lund, M. N., & Ray, C. A. (2017). Control of Maillard Reactions in Foods: Strategies and Chemical Mechanisms. *Journal of Agricultural and Food Chemistry*, *65*(23), 4537–4552. <https://doi.org/10.1021/acs.jafc.7b00882>
- Madiah, K. Y. K., Zaibunnisa, A. H., Norashikin, S., Rozita, O., & Misnawi, J. (2012). Optimization of Roasting Conditions for High-Quality Robusta Coffee. *APCBEE Procedia*, *4*, 209–214. <https://doi.org/10.1016/j.apcbee.2012.11.035>
- Matoso, V., Bargi-Souza, P., Ivanski, F., Romano, M. A., & Romano, R. M. (2019). Acrylamide: A review about its toxic effects in the light of Developmental Origin of Health and Disease (DOHaD) concept. *Food Chemistry*, *283*, 422–430. <https://doi.org/10.1016/j.foodchem.2019.01.054>
- Mauron J. (1981). The Maillard reaction in food; a critical review from the nutritional standpoint. *Prog Food Nutr Sci.*, *5*(1-6), 5–35. <https://doi.org/doi:10.1159/000416696>.
- McCafferty, J., Griffiths, A. D., Winter, G., & Chiswell, D. J. (1990). Phage antibodies: filamentous phage displaying antibody variable domains. *Nature*, *348*(6301), 552–554. <https://doi.org/10.1038/348552a0>
- Mottram, D. S., Wedzicha, B. L., & Dodson, A. T. (2002). Acrylamide is formed in the Maillard reaction. *Nature*, *419*(6906), 448–449. <https://doi.org/10.1038/419448a>
- Murdock, R. C., Shen, L., Griffin, D. K., Kelley-Loughnane, N., Papautsky, I., & Hagen, J. A. (2013). Optimization of a Paper-Based ELISA for a Human Performance Biomarker. *Analytical Chemistry*, *85*(23), 11634–11642. <https://doi.org/10.1021/ac403040a>
- Neuhäuser-Klaus, A., & Schmahl, W. (1989). Mutagenic and teratogenic effects of acrylamide in the mammalian spot test. *Mutation Research Letters*, *226*(3), 157–162. [https://doi.org/10.1016/0165-7992\(89\)90013-4](https://doi.org/10.1016/0165-7992(89)90013-4)
- Okuno, T., Matsuoka, M., Sumizawa, T., & Igisu, H. (2006). Involvement of the extracellular signal-regulated protein kinase pathway in phosphorylation of p53 protein and exerting cytotoxicity in human neuroblastoma cells (SH-SY5Y) exposed to acrylamide. *Archives of Toxicology*, *80*(3), 146–153. <https://doi.org/10.1007/s00204-005-0022-8>
- P. Tijssen. (1985). *Chapter 14 Quantitative enzyme immunoassay techniques* (pp. 329–384). [https://doi.org/10.1016/S0075-7535\(08\)70144-X](https://doi.org/10.1016/S0075-7535(08)70144-X)

- Pande, J., Szewczyk, M. M., & Grover, A. K. (2010). Phage display: Concept, innovations, applications and future. *Biotechnology Advances*, 28(6), 849–858. <https://doi.org/10.1016/j.biotechadv.2010.07.004>
- Pingot, D., Pyrzanowski, K., Michałowicz, J., & Bukowska, B. (2013). TOXICITY OF ACRYLAMIDE AND ITS METABOLITE - GLICYDAMIDE. *Medycyna Pracy*. <https://doi.org/10.13075/mp.5893/2013/0022>
- Pundir, C. S., Yadav, N., & Chhillar, A. K. (2019a). Occurrence, synthesis, toxicity and detection methods for acrylamide determination in processed foods with special reference to biosensors: A review. *Trends in Food Science & Technology*, 85, 211–225. <https://doi.org/10.1016/j.tifs.2019.01.003>
- Pundir, C. S., Yadav, N., & Chhillar, A. K. (2019b). Occurrence, synthesis, toxicity and detection methods for acrylamide determination in processed foods with special reference to biosensors: A review. *Trends in Food Science & Technology*, 85, 211–225. <https://doi.org/10.1016/j.tifs.2019.01.003>
- Quan, Y., Chen, M., Zhan, Y., & Zhang, G. (2011a). Development of an Enhanced Chemiluminescence ELISA for the Rapid Detection of Acrylamide in Food Products. *Journal of Agricultural and Food Chemistry*, 59(13), 6895–6899. <https://doi.org/10.1021/jf200954w>
- Quan, Y., Chen, M., Zhan, Y., & Zhang, G. (2011b). Development of an Enhanced Chemiluminescence ELISA for the Rapid Detection of Acrylamide in Food Products. *Journal of Agricultural and Food Chemistry*, 59(13), 6895–6899. <https://doi.org/10.1021/jf200954w>
- Rahbarnia, L., Farajnia, S., Babaei, H., Majidi, J., Veisi, K., Ahmadzadeh, V., & Akbari, B. (2017). Evolution of phage display technology: from discovery to application. *Journal of Drug Targeting*, 25(3), 216–224. <https://doi.org/10.1080/1061186X.2016.1258570>
- Rakonjac, J., Russel, M., Khanum, S., Brooke, S. J., & Rajič, M. (2017). *Filamentous Phage: Structure and Biology* (pp. 1–20). https://doi.org/10.1007/978-3-319-72077-7_1
- Reshmitha, T. R., & Nisha, P. (2021). Lycopene mitigates acrylamide and glycidamide induced cellular toxicity via oxidative stress modulation in HepG2 cells. *Journal of Functional Foods*, 80, 104390. <https://doi.org/10.1016/j.jff.2021.104390>

- Rifai, L., & Saleh, F. A. (2020). A Review on Acrylamide in Food: Occurrence, Toxicity, and Mitigation Strategies. *International Journal of Toxicology*, *39*(2), 93–102. <https://doi.org/10.1177/1091581820902405>
- Rosén, J., & Hellenäs, K.-E. (2002). Analysis of acrylamide in cooked foods by liquid chromatography tandem mass spectrometry. *The Analyst*, *127*(7), 880–882. <https://doi.org/10.1039/b204938d>
- Rubayiza, A. B., & Meurens, M. (2005). Chemical Discrimination of Arabica and Robusta Coffees by Fourier Transform Raman Spectroscopy. *Journal of Agricultural and Food Chemistry*, *53*(12), 4654–4659. <https://doi.org/10.1021/jf0478657>
- S. Rath & Madeleine E. Devey. (1988). IgG subclass composition of antibodies to HBsAg in circulating immune complexes from patients with hepatitis B virus infections. *Clin. Exp. Immunol.*, *72*, 164–167. <https://pubmed.ncbi.nlm.nih.gov/3396217/>
- Sáez-Hernández, R., Ruiz, P., Mauri-Aucejo, A. R., Yusa, V., & Cervera, M. L. (2022). Determination of acrylamide in toasts using digital image colorimetry by smartphone. *Food Control*, *141*, 109163. <https://doi.org/10.1016/j.foodcont.2022.109163>
- Schabacker, J., Schwend, T., & Wink, M. (2004). Reduction of Acrylamide Uptake by Dietary Proteins in a Caco-2 Gut Model. *Journal of Agricultural and Food Chemistry*, *52*(12), 4021–4025. <https://doi.org/10.1021/jf035238w>
- Schouten, M. A., Frygasas, C., Tappi, S., Romani, S., & Fogliano, V. (2022). The use of kidney bean flour with intact cell walls reduces the formation of acrylamide in biscuits. *Food Control*, *140*, 109054. <https://doi.org/10.1016/j.foodcont.2022.109054>
- Schouten, M. A., Genovese, J., Tappi, S., Di Francesco, A., Baraldi, E., Cortese, M., Caprioli, G., Angeloni, S., Vittori, S., Rocculi, P., & Romani, S. (2020). Effect of innovative pre-treatments on the mitigation of acrylamide formation in potato chips. *Innovative Food Science & Emerging Technologies*, *64*, 102397. <https://doi.org/10.1016/j.ifset.2020.102397>
- Schouten, M. A., Tappi, S., Angeloni, S., Cortese, M., Caprioli, G., Vittori, S., & Romani, S. (2021). Acrylamide formation and antioxidant activity in coffee during roasting

- A systematic study. *Food Chemistry*, 343, 128514.
<https://doi.org/10.1016/j.foodchem.2020.128514>
- Sheikholvaezin, A., Sandström, P., Eriksson, D., Norgren, N., Riklund, K., & Stigbrand, T. (2006). Optimizing the Generation of Recombinant Single-Chain Antibodies Against Placental Alkaline Phosphatase. *Hybridoma*, 25(4), 181–192.
<https://doi.org/10.1089/hyb.2006.25.181>
- Shin, D.-C., Kim, C.-T., Lee, Y.-C., Choi, W.-J., Na, Y.-J., & Lee, K.-W. (2010). Reduction of acrylamide by taurine in aqueous and potato chip model systems. *Food Research International*, 43(5), 1356–1360.
<https://doi.org/10.1016/j.foodres.2010.03.024>
- Sidhu, S. S., Lowman, H. B., Cunningham, B. C., & Wells, J. A. (2000). [21] Phage display for selection of novel binding peptides (pp. 333-IN5).
[https://doi.org/10.1016/S0076-6879\(00\)28406-1](https://doi.org/10.1016/S0076-6879(00)28406-1)
- Sidney, J., Southwood, S., Moore, C., Oseroff, C., Pinilla, C., Grey, H. M., & Sette, A. (2013). Measurement of MHC/Peptide Interactions by Gel Filtration or Monoclonal Antibody Capture. *Current Protocols in Immunology*, 100(1).
<https://doi.org/10.1002/0471142735.im1803s100>
- Singh, G., Brady, B., Koerner, T., Becalski, A., Zhao, T., Feng, S., Godefroy, S. B., Huet, A.-C., & Delahaut, P. (2014). Development of a Highly Sensitive Competitive Indirect Enzyme-Linked Immunosorbent Assay for Detection of Acrylamide in Foods and Water. *Food Analytical Methods*, 7(6), 1298–1304.
<https://doi.org/10.1007/s12161-013-9749-7>
- Skerra, A., & Plückthun, A. (1988). Assembly of a Functional Immunoglobulin F_v Fragment in *Escherichia coli*. *Science*, 240(4855), 1038–1041.
<https://doi.org/10.1126/science.3285470>
- Smith, G. P. (1985). Filamentous Fusion Phage: Novel Expression Vectors That Display Cloned Antigens on the Virion Surface. *Science*, 228(4705), 1315–1317.
<https://doi.org/10.1126/science.4001944>
- Sörgel, F., Weissenbacher, R., Kinzig-Schippers, M., Hofmann, A., Illauer, M., Skott, A., & Landersdorfer, C. (2002). Acrylamide: Increased Concentrations in Homemade Food and First Evidence of Its Variable Absorption from Food, Variable

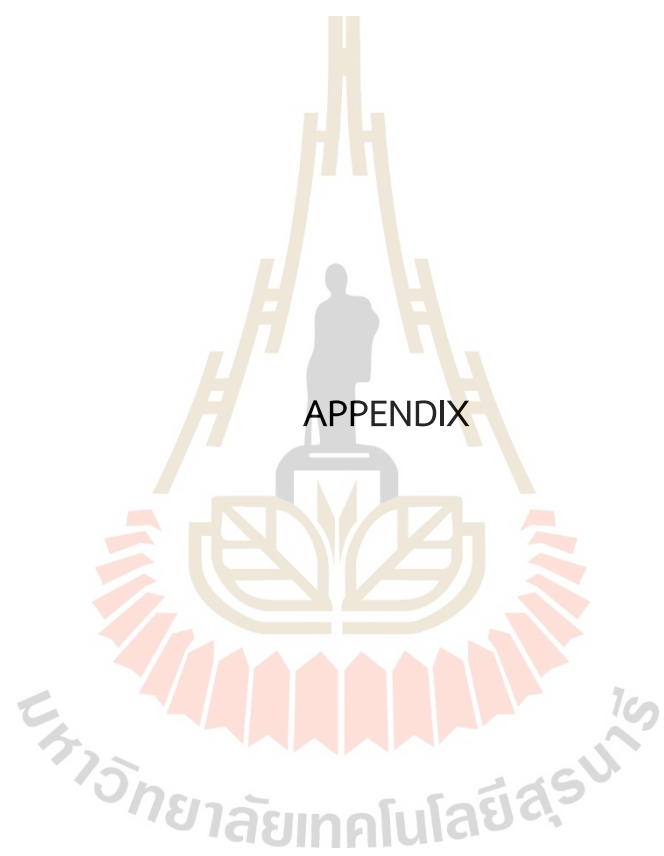
- Metabolism and Placental and Breast Milk Transfer in Humans. *Chemotherapy*, 48(6), 267–274. <https://doi.org/10.1159/000069715>
- Stadler, R. H., Blank, I., Varga, N., Robert, F., Hau, J., Guy, P. A., Robert, M.-C., & Riediker, S. (2002). Acrylamide from Maillard reaction products. *Nature*, 419(6906), 449–450. <https://doi.org/10.1038/419449a>
- Steinegger, A., Wolfbeis, O. S., & Borisov, S. M. (2020). Optical Sensing and Imaging of pH Values: Spectroscopies, Materials, and Applications. *Chemical Reviews*, 120(22), 12357–12489. <https://doi.org/10.1021/acs.chemrev.0c00451>
- Stephanie D, G. S. P. K. et al. (2013). Enzyme immunoassay and enzyme-linked immunosorbent assay. *J Invest Dermatol*, 133(9), 12. <https://doi.org/doi:10.1038/jid.2013.287>
- Stura E.A., F. G. G. , W. I. A. (1993). Crystallization of Antibodies and Antibody-Antigen Complexes. . *Immunomethods*, 3, 164–179. <https://doi.org/doi:10.1107/S0907444910026041>
- Suriben, R., Chen, M., Higbee, J., Oeffinger, J., Ventura, R., Li, B., Mondal, K., Gao, Z., Ayupova, D., Taskar, P., Li, D., Starck, S. R., Chen, H.-I. H., McEntee, M., Katewa, S. D., Phung, V., Wang, M., Kekatpure, A., Lakshminarasimhan, D., ... Allan, B. B. (2020). Antibody-mediated inhibition of GDF15–GFRAL activity reverses cancer cachexia in mice. *Nature Medicine*, 26(8), 1264–1270. <https://doi.org/10.1038/s41591-020-0945-x>
- Svensson, K., Abramsson, L., Becker, W., Glynn, A., Hellenäs, K.-E., Lind, Y., & Rosén, J. (2003). Dietary intake of acrylamide in Sweden. *Food and Chemical Toxicology*, 41(11), 1581–1586. [https://doi.org/10.1016/S0278-6915\(03\)00188-1](https://doi.org/10.1016/S0278-6915(03)00188-1)
- Sylvia, J. M., Janni, J. A., Klein, J. D., & Spencer, K. M. (2000). Surface-Enhanced Raman Detection of 2,4-Dinitrotoluene Impurity Vapor as a Marker To Locate Landmines. *Analytical Chemistry*, 72(23), 5834–5840. <https://doi.org/10.1021/ac0006573>
- TAEYMANS, D., WOOD, J., ASHBY, P., BLANK, I., STUDER, A., STADLER, R. H., GONDÉ, P., EIJCK, P., LALLJIE, S., LINGNERT, H., LINDBLOM, M., MATISSEK, R., MÜLLER, D., TALLMADGE, D., O'BRIEN, J., THOMPSON, S., SILVANI, D., & WHITMORE, T. (2004). A Review of Acrylamide: An Industry Perspective on Research, Analysis,

- Formation, and Control. *Critical Reviews in Food Science and Nutrition*, 44(5), 323–347. <https://doi.org/10.1080/10408690490478082>
- Tam, J. O., de Puig, H., Yen, C., Bosch, I., Gómez-Márquez, J., Clavet, C., Hamad-Schifferli, K., & Gehrke, L. (2017). A comparison of nanoparticle-antibody conjugation strategies in sandwich immunoassays. *Journal of Immunoassay and Immunochemistry*, 38(4), 355–377. <https://doi.org/10.1080/15321819.2016.1269338>
- Tareke, E., Lyn-Cook, B., Robinson, B., & Ali, S. F. (2008). Acrylamide: A Dietary Carcinogen Formed in Vivo? *Journal of Agricultural and Food Chemistry*, 56(15), 6020–6023. <https://doi.org/10.1021/jf703749h>
- Tareke, E., Rydberg, P., Karlsson, P., Eriksson, S., & Törnqvist, M. (2000). Acrylamide: A Cooking Carcinogen? *Chemical Research in Toxicology*, 13(6), 517–522. <https://doi.org/10.1021/tx9901938>
- Thanongsaksrikul, J., Srimanote, P., Maneewatch, S., Choowongkamon, K., Tapchaisri, P., Makino, S., Kurazono, H., & Chaicumpa, W. (2010). A VHH That Neutralizes the Zinc Metalloproteinase Activity of Botulinum Neurotoxin Type A. *Journal of Biological Chemistry*, 285(13), 9657–9666. <https://doi.org/10.1074/jbc.M109.073163>
- Thanongsaksrikul, J., Srimanote, P., Tongtawe, P., Glab-ampai, K., Malik, A. A., Supasorn, O., Chiawwit, P., Poovorawan, Y., & Chaicumpa, W. (2018). Identification and production of mouse scFv to specific epitope of enterovirus-71 virion protein-2 (VP2). *Archives of Virology*, 163(5), 1141–1152. <https://doi.org/10.1007/s00705-018-3731-z>
- Thattanon, P., Thanongsaksrikul, J., Petvises, S., & Nathalang, O. (2020). Monoclonal antibody specific to the Di blood group antigen generated by phage display technology. *Blood Transfusion*, 18(5), 366–373. <https://doi.org/10.2450/2020.0031-20>
- Thobhani, S., Attree, S., Boyd, R., Kumarswami, N., Noble, J., Szymanski, M., & Porter, R. A. (2010). Bioconjugation and characterisation of gold colloid-labelled proteins. *Journal of Immunological Methods*, 356(1–2), 60–69. <https://doi.org/10.1016/j.jim.2010.02.007>

- Thorpe, S. R., & Baynes, J. W. (2003). Maillard reaction products in tissue proteins: New products and new perspectives. *Amino Acids*, *25*(3–4), 275–281. <https://doi.org/10.1007/s00726-003-0017-9>
- Tilson HA. (1981). The neurotoxicity of acrylamide: an overview. *Neurobehav Toxicol Teratol*. *Neurobehav Toxicol Teratol*, *3*(4), 445–461.
- Verma, V., & Yadav, N. (2022). Acrylamide content in starch based commercial foods by using high performance liquid chromatography and its association with browning index. *Current Research in Food Science*, *5*, 464–470. <https://doi.org/10.1016/j.crfs.2022.01.010>
- Vikström, A. C., Warholm, M., Paulsson, B., Axmon, A., Wirfält, E., & Törnqvist, M. (2012). Hemoglobin adducts as a measure of variations in exposure to acrylamide in food and comparison to questionnaire data. *Food and Chemical Toxicology*, *50*(7), 2531–2539. <https://doi.org/10.1016/j.fct.2012.04.004>
- Wang, F., Fan, B., Chen, C., & Zhang, W. (2022). Acrylamide causes neurotoxicity by inhibiting glycolysis and causing the accumulation of carbonyl compounds in BV2 microglial cells. *Food and Chemical Toxicology*, *163*, 112982. <https://doi.org/10.1016/j.fct.2022.112982>
- Wang L, L. N. F. D. (2015). Persistence of prolonged C peptide production in type 1 diabetes as measured with an ultrasensitive C-peptide assay. *Diabetes Care*, *35*(3), 465–470. <https://doi.org/doi:10.2337/dc11-1236>.
- Whitlow, M., Bell, B. A., Feng, S.-L., Filpula, D., Hardman, K. D., Hubert, S. L., Rollence, M. L., Wood, J. F., Schott, M. E., Milenic, D. E., Yokota, T., & Schlom, J. (1993). An improved linker for single-chain Fv with reduced aggregation and enhanced proteolytic stability. *Protein Engineering, Design and Selection*, *6*(8), 989–995. <https://doi.org/10.1093/protein/6.8.989>
- Wilson, D. R., Siebers, A., & Finlay, B. B. (1998). Antigenic Analysis of *Bordetella pertussis* Filamentous Hemagglutinin with Phage Display Libraries and Rabbit Anti-Filamentous Hemagglutinin Polyclonal Antibodies. *Infection and Immunity*, *66*(10), 4884–4894. <https://doi.org/10.1128/IAI.66.10.4884-4894.1998>
- Xian, Y., Wu, Y., Dong, H., Chen, L., Zhang, C., Hou, X., Zeng, X., Bai, W., & Guo, X. (2019). Modified QuEChERS purification and Fe₃O₄ nanoparticle decoloration for robust analysis of 14 heterocyclic aromatic amines and acrylamide in coffee

- products using UHPLC-MS/MS. *Food Chemistry*, *285*, 77–85.
<https://doi.org/10.1016/j.foodchem.2019.01.132>
- Xu, Y., Cui, B., Ran, R., Liu, Y., Chen, H., Kai, G., & Shi, J. (2014). Risk assessment, formation, and mitigation of dietary acrylamide: Current status and future prospects. *Food and Chemical Toxicology*, *69*, 1–12.
<https://doi.org/10.1016/j.fct.2014.03.037>
- Yang, L., Zhang, G., Yang, L., & He, Y. (2012). LC-MS/MS determination of acrylamide in instant noodles from supermarkets in the Hebei province of China. *Food Additives and Contaminants: Part B*, *5*(2), 100–104.
<https://doi.org/10.1080/19393210.2012.658874>
- Yasuhara, A., Tanaka, Y., Hengel, M., & Shibamoto, T. (2003). Gas Chromatographic Investigation of Acrylamide Formation in Browning Model Systems. *Journal of Agricultural and Food Chemistry*, *51*(14), 3999–4003.
<https://doi.org/10.1021/jf0300947>
- Yaylayan, V. A., Machiels, D., & Istasse, L. (2003). Thermal Decomposition of Specifically Phosphorylated α -Glucoses and Their Role in the Control of the Maillard Reaction. *Journal of Agricultural and Food Chemistry*, *51*(11), 3358–3366. <https://doi.org/10.1021/jf034037p>
- Yuan, Y., Yucai, L., Lu, L., Hui, L., Yong, P., & Haiyang, Y. (2022a). Acrylamide induces ferroptosis in HSC-T6 cells by causing antioxidant imbalance of the XCT-GSH-GPX4 signaling and mitochondrial dysfunction. *Toxicology Letters*, *368*, 24–32.
<https://doi.org/10.1016/j.toxlet.2022.08.007>
- Yuan, Y., Yucai, L., Lu, L., Hui, L., Yong, P., & Haiyang, Y. (2022b). Acrylamide induces ferroptosis in HSC-T6 cells by causing antioxidant imbalance of the XCT-GSH-GPX4 signaling and mitochondrial dysfunction. *Toxicology Letters*, *368*, 24–32.
<https://doi.org/10.1016/j.toxlet.2022.08.007>
- Yuxin Ma, Jing Shi, Meige Zheng, Jing Liu, Sumin Tian, Xinhong He, Dexing Zhang, Guoying Li, & Jiayong Zhu. (2011). Toxicological effects of acrylamide on the reproductive system of weaning male rats. *Toxicology and Industrial Health*, *27*(7), 617–627. <https://doi.org/10.1177/0748233710394235>

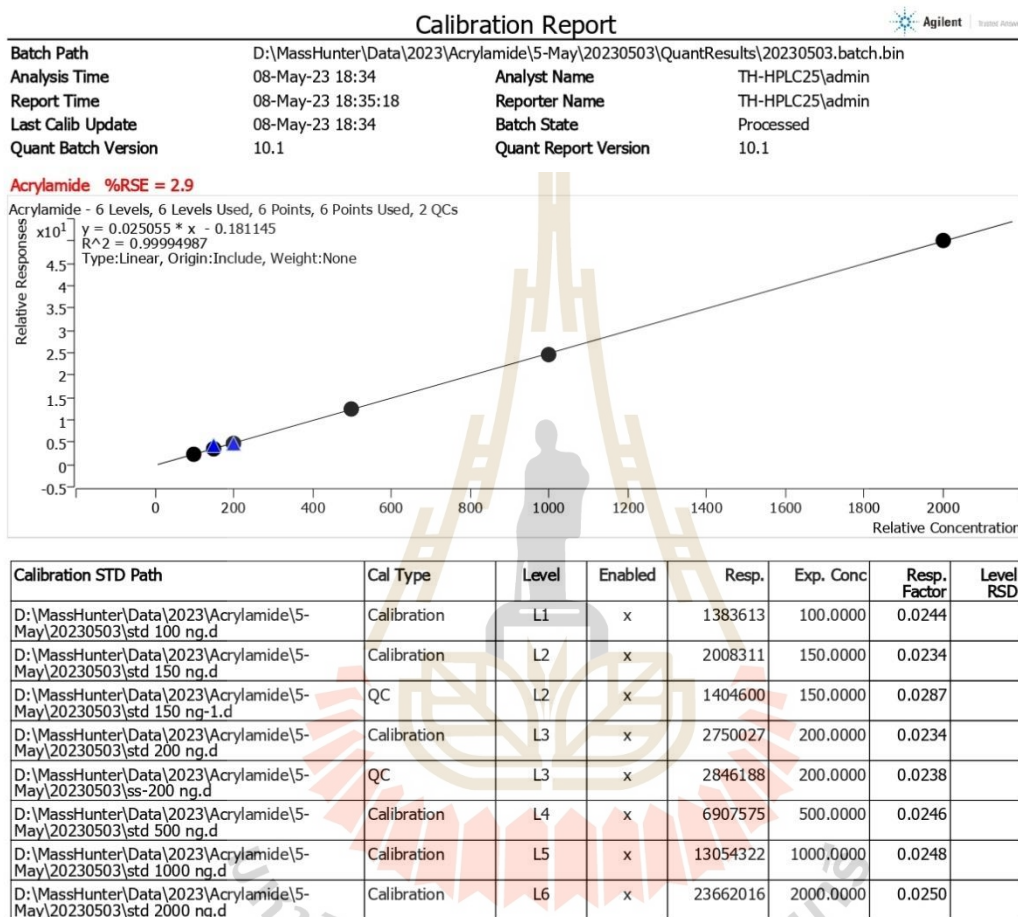
- Zalewska-Piątek, B., & Piątek, R. (2021). Bacteriophages as Potential Tools for Use in Antimicrobial Therapy and Vaccine Development. *Pharmaceuticals*, *14*(4), 331. <https://doi.org/10.3390/ph14040331>
- Zhang, H., Shan, L., Aniaqu, S., Jiang, Y., & Chen, T. (2022). Paternal acrylamide exposure induces transgenerational effects on sperm parameters and learning capability in mice. *Food and Chemical Toxicology*, *161*, 112817. <https://doi.org/10.1016/j.fct.2022.112817>
- Zhang, Y., Ren, Y., Jiao, J., Li, D., & Zhang, Y. (2011). Ultra High-Performance Liquid Chromatography–Tandem Mass Spectrometry for the Simultaneous Analysis of Asparagine, Sugars, and Acrylamide in Maillard Reactions. *Analytical Chemistry*, *83*(9), 3297–3304. <https://doi.org/10.1021/ac1029538>
- Zhao, T., Guo, Y., Ji, H., Mao, G., Feng, W., Chen, Y., Wu, X., & Yang, L. (2022). Short-term exposure to acrylamide exacerbated metabolic disorders and increased metabolic toxicity susceptibility on adult male mice with diabetes. *Toxicology Letters*, *356*, 41–53. <https://doi.org/10.1016/j.toxlet.2021.12.004>
- Zhou, S., Zhang, C., Wang, D., & Zhao, M. (2008). Antigen synthetic strategy and immunoassay development for detection of acrylamide in foods. *The Analyst*, *133*(7), 903. <https://doi.org/10.1039/b716526a>
- Zödl, B., Schmid, D., Wassler, G., Gundacker, C., Leibetseder, V., Thalhammer, T., & Ekmekcioglu, C. (2007). Intestinal transport and metabolism of acrylamide. *Toxicology*, *232*(1–2), 99–108. <https://doi.org/10.1016/j.tox.2006.12.014>



APPENDIX

APPENDIX A

The verified by High- performance liquid chromatography (HPLC).



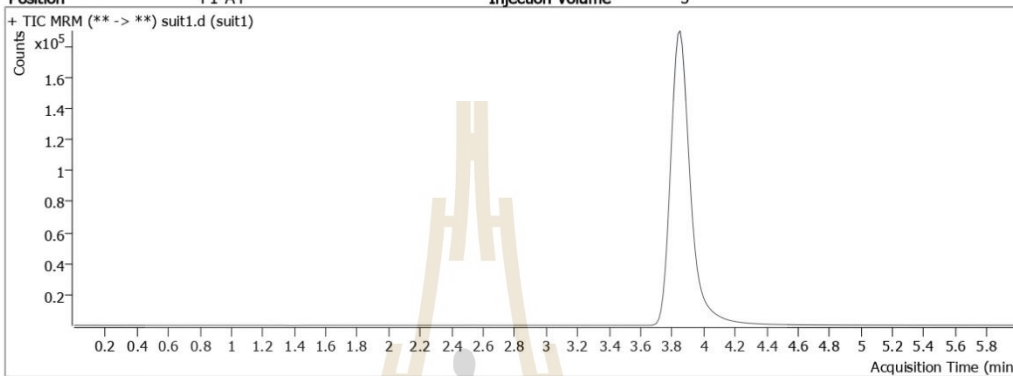
By Sample Quant Report



Batch Path D:\MassHunter\Data\2023\Acrylamide\5-May\20230511+H2o\QuantResults\20230511-n.batch.bin
 Analysis Time 15-May-23 11:27 Analyst Name TH-HPLC25\admin
 Report Time 18-May-23 13:52:04 Reporter Name TH-HPLC25\admin
 Last Calib Update 15-May-23 11:27 Batch State Processed
 Quant Batch Version 10.1 Quant Report Version 10.1

Analysis Info

Instrument 1 Instrument 1 Operator
 Data File suit1.d Sample Name suit1
 Sample Type Sample Dilution 1
 Acq. Method Acrylamide for coffee.m Acq. Date 11-May-23 22:06
 Position P1-A4 Injection Volume 5

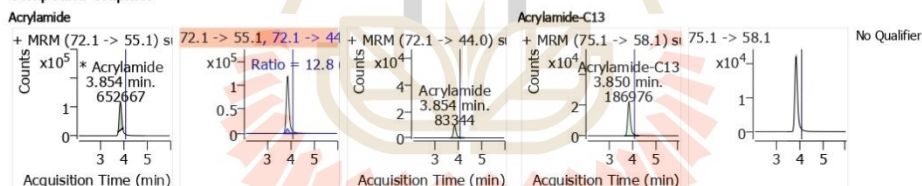


ISTD Compounds	Compound Type	RT	Transition(T)	ISTD Resp.
Acrylamide-C13	ISTD	3.850	75.1 -> 58.1	186976

Quantitation Results

Compound	RT	Ref RT	Transition(T)	Transition(Q)	T-Resp	Q-Resp	QRatio	Ref QRatio	ISTD Compounds	IS Ratio	Final Conc.	Units
Acrylamide	3.854	4.042	72.1 -> 55.1	72.1 -> 44.0	652667	83344	12.8	8.5	Acrylamide-C13	3.4906	123.1534	ng/ml

Compound Graphics



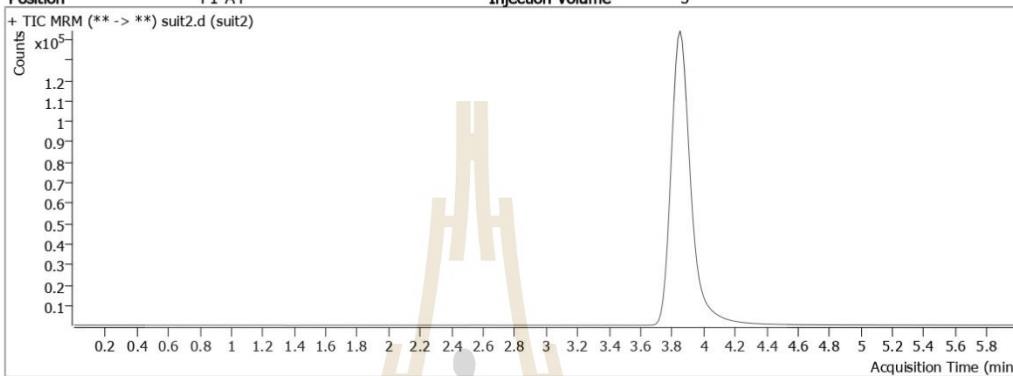
By Sample Quant Report



Batch Path D:\MassHunter\Data\2023\Acrylamide\5-May\20230511+H2o\QuantResults\20230511-n.batch.bin
Analysis Time 15-May-23 11:27 **Analyst Name** TH-HPLC25\admin
Report Time 18-May-23 13:52:06 **Reporter Name** TH-HPLC25\admin
Last Calib Update 15-May-23 11:27 **Batch State** Processed
Quant Batch Version 10.1 **Quant Report Version** 10.1

Analysis Info

Instrument 1 Instrument 1 **Operator**
Data File suit2.d **Sample Name** suit2
Sample Type Sample **Dilution** 1
Acq. Method Acrylamide for coffee.m **Acq. Date** 11-May-23 22:12
Position P1-A4 **Injection Volume** 5

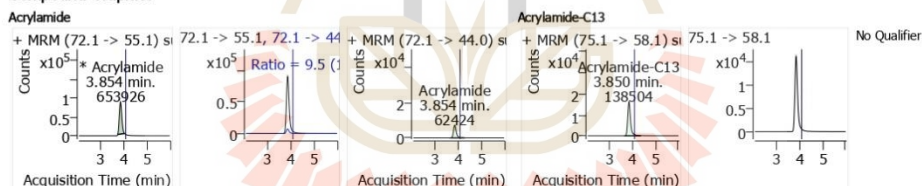


ISTD Compounds	Compound Type	RT	Transition(T)	ISTD Resp.
Acrylamide-C13	ISTD	3.850	75.1 -> 58.1	138504

Quantitation Results

Compound	RT	Ref RT	Transition(T)	Transition(Q)	T-Resp	Q-Resp	QRatio	Ref QRatio	ISTD Compounds	IS Ratio	Final Conc.	Units
Acrylamide	3.854	4.042	72.1 -> 55.1	72.1 -> 44.0	653926	62424	9.5	8.5	Acrylamide-C13	4.7213	165.6773	ng/ml

Compound Graphics



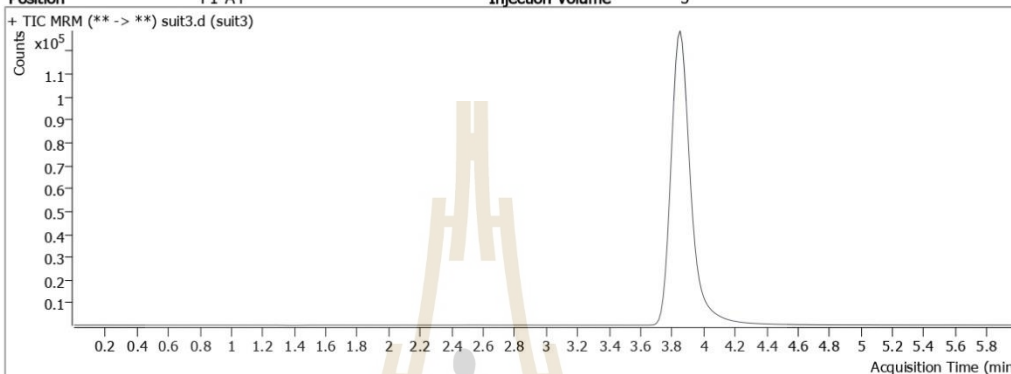
By Sample Quant Report



Batch Path D:\MassHunter\Data\2023\Acrylamide\5-May\20230511+H2o\QuantResults\20230511-n.batch.bin
 Analysis Time 15-May-23 11:27 Analyst Name TH-HPLC25\admin
 Report Time 18-May-23 13:52:08 Reporter Name TH-HPLC25\admin
 Last Calib Update 15-May-23 11:27 Batch State Processed
 Quant Batch Version 10.1 Quant Report Version 10.1

Analysis Info

Instrument 1 Instrument 1 Operator
 Data File suit3.d Sample Name suit3
 Sample Type Sample Dilution 1
 Acq. Method Acrylamide for coffee.m Acq. Date 11-May-23 22:19
 Position P1-A4 Injection Volume 5

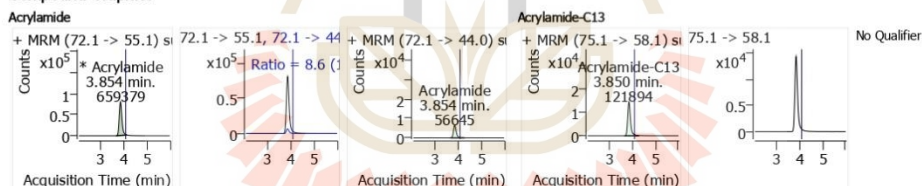


ISTD Compounds	Compound Type	RT	Transition(T)	ISTD Resp.
Acrylamide-C13	ISTD	3.850	75.1 -> 58.1	121894

Quantitation Results

Compound	RT	Ref RT	Transition(T)	Transition(Q)	T-Resp	Q-Resp	QRatio	Ref QRatio	ISTD Compounds	IS Ratio	Final Conc.	Units
Acrylamide	3.854	4.042	72.1 -> 55.1	72.1 -> 44.0	659379	56645	8.6	8.5	Acrylamide-C13	5.4094	189.4529	ng/ml

Compound Graphics



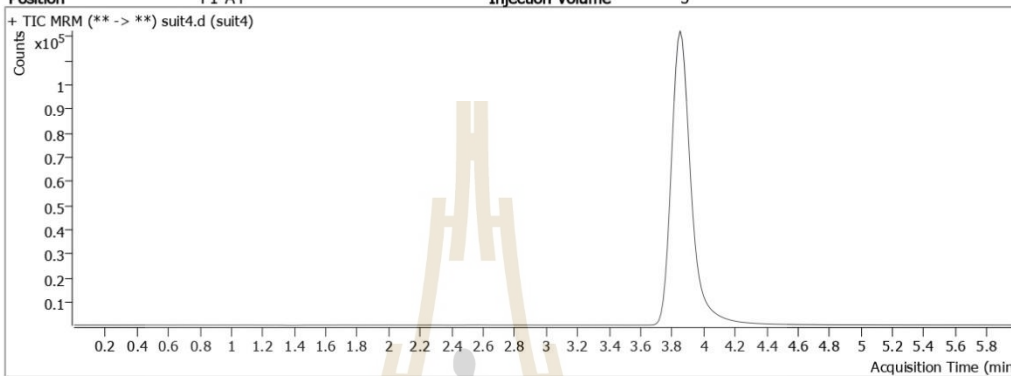
By Sample Quant Report



Batch Path D:\MassHunter\Data\2023\Acrylamide\5-May\20230511+H2o\QuantResults\20230511-n.batch.bin
 Analysis Time 15-May-23 11:27 Analyst Name TH-HPLC25\admin
 Report Time 18-May-23 13:52:10 Reporter Name TH-HPLC25\admin
 Last Calib Update 15-May-23 11:27 Batch State Processed
 Quant Batch Version 10.1 Quant Report Version 10.1

Analysis Info

Instrument 1 Instrument 1 Operator
 Data File suit4.d Sample Name suit4
 Sample Type Sample Dilution 1
 Acq. Method Acrylamide for coffee.m Acq. Date 11-May-23 22:26
 Position P1-A4 Injection Volume 5

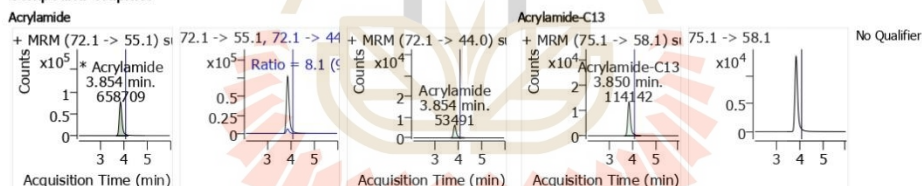


ISTD Compounds	Compound Type	RT	Transition(T)	ISTD Resp.
Acrylamide-C13	ISTD	3.850	75.1 -> 58.1	114142

Quantitation Results

Compound	RT	Ref RT	Transition(T)	Transition(Q)	T-Resp	Q-Resp	QRatio	Ref QRatio	ISTD Compounds	IS Ratio	Final Conc.	Units
Acrylamide	3.854	4.042	72.1 -> 55.1	72.1 -> 44.0	658709	53491	8.1	8.5	Acrylamide-C13	5.7709	201.9437	ng/ml

Compound Graphics



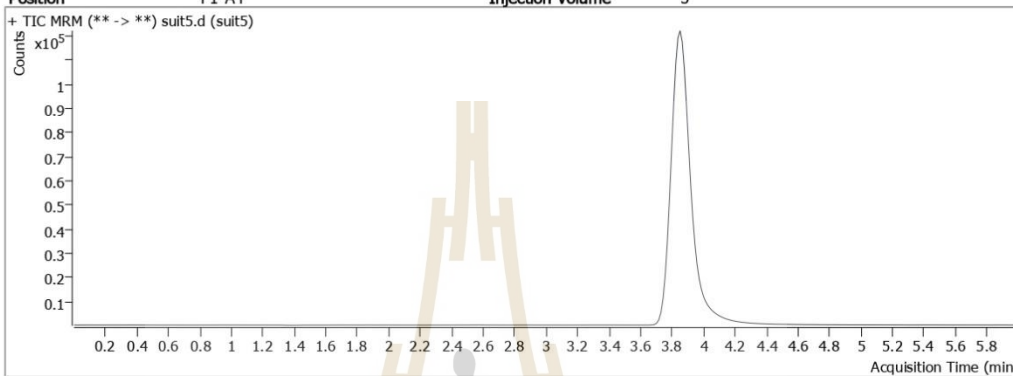
By Sample Quant Report



Batch Path D:\MassHunter\Data\2023\Acrylamide\5-May\20230511+H2o\QuantResults\20230511-n.batch.bin
 Analysis Time 15-May-23 11:27 Analyst Name TH-HPLC25\admin
 Report Time 18-May-23 13:52:12 Reporter Name TH-HPLC25\admin
 Last Calib Update 15-May-23 11:27 Batch State Processed
 Quant Batch Version 10.1 Quant Report Version 10.1

Analysis Info

Instrument 1 Instrument 1 Operator
 Data File suit5.d Sample Name suit5
 Sample Type Sample Dilution 1
 Acq. Method Acrylamide for coffee.m Acq. Date 11-May-23 22:33
 Position P1-A4 Injection Volume 5

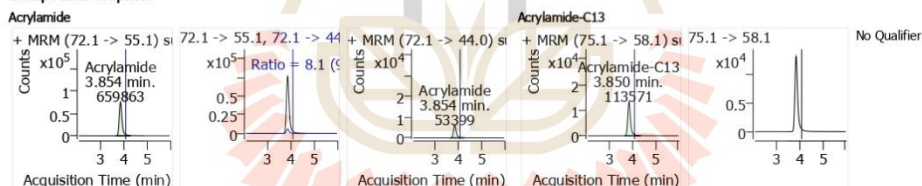


ISTD Compounds	Compound Type	RT	Transition(T)	ISTD Resp.
Acrylamide-C13	ISTD	3.850	75.1 -> 58.1	113571

Quantitation Results

Compound	RT	Ref RT	Transition(T)	Transition(Q)	T-Resp	Q-Resp	QRatio	Ref QRatio	ISTD Compounds	IS Ratio	Final Conc.	Units
Acrylamide	3.854	4.042	72.1 -> 55.1	72.1 -> 44.0	659863	53399	8.1	8.5	Acrylamide-C13	5.8101	203.2973	ng/ml

Compound Graphics



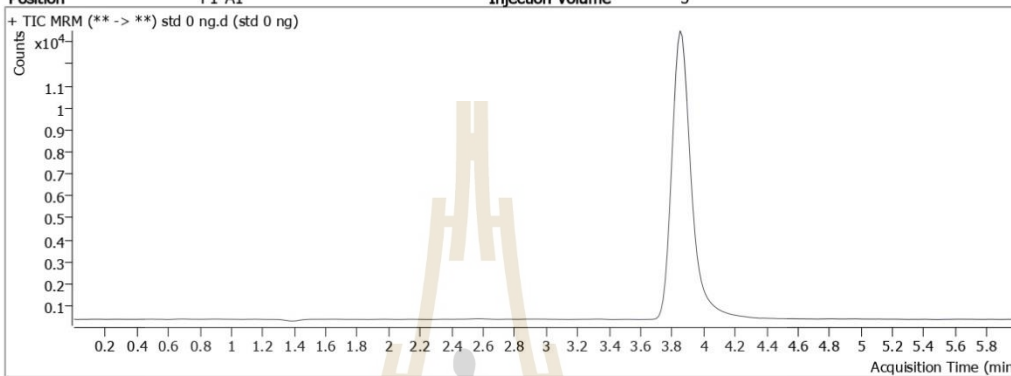
By Sample Quant Report



Batch Path D:\MassHunter\Data\2023\Acrylamide\5-May\20230511+H2o\QuantResults\20230511-n.batch.bin
Analysis Time 15-May-23 11:27 **Analyst Name** TH-HPLC25\admin
Report Time 18-May-23 13:52:14 **Reporter Name** TH-HPLC25\admin
Last Calib Update 15-May-23 11:27 **Batch State** Processed
Quant Batch Version 10.1 **Quant Report Version** 10.1

Analysis Info

Instrument 1 Instrument 1 **Operator**
Data File std 0 ng.d **Sample Name** std 0 ng
Sample Type Sample **Dilution** 1
Acq. Method Acrylamide for coffee.m **Acq. Date** 11-May-23 22:39
Position P1-A1 **Injection Volume** 5

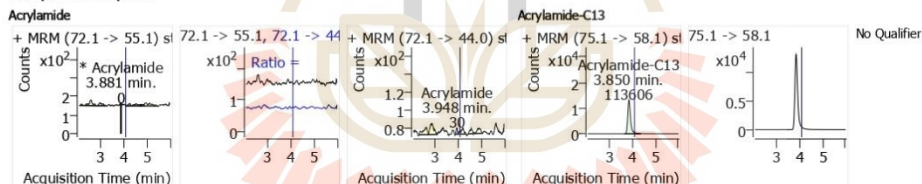


ISTD Compounds	Compound Type	RT	Transition(T)	ISTD Resp.
Acrylamide-C13	ISTD	3.850	75.1 -> 58.1	113606

Quantitation Results

Compound	RT	Ref RT	Transition(T)	Transition(Q)	T-Resp	Q-Resp	QRatio	Ref QRatio	ISTD Compounds	IS Ratio	Final Conc.	Units
Acrylamide	3.881	4.042	72.1 -> 55.1	72.1 -> 44.0	0	30		8.5	Acrylamide-C13	0.0000	ND	ng/ml

Compound Graphics

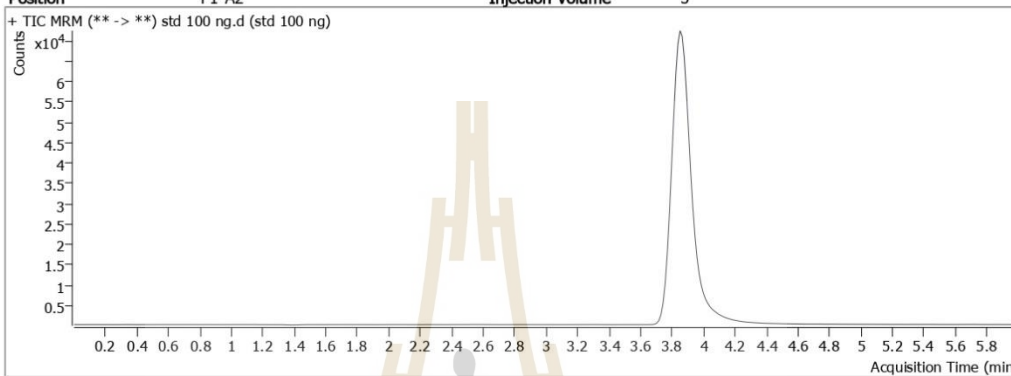


By Sample Quant Report



Batch Path D:\MassHunter\Data\2023\Acrylamide\5-May\20230511+H2o\QuantResults\20230511-n.batch.bin
 Analysis Time 15-May-23 11:27 Analyst Name TH-HPLC25\admin
 Report Time 18-May-23 13:52:16 Reporter Name TH-HPLC25\admin
 Last Calib Update 15-May-23 11:27 Batch State Processed
 Quant Batch Version 10.1 Quant Report Version 10.1

Analysis Info
 Instrument 1 Instrument 1 Operator
 Data File std 100 ng.d Sample Name std 100 ng
 Sample Type Cal Dilution 1
 Acq. Method Acrylamide for coffee.m Acq. Date 11-May-23 22:46
 Position P1-A2 Injection Volume 5

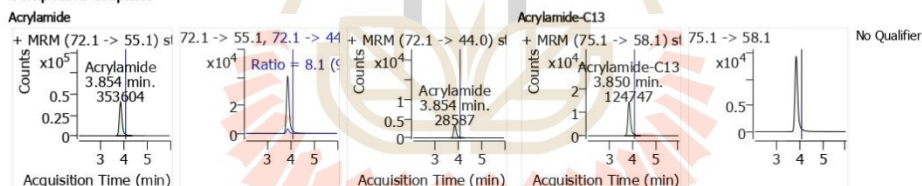


ISTD Compounds	Compound Type	RT	Transition(T)	ISTD Resp.
Acrylamide-C13	ISTD	3.850	75.1 -> 58.1	124747

Quantitation Results

Compound	RT	Ref RT	Transition(T)	Transition(Q)	T-Resp	Q-Resp	QRatio	Ref QRatio	ISTD Compounds	IS Ratio	Final Conc.	Units
Acrylamide	3.854	4.042	72.1 -> 55.1	72.1 -> 44.0	353604	28587	8.1	8.5	Acrylamide-C13	2.8346	100.4843	ng/ml

Compound Graphics



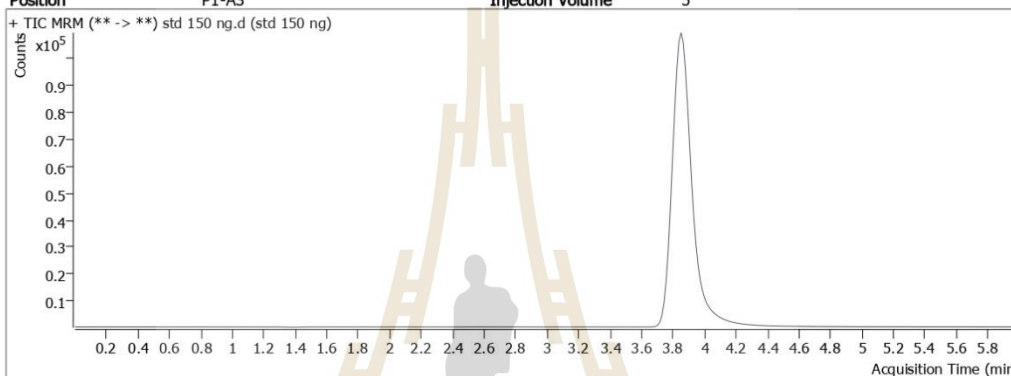
By Sample Quant Report



Batch Path D:\MassHunter\Data\2023\Acrylamide\5-May\20230511+H2o\QuantResults\20230511-n.batch.bin
Analysis Time 15-May-23 11:27 **Analyst Name** TH-HPLC25\admin
Report Time 18-May-23 13:52:18 **Reporter Name** TH-HPLC25\admin
Last Calib Update 15-May-23 11:27 **Batch State** Processed
Quant Batch Version 10.1 **Quant Report Version** 10.1

Analysis Info

Instrument Instrument 1 **Operator**
Data File std 150 ng.d **Sample Name** std 150 ng
Sample Type Cal **Dilution** 1
Acq. Method Acrylamide for coffee.m **Acq. Date** 11-May-23 22:53
Position P1-A3 **Injection Volume** 5

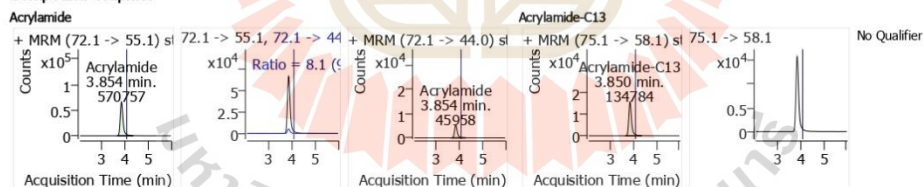


ISTD Compounds	Compound Type	RT	Transition(T)	ISTD Resp.
Acrylamide-C13	ISTD	3.850	75.1 -> 58.1	134784

Quantitation Results

Compound	RT	Ref RT	Transition(T)	Transition(Q)	T-Resp	Q-Resp	QRatio	Ref QRatio	ISTD Compounds	IS Ratio	Final Conc.	Units
Acrylamide	3.854	4.042	72.1 -> 55.1	72.1 -> 44.0	570757	45958	8.1	8.5	Acrylamide-C13	4.2346	148.8588	ng/ml

Compound Graphics



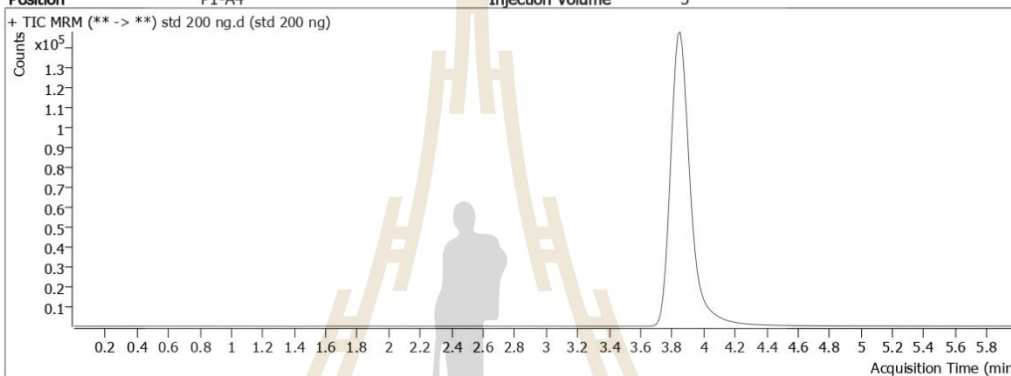
By Sample Quant Report



Batch Path D:\MassHunter\Data\2023\Acrylamide\5-May\20230511+H2o\QuantResults\20230511-n.batch.bin
 Analysis Time 15-May-23 11:27 Analyst Name TH-HPLC25\admin
 Report Time 18-May-23 13:52:20 Reporter Name TH-HPLC25\admin
 Last Calib Update 15-May-23 11:27 Batch State Processed
 Quant Batch Version 10.1 Quant Report Version 10.1

Analysis Info

Instrument Instrument 1 Operator
 Data File std 200 ng.d Sample Name std 200 ng
 Sample Type Cal Dilution 1
 Acq. Method Acrylamide for coffee.m Acq. Date 11-May-23 23:00
 Position P1-A4 Injection Volume 5

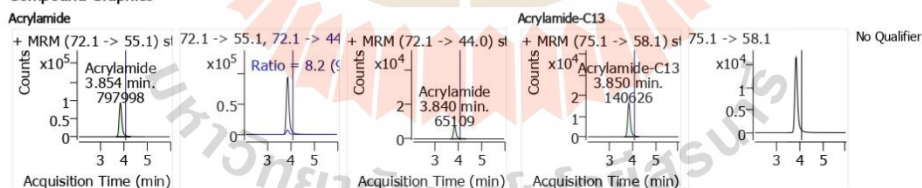


ISTD Compounds	Compound Type	RT	Transition(T)	ISTD Resp.
Acrylamide-C13	ISTD	3.850	75.1 -> 58.1	140626

Quantitation Results

Compound	RT	Ref RT	Transition(T)	Transition(Q)	T-Resp	Q-Resp	QRatio	Ref QRatio	ISTD Compounds	IS Ratio	Final Conc.	Units
Acrylamide	3.854	4.042	72.1 -> 55.1	72.1 -> 44.0	797998	65109	8.2	8.5	Acrylamide-C13	5.6746	198.6150	ng/ml

Compound Graphics



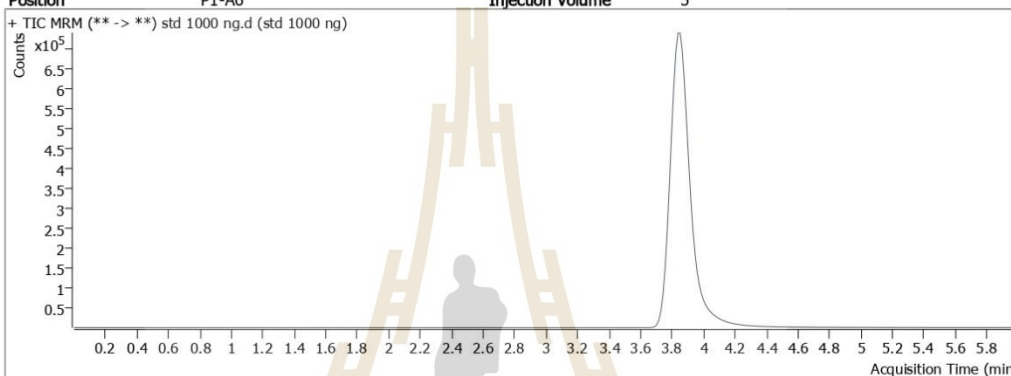
By Sample Quant Report



Batch Path D:\MassHunter\Data\2023\Acrylamide\5-May\20230511+H2o\QuantResults\20230511-n.batch.bin
Analysis Time 15-May-23 11:27 **Analyst Name** TH-HPLC25\admin
Report Time 18-May-23 13:52:24 **Reporter Name** TH-HPLC25\admin
Last Calib Update 15-May-23 11:27 **Batch State** Processed
Quant Batch Version 10.1 **Quant Report Version** 10.1

Analysis Info

Instrument 1 Instrument 1 **Operator**
Data File std 1000 ng.d **Sample Name** std 1000 ng
Sample Type Cal **Dilution** 1
Acq. Method Acrylamide for coffee.m **Acq. Date** 11-May-23 23:13
Position P1-A6 **Injection Volume** 5

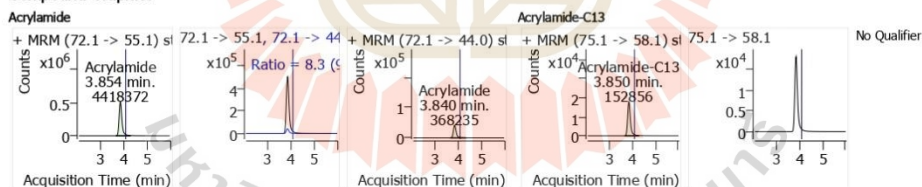


ISTD Compounds	Compound Type	RT	Transition(T)	ISTD Resp.
Acrylamide-C13	ISTD	3.850	75.1 -> 58.1	152856

Quantitation Results

Compound	RT	Ref RT	Transition(T)	Transition(Q)	T-Resp	Q-Resp	QRatio	Ref QRatio	ISTD Compounds	IS Ratio	Final Conc.	Units
Acrylamide	3.854	4.042	72.1 -> 55.1	72.1 -> 44.0	4418372	368235	8.3	8.5	Acrylamide-C13	28.9055	1001.3008	ng/ml

Compound Graphics



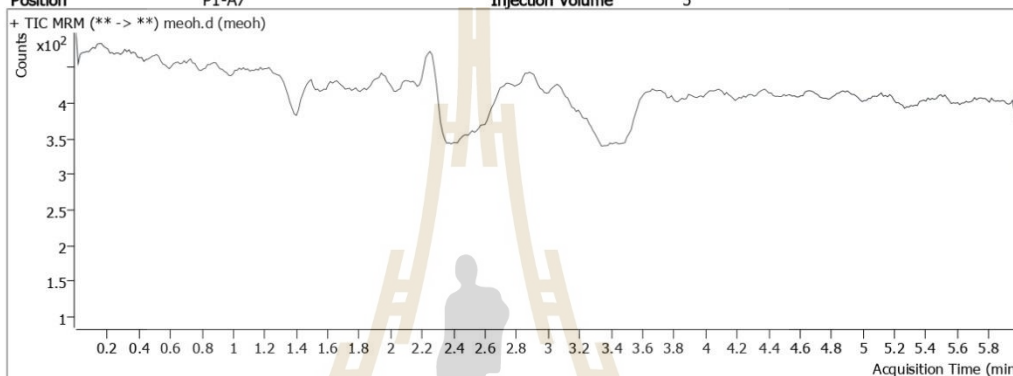
By Sample Quant Report



Batch Path D:\MassHunter\Data\2023\Acrylamide\5-May\20230511+H2o\QuantResults\20230511-n.batch.bin
Analysis Time 15-May-23 11:27 **Analyst Name** TH-HPLC25\admin
Report Time 18-May-23 13:52:26 **Reporter Name** TH-HPLC25\admin
Last Calib Update 15-May-23 11:27 **Batch State** Processed
Quant Batch Version 10.1 **Quant Report Version** 10.1

Analysis Info

Instrument 1 Instrument 1 **Operator**
Data File meoh.d **Sample Name** meoh
Sample Type Sample **Dilution** 1
Acq. Method Acrylamide for coffee.m **Acq. Date** 11-May-23 23:20
Position P1-A7 **Injection Volume** 5

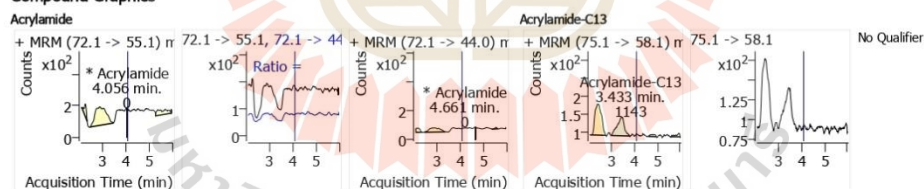


ISTD Compounds	Compound Type	RT	Transition(T)	ISTD Resp.
Acrylamide-C13	ISTD	3.433	75.1 -> 58.1	1143

Quantitation Results

Compound	RT	Ref RT	Transition(T)	Transition(Q)	T-Resp	Q-Resp	QRatio	Ref QRatio	ISTD Compounds	IS Ratio	Final Conc.	Units
Acrylamide	4.056	4.042	72.1 -> 55.1	72.1 -> 44.0	0	0		8.5	Acrylamide-C13	0.0000	ND	ng/ml

Compound Graphics



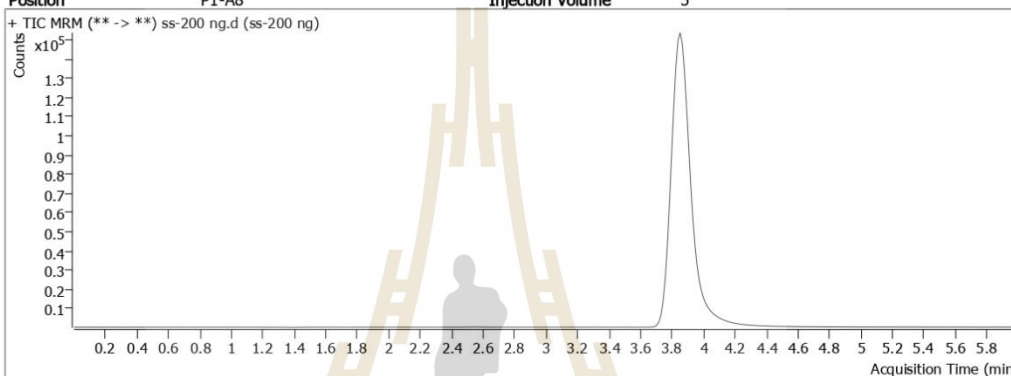
By Sample Quant Report



Batch Path D:\MassHunter\Data\2023\Acrylamide\5-May\20230511+H2o\QuantResults\20230511-n.batch.bin
Analysis Time 15-May-23 11:27 **Analyst Name** TH-HPLC25\admin
Report Time 18-May-23 13:52:28 **Reporter Name** TH-HPLC25\admin
Last Calib Update 15-May-23 11:27 **Batch State** Processed
Quant Batch Version 10.1 **Quant Report Version** 10.1

Analysis Info

Instrument 1 Instrument 1 **Operator**
Data File ss-200 ng.d **Sample Name** ss-200 ng
Sample Type QC **Dilution** 1
Acq. Method Acrylamide for coffee.m **Acq. Date** 11-May-23 23:27
Position P1-A8 **Injection Volume** 5

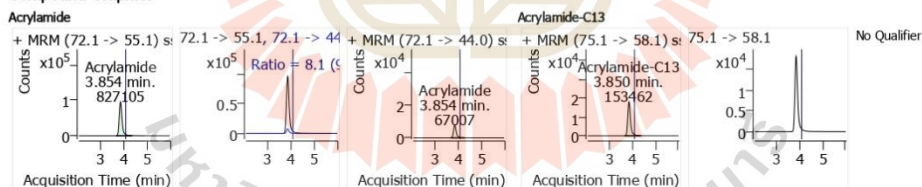


ISTD Compounds	Compound Type	RT	Transition(T)	ISTD Resp.
Acrylamide-C13	ISTD	3.850	75.1 -> 58.1	153462

Quantitation Results

Compound	RT	Ref RT	Transition(T)	Transition(Q)	T-Resp	Q-Resp	QRatio	Ref QRatio	ISTD Compounds	IS Ratio	Final Conc.	Units
Acrylamide	3.854	4.042	72.1 -> 55.1	72.1 -> 44.0	827105	67007	8.1	8.5	Acrylamide-C13	5.3896	188.7682	ng/ml

Compound Graphics



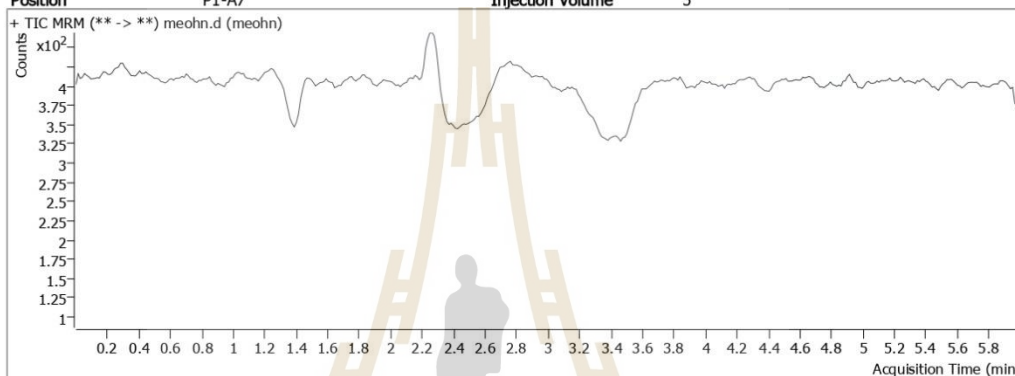
By Sample Quant Report



Batch Path D:\MassHunter\Data\2023\Acrylamide\5-May\20230511+H2o\QuantResults\20230511-n.batch.bin
Analysis Time 15-May-23 11:27 **Analyst Name** TH-HPLC25\admin
Report Time 18-May-23 13:52:31 **Reporter Name** TH-HPLC25\admin
Last Calib Update 15-May-23 11:27 **Batch State** Processed
Quant Batch Version 10.1 **Quant Report Version** 10.1

Analysis Info

Instrument 1 Instrument 1 **Operator**
Data File meohn.d **Sample Name** meohn
Sample Type Sample **Dilution** 1
Acq. Method Acrylamide for coffee.m **Acq. Date** 11-May-23 23:34
Position P1-A7 **Injection Volume** 5

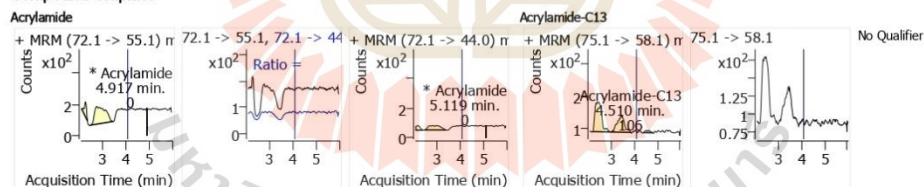


ISTD Compounds	Compound Type	RT	Transition(T)	ISTD Resp.
Acrylamide-C13	ISTD	4.510	75.1 -> 58.1	106

Quantitation Results

Compound	RT	Ref RT	Transition(T)	Transition(Q)	T-Resp	Q-Resp	QRatio	Ref QRatio	ISTD Compounds	IS Ratio	Final Conc.	Units
Acrylamide	4.917	4.042	72.1 -> 55.1	72.1 -> 44.0	0	0		8.5	Acrylamide-C13	0.0000	ND	ng/ml

Compound Graphics



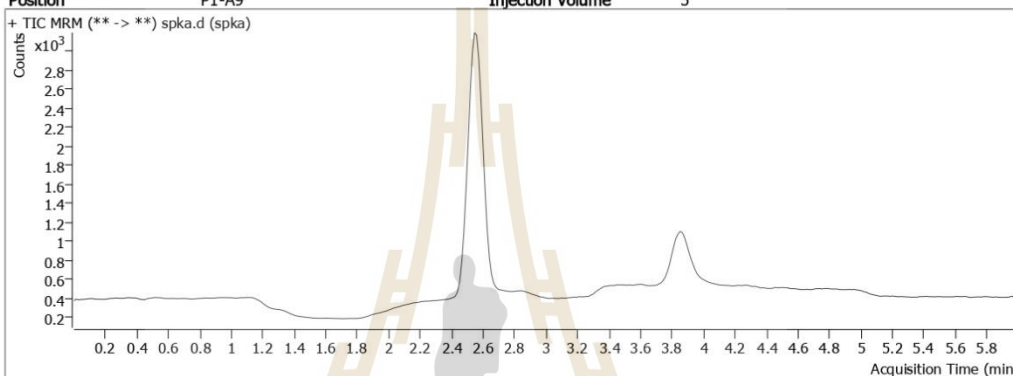
By Sample Quant Report



Batch Path D:\MassHunter\Data\2023\Acrylamide\5-May\20230511+H2o\QuantResults\20230511-n.batch.bin
Analysis Time 15-May-23 11:27 **Analyst Name** TH-HPLC25\admin
Report Time 18-May-23 13:52:33 **Reporter Name** TH-HPLC25\admin
Last Calib Update 15-May-23 11:27 **Batch State** Processed
Quant Batch Version 10.1 **Quant Report Version** 10.1

Analysis Info

Instrument 1 Instrument 1 **Operator**
Data File spka.d **Sample Name** spka
Sample Type QC **Dilution** 1
Acq. Method Acrylamide for coffee.m **Acq. Date** 11-May-23 23:40
Position P1-A9 **Injection Volume** 5

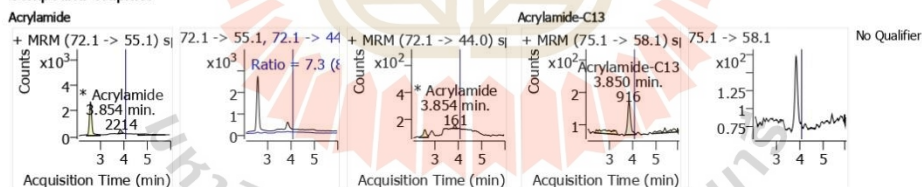


ISTD Compounds	Compound Type	RT	Transition(T)	ISTD Resp.
Acrylamide-C13	ISTD	3.850	75.1 -> 58.1	916

Quantitation Results

Compound	RT	Ref RT	Transition(T)	Transition(Q)	T-Resp	Q-Resp	QRatio	Ref QRatio	ISTD Compounds	IS Ratio	Final Conc.	Units
Acrylamide	3.854	4.042	72.1 -> 55.1	72.1 -> 44.0	2214	161	7.3	8.5	Acrylamide-C13	2.4168	86.0512	ng/ml

Compound Graphics



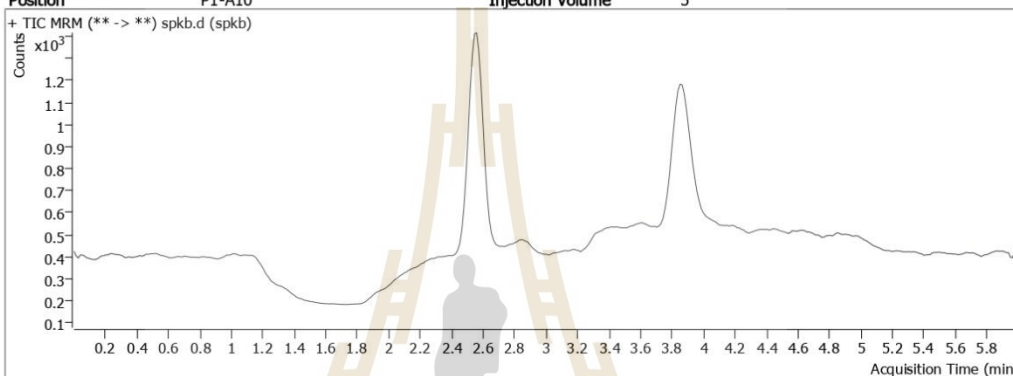
By Sample Quant Report



Batch Path D:\MassHunter\Data\2023\Acrylamide\5-May\20230511+H2o\QuantResults\20230511-n.batch.bin
Analysis Time 15-May-23 11:27 **Analyst Name** TH-HPLC25\admin
Report Time 18-May-23 13:52:35 **Reporter Name** TH-HPLC25\admin
Last Calib Update 15-May-23 11:27 **Batch State** Processed
Quant Batch Version 10.1 **Quant Report Version** 10.1

Analysis Info

Instrument 1 Instrument 1 **Operator**
Data File spkb.d **Sample Name** spkb
Sample Type QC **Dilution** 1
Acq. Method Acrylamide for coffee.m **Acq. Date** 11-May-23 23:47
Position P1-A10 **Injection Volume** 5

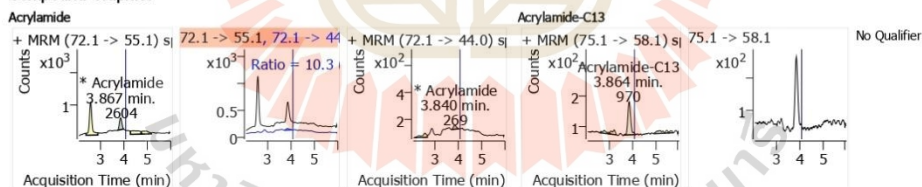


ISTD Compounds	Compound Type	RT	Transition(T)	ISTD Resp.
Acrylamide-C13	ISTD	3.864	75.1 -> 58.1	970

Quantitation Results

Compound	RT	Ref RT	Transition(T)	Transition(Q)	T-Resp	Q-Resp	QRatio	Ref QRatio	ISTD Compounds	IS Ratio	Final Conc.	Units
Acrylamide	3.867	4.042	72.1 -> 55.1	72.1 -> 44.0	2604	269	10.3	8.5	Acrylamide-C13	2.6835	95.2646	ng/ml

Compound Graphics



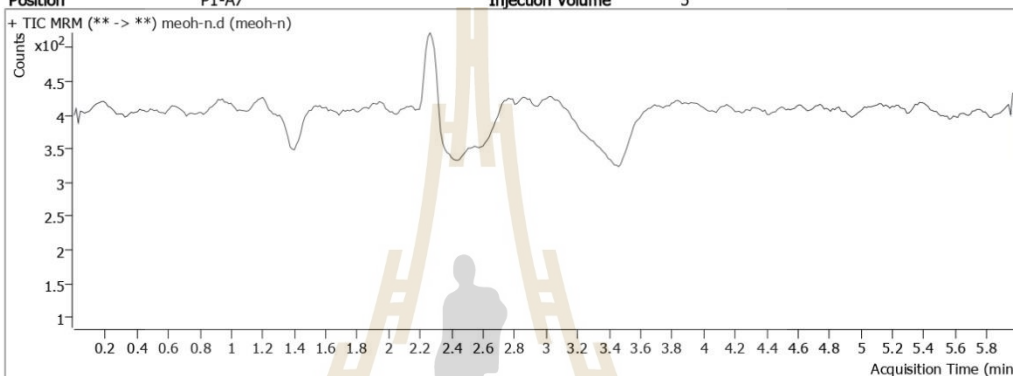
By Sample Quant Report



Batch Path D:\MassHunter\Data\2023\Acrylamide\5-May\20230511+H2o\QuantResults\20230511-n.batch.bin
Analysis Time 15-May-23 11:27 **Analyst Name** TH-HPLC25\admin
Report Time 18-May-23 13:52:37 **Reporter Name** TH-HPLC25\admin
Last Calib Update 15-May-23 11:27 **Batch State** Processed
Quant Batch Version 10.1 **Quant Report Version** 10.1

Analysis Info

Instrument 1 Instrument 1 **Operator**
Data File meoh-n.d **Sample Name** meoh-n
Sample Type Sample **Dilution** 1
Acq. Method Acrylamide for coffee.m **Acq. Date** 11-May-23 23:54
Position P1-A7 **Injection Volume** 5

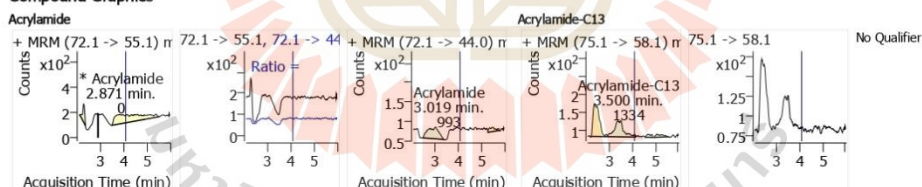


ISTD Compounds	Compound Type	RT	Transition(T)	ISTD Resp.
Acrylamide-C13	ISTD	3.500	75.1 -> 58.1	1334

Quantitation Results

Compound	RT	Ref RT	Transition(T)	Transition(Q)	T-Resp	Q-Resp	QRatio	Ref QRatio	ISTD Compounds	IS Ratio	Final Conc.	Units
Acrylamide	2.871	4.042	72.1 -> 55.1	72.1 -> 44.0	0	993		8.5	Acrylamide-C13	0.0000	ND	ng/ml

Compound Graphics



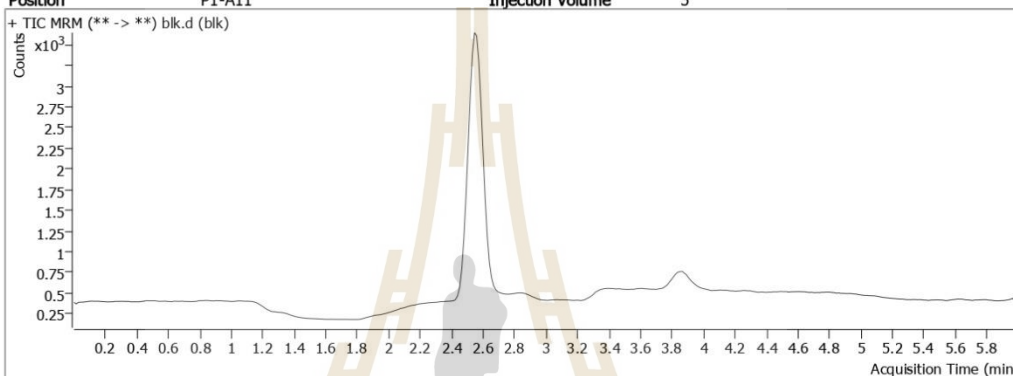
By Sample Quant Report



Batch Path D:\MassHunter\Data\2023\Acrylamide\5-May\20230511+H2o\QuantResults\20230511-n.batch.bin
 Analysis Time 15-May-23 11:27 Analyst Name TH-HPLC25\admin
 Report Time 18-May-23 13:52:39 Reporter Name TH-HPLC25\admin
 Last Calib Update 15-May-23 11:27 Batch State Processed
 Quant Batch Version 10.1 Quant Report Version 10.1

Analysis Info

Instrument 1 Instrument 1 Operator
 Data File blk.d Sample Name blk
 Sample Type Sample Dilution 1
 Acq. Method Acrylamide for coffee.m Acq. Date 12-May-23 0:01
 Position P1-A11 Injection Volume 5

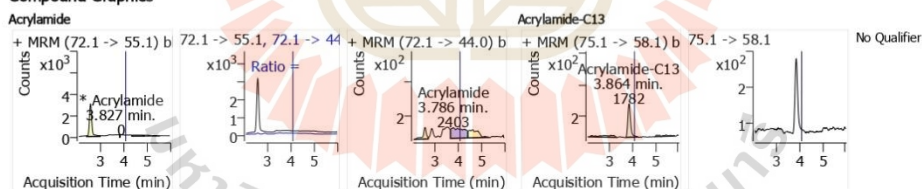


ISTD Compounds	Compound Type	RT	Transition(T)	ISTD Resp.
Acrylamide-C13	ISTD	3.864	75.1 -> 58.1	1782

Quantitation Results

Compound	RT	Ref RT	Transition(T)	Transition(Q)	T-Resp	Q-Resp	QRatio	Ref QRatio	ISTD Compounds	IS Ratio	Final Conc.	Units
Acrylamide	3.827	4.042	72.1 -> 55.1	72.1 -> 44.0	0	2403		8.5	Acrylamide-C13	0.0000	ND	ng/ml

Compound Graphics



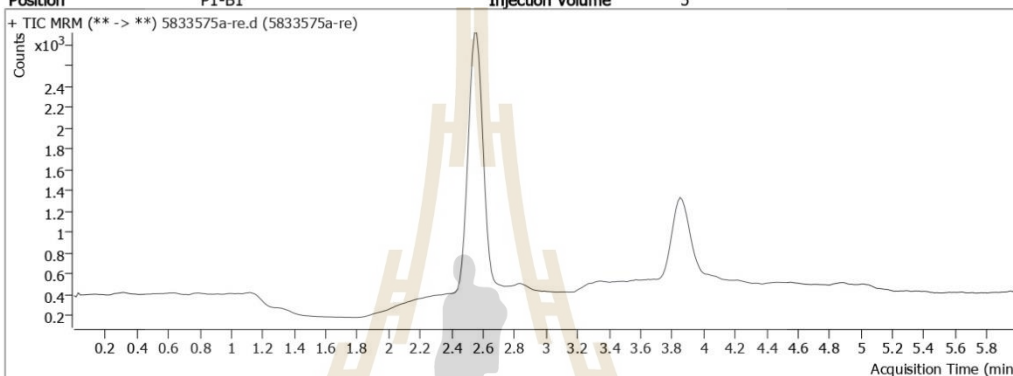
By Sample Quant Report



Batch Path D:\MassHunter\Data\2023\Acrylamide\5-May\20230511+H2o\QuantResults\20230511-n.batch.bin
Analysis Time 15-May-23 11:27 **Analyst Name** TH-HPLC25\admin
Report Time 18-May-23 13:52:41 **Reporter Name** TH-HPLC25\admin
Last Calib Update 15-May-23 11:27 **Batch State** Processed
Quant Batch Version 10.1 **Quant Report Version** 10.1

Analysis Info

Instrument 1 Instrument 1 **Operator**
Data File 5833575a-re.d **Sample Name** 5833575a-re
Sample Type Sample **Dilution** 1
Acq. Method Acrylamide for coffee.m **Acq. Date** 12-May-23 0:08
Position P1-B1 **Injection Volume** 5

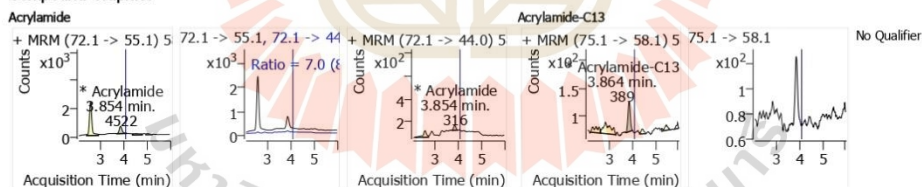


ISTD Compounds	Compound Type	RT	Transition(T)	ISTD Resp.
Acrylamide-C13	ISTD	3.864	75.1 -> 58.1	389

Quantitation Results

Compound	RT	Ref RT	Transition(T)	Transition(Q)	T-Resp	Q-Resp	QRatio	Ref QRatio	ISTD Compounds	IS Ratio	Final Conc.	Units
Acrylamide	3.854	4.042	72.1 -> 55.1	72.1 -> 44.0	4522	316	7.0	8.5	Acrylamide-C13	11.6200	404.0414	ng/ml

Compound Graphics



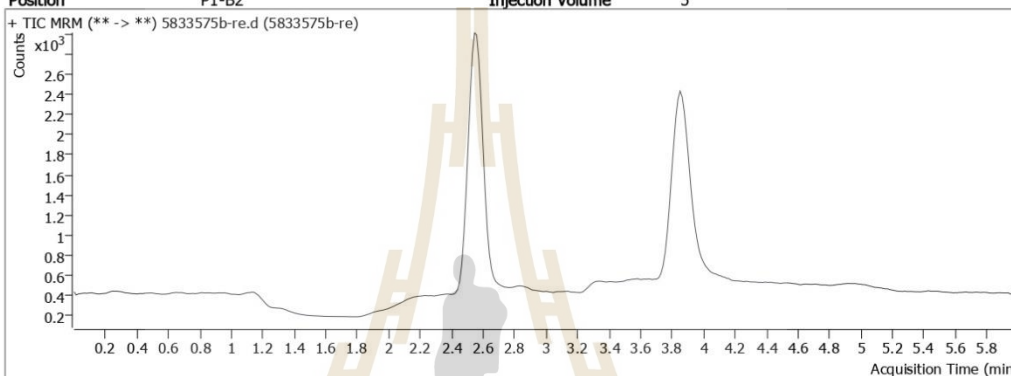
By Sample Quant Report



Batch Path D:\MassHunter\Data\2023\Acrylamide\5-May\20230511+H2o\QuantResults\20230511-n.batch.bin
Analysis Time 15-May-23 11:27 **Analyst Name** TH-HPLC25\admin
Report Time 18-May-23 13:52:43 **Reporter Name** TH-HPLC25\admin
Last Calib Update 15-May-23 11:27 **Batch State** Processed
Quant Batch Version 10.1 **Quant Report Version** 10.1

Analysis Info

Instrument 1 Instrument 1 **Operator**
Data File 5833575b-re.d **Sample Name** 5833575b-re
Sample Type Sample **Dilution** 1
Acq. Method Acrylamide for coffee.m **Acq. Date** 12-May-23 0:14
Position P1-B2 **Injection Volume** 5

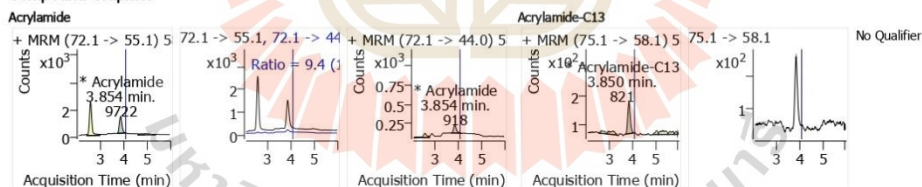


ISTD Compounds	Compound Type	RT	Transition(T)	ISTD Resp.
Acrylamide-C13	ISTD	3.850	75.1 -> 58.1	821

Quantitation Results

Compound	RT	Ref RT	Transition(T)	Transition(Q)	T-Resp	Q-Resp	QRatio	Ref QRatio	ISTD Compounds	IS Ratio	Final Conc.	Units
Acrylamide	3.854	4.042	72.1 -> 55.1	72.1 -> 44.0	9722	918	9.4	8.5	Acrylamide-C13	11.8452	411.8239	ng/ml

Compound Graphics



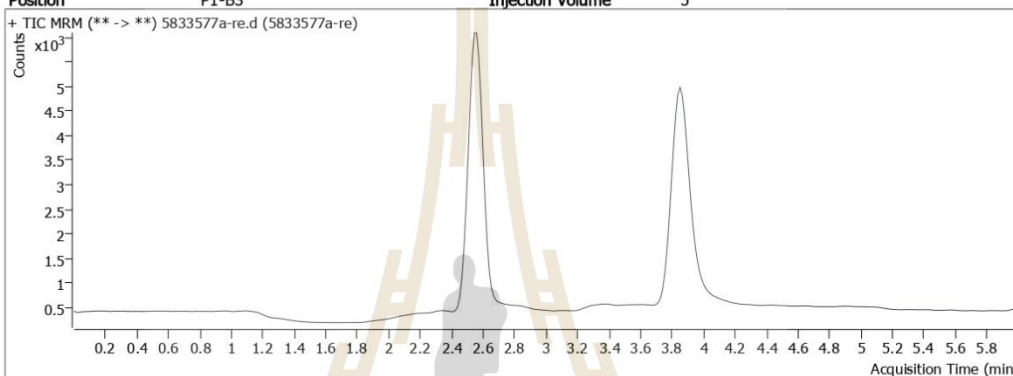
By Sample Quant Report



Batch Path D:\MassHunter\Data\2023\Acrylamide\5-May\20230511+H2o\QuantResults\20230511-n.batch.bin
Analysis Time 15-May-23 11:27 **Analyst Name** TH-HPLC25\admin
Report Time 18-May-23 13:52:45 **Reporter Name** TH-HPLC25\admin
Last Calib Update 15-May-23 11:27 **Batch State** Processed
Quant Batch Version 10.1 **Quant Report Version** 10.1

Analysis Info

Instrument 1 Instrument 1 **Operator**
Data File 5833577a-re.d **Sample Name** 5833577a-re
Sample Type Sample **Dilution** 1
Acq. Method Acrylamide for coffee.m **Acq. Date** 12-May-23 0:21
Position P1-B3 **Injection Volume** 5

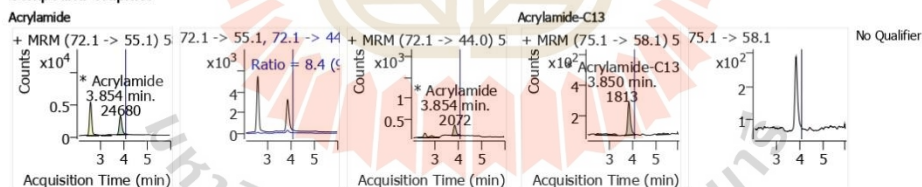


ISTD Compounds	Compound Type	RT	Transition(T)	ISTD Resp.
Acrylamide-C13	ISTD	3.850	75.1 -> 58.1	1813

Quantitation Results

Compound	RT	Ref RT	Transition(T)	Transition(Q)	T-Resp	Q-Resp	QRatio	Ref QRatio	ISTD Compounds	IS Ratio	Final Conc.	Units
Acrylamide	3.854	4.042	72.1 -> 55.1	72.1 -> 44.0	24680	2072	8.4	8.5	Acrylamide-C13	13.6110	472.8354	ng/ml

Compound Graphics



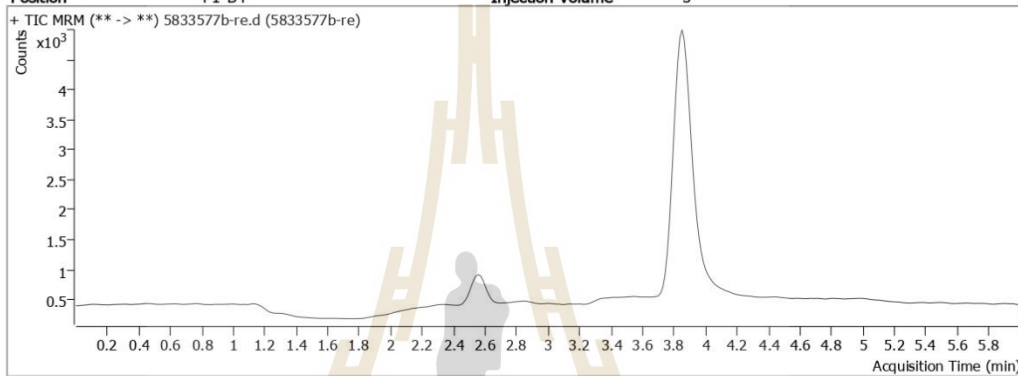
By Sample Quant Report



Batch Path D:\MassHunter\Data\2023\Acrylamide\5-May\20230511+H2o\QuantResults\20230511-n.batch.bin
Analysis Time 15-May-23 11:27 **Analyst Name** TH-HPLC25\admin
Report Time 18-May-23 13:52:47 **Reporter Name** TH-HPLC25\admin
Last Calib Update 15-May-23 11:27 **Batch State** Processed
Quant Batch Version 10.1 **Quant Report Version** 10.1

Analysis Info

Instrument 1 Instrument 1 **Operator**
Data File 5833577b-re.d **Sample Name** 5833577b-re
Sample Type Sample **Dilution** 1
Acq. Method Acrylamide for coffee.m **Acq. Date** 12-May-23 0:28
Position P1-B4 **Injection Volume** 5

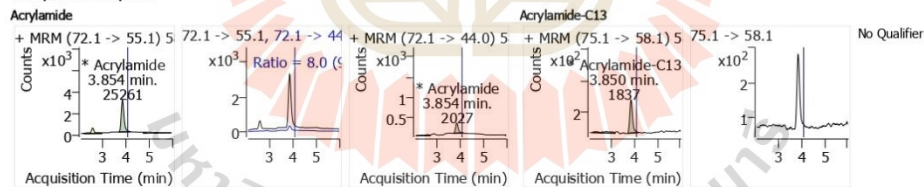


ISTD Compounds	Compound Type	RT	Transition(T)	ISTD Resp.
Acrylamide-C13	ISTD	3.850	75.1 -> 58.1	1837

Quantitation Results

Compound	RT	Ref RT	Transition(T)	Transition(Q)	T-Resp	Q-Resp	QRatio	Ref QRatio	ISTD Compounds	IS Ratio	Final Conc.	Units
Acrylamide	3.854	4.042	72.1 -> 55.1	72.1 -> 44.0	25261	2027	8.0	8.5	Acrylamide-C13	13.7515	477.6919	ng/ml

Compound Graphics



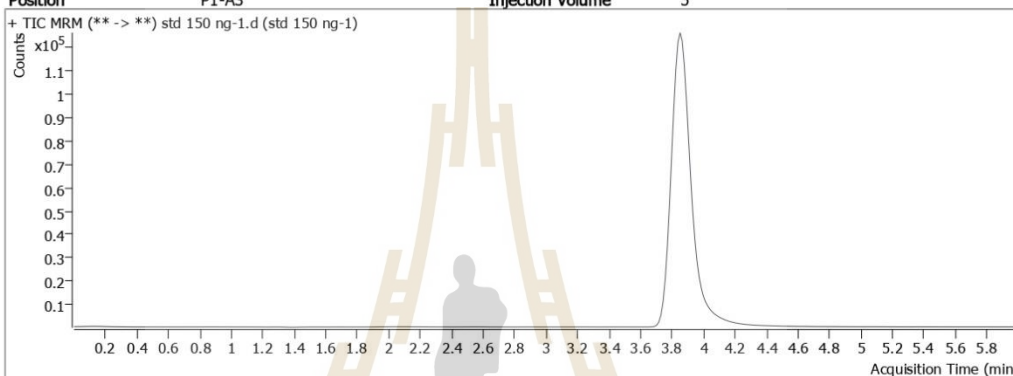
By Sample Quant Report



Batch Path D:\MassHunter\Data\2023\Acrylamide\5-May\20230511+H2o\QuantResults\20230511-n.batch.bin
Analysis Time 15-May-23 11:27 **Analyst Name** TH-HPLC25\admin
Report Time 18-May-23 13:52:49 **Reporter Name** TH-HPLC25\admin
Last Calib Update 15-May-23 11:27 **Batch State** Processed
Quant Batch Version 10.1 **Quant Report Version** 10.1

Analysis Info

Instrument 1 Instrument 1 **Operator**
Data File std 150 ng-1.d **Sample Name** std 150 ng-1
Sample Type QC **Dilution** 1
Acq. Method Acrylamide for coffee.m **Acq. Date** 12-May-23 1:08
Position P1-A3 **Injection Volume** 5

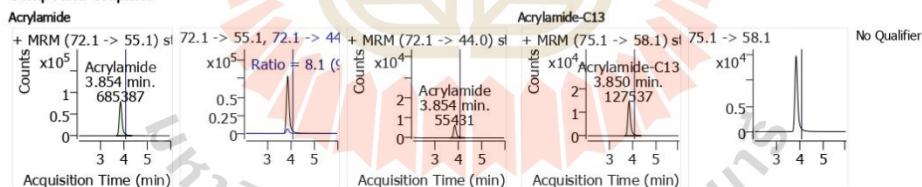


ISTD Compounds	Compound Type	RT	Transition(T)	ISTD Resp.
Acrylamide-C13	ISTD	3.850	75.1 -> 58.1	127537

Quantitation Results

Compound	RT	Ref RT	Transition(T)	Transition(Q)	T-Resp	Q-Resp	QRatio	Ref QRatio	ISTD Compounds	IS Ratio	Final Conc.	Units
Acrylamide	3.854	4.042	72.1 -> 55.1	72.1 -> 44.0	685387	55431	8.1	8.5	Acrylamide-C13	5.3740	188.2298	ng/ml

Compound Graphics



APPENDIX B

Reagents for DNA manipulation

1. Tris-acetate-EDTA (TAE) (50x stock)

The stock of TAE buffer was prepared by dissolving the below ingredients in 700 mL of ultrapure deionized water (UDW)

Tris (Affymetrix, California, USA)	240.0g
EDTA (Affymetrix)	18.6 g
Glacial acetic acid (Merck, New Jersey, USA)	57.1 mL

The pH and the volume were adjusted to 8.3 and 1 L, respectively. The TAE stock was autoclaved. Working TAE (1x) was prepared by diluting 20 mL of the stock buffer with 980 mL of UDW.

2. DNA loading dye (10x)

The DNA loading dye for electrophoresis was prepared by dissolving all of the below ingredients in UDW.

Bromophenol blue (Bio-Rad, California, USA)	240.0 g
Xylene cyanol (Affymetrix)	18.6 g
Glacial acetic acid (Merck)	57.1 mL

The volume was made to 100 mL with UDW.

4. Tris-borate-EDTA (TBE) (5x stock)

The TBE was made from:

Tris-base (Affymetrix)	52.0 g
EDTA (Affymetrix)	4.65 g
Clycerol (Univar, Washington, USA)	27.5 mL

All ingredients were dissolved in 700 mL of UDW. The pH was adjusted to 8.3. The volume was brought up to 1 L with UDW. The preparation was autoclaved. For making 1 L of a working buffer, 200 mL of 5x TBE buffer were added to 800 mL of UDW.

APPENDIX C

Bacterial culture media

1. Luria-Bertani (LB) broth (basal LB broth)

The medium was prepared by dissolving the following ingredients in 1 L of UDW and autoclaved:

Bacto-tryptone (Himedia, Mumbai, India)	10g
Bacto-yeast extract (Himedia)	5g
NaCl (Univar)	5g

2. LB-ampicillin (LB-A) broth

The LB broth prepared as described above was added with ampicillin to a final concentration of 100 ug/mL. The medium was kept at 4°C until use.

3. LB-ampicillin, glucose (LB-AG) broth

One L of the sterilized LB broth was added with ampicillin to the final concentration of 100 ug/mL and 55.6 mL of 2 M glucose. The broth was kept at 4°C until use.

4. LB agar

This agar was prepared by dissolving the following ingredients in 1 L of UDW.

Bacto-tryptone (Himedia)	10g
Bacto-yeast extract (Himedia)	5g
NaCl (Univar)	5g
Agar powder (Himedia)	15 g

The preparation was sterilized by autoclaving. After cooling down to ~ 55-60°C, 25 mL aliquots were poured into 100-mm Petri-dishes. The agar was allowed to be set in a biosafety cabinet. The plates were kept at 4°C. The agar surface was dried appropriately before use.

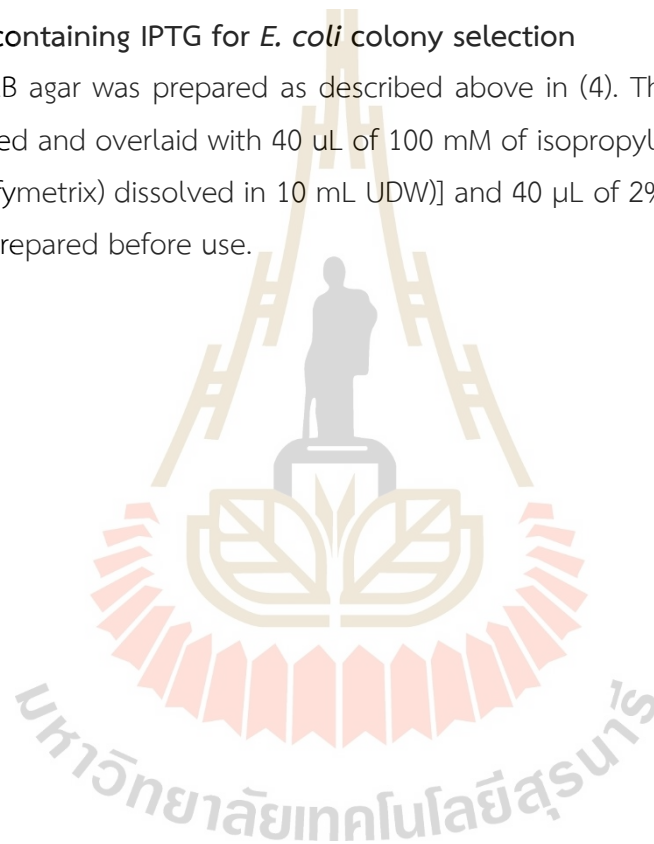
5. LB-ampicillin (LB-Amp), LB-ampicillin-glucose (LB-AG) agar

For preparing the LB-A agar, the LB agar was prepared as described above in (4). After cooling down-55-60°C, ampicillin was added to the final concentration of 100 µg/mL. Twenty-five mL aliquots of the preparation were poured into 100-mm petridishes; the agar was allowed to set and the plates were kept at 4°C until use.

For preparing the LB-AG agar, 55.6 mL of 2 M glucose solution were added to mix with 1 L of the molten LB-A agar. The LB-AG agar plates were prepared as for the LB-A plates.

6. LB-A agar containing IPTG for *E. coli* colony selection

The LB agar was prepared as described above in (4). The surface of the agar plate was dried and overlaid with 40 µL of 100 mM of isopropyl thio-β-D galactoside [(2 g IPTG (Affymetrix) dissolved in 10 mL UDW)] and 40 µL of 2% w/v of This medium was freshly prepared before use.



APPENDIX D

Reagents for protein purification

1.Ni-NTA™ beads for protein purification under native condition

1.1 Buffer C (native lysis Buffer) (100 mM NaH₂PO₄, 10 mM Tris-HCl, 500 mM NaCl, pH 6.3)

All ingredients listed below were dissolved in 700 mL of UDW by stirring.

NaH ₂ PO ₄ .2H ₂ O (Univar)	15.6 g
Tris-HCl (Affymetrix)	1.2 g
NaCl (Univar)	29.2 g

After dissolving completely, the pH was adjusted to 6.3 with 1 M HCl or 1 N NaOH. The volume was brought up to 1 L. The buffer was filtered through an 11- μ m Whatman filter paper.

1.2 Imidazole solution (1 M stock solution)

The imidazole stock solution was prepared by dissolving 20.4 g of imidazole (Affymetrix) in 70 mL of buffer C. After dissolving completely by stirring, the volume was made up to 100 mL by adding buffer C. The solution was filtered through an 11- μ m Whatman filter paper.

1.3 Wash buffer (Buffer C containing 30 mM imidazole)

The wash buffer was prepared by adding 30 mL of imidazole stock solution in 970 mL of buffer C. The homogeneous buffer was filtered through an 11- μ m Whatman filter paper.

1.4 Elution buffer (100 mM NaH₂PO₄, 10 mM Tris-HCl, 500 mM NaCl, 500 mM imidazole, pH 6.3)

This buffer was prepared by adding the stock imidazole solution to Buffer C as described above in (1.2) to a final concentration of 10 mM, 50 mM, 75 mM, 100 mM, 500 mM

APPENDIX E

Reagents for indirect ELISA

1. Coating buffer (0.05 M carbonate-bicarbonate buffer, pH 9.6)

NaHCO₃ (Univar) (4.2 g) was dissolved in 800 mL of UDW. The pH of the preparation was adjusted to 9.6. The volume of the buffer was made up to 1 L with UDW and filtered through an 11-um Whatman filter paper before keeping at 4°C.

2. Phosphate buffered saline (0.01 M PBS, pH 7.4)

The buffer was prepared by dissolving the following ingredients in 900 mL of UDW:

NaCl (Univar)	8 g
KCl (Merck)	0.2 g
Na ₂ HPO ₄ (Univar)	1.44 g
KH ₂ PO ₄ (Univar)	0.24 g

The pH of the preparation was adjusted to 7.4. The volume was made to 1 L with UDW and autoclaved.

3. PBS-T buffer (0.05% Tween-20 in PBS)

One L of PBS was added with 0.5 mL of Tween-20 (Sigma-Aldrich). The solution was sterilized by autoclaving.

4. BSA in PBS (3%)

The preparation was prepared by dissolving 3 g of BSA (Calbiochem) in 100 mL of UDW.

APPENDIX F

Reagents for sodium dodecyl sulfate-polyacrylamide gel electrophoresis (SDS-PAGE) and Western blotting (WB)

1. Reducing sample buffer for SDS-PAGE (6x)

All ingredients listed below were combined and dissolved.

SDS (Affymetrix)	0.6 mg
Bromophenol blue (Bio-Rad, California, USA)	0.5 mg
0.5 M Tris-HCl, pH 8.8 (Affymetrix)	3.75 mL
Glycerol (Univar)	4.6 mL
β -mercaptoethanol (Amersham Biosciences, Little Chalfont, UK)	1.5 mL

The volume was made up to 10 mL with UDW. The solution was kept at -20°C until use. For SDS-PAGE, the sample for gel loading was prepared by mixing 5 parts of the sample with 1 part of the 6x sample buffer.

2. Tris-HCl (1.5 M, pH 8.8)

The solution was prepared by dissolving 181.5 g of Tris-base (Affymetrix) in 500 mL of UDW. The pH was adjusted to 8.8 using 1 N HCl. The volume was adjusted to 1 L with UDW. The solution was filtered through an 11- μm Whatman filter paper and stored at 4°C .

3. Tris-HCl (0.5 M, pH 6.8)

Tris-base (60.5 g) (Affymetrix) was dissolved in 500 mL of UDW. The pH was adjusted to 6.8. The volume was made up to 1 L with UDW. The preparation was filtered through an 11- μm Whatman filter paper and kept at 4°C .

4. Sodium dodecyl sulfate solution (10% SDS)

The solution was prepared by dissolving 10% (w/v) of SDS (Affymetrix) in 100 mL of UDW. The solution was filtered through an 11- μm Whatman filter paper.

5. Ammonium persulfate solution (10%)

The solution was freshly prepared by dissolving 50 mg of ammonium persulfate (Bio-Rad) in 0.5 mL of UDW.

6. Polyacrylamide resolving gel (12%)

All ingredients listed below were mixed and added with 50 μ L of 10% ammonium persulfate and 5 μ L of TEMED just before pouring into the gel casting apparatus (Bio-Rad). The gel was overlaid with UDW and polymerized.

Tris-HCl (1.5 M, pH 8.8) (Affymetrix)	2.5 mL
SDS (10%) (Affymetrix)	0.1 mL
Acrylamide solution (30%) (Bio-Rad)	4.0 mL
UDW	3.5 mL

7. Polyacrylamide resolving gel (4%)

All ingredients listed below were mixed and added with 50 μ L of 10% ammonium persulfate and 5 μ L of TEMED just before pouring into the gel casting apparatus.

Tris-HCl (0.5 M, pH 6.8) (Affymetrix)	2.5 mL
SDS (10%) (Affymetrix)	0.1 mL
Acrylamide solution (30%) (Bio-Rad)	1.3 mL
UDW	6.2 mL

A comb was placed into the gel before allowing the gel to polymerize.

8. SDS electrophoresis buffer (10x)

The buffer was prepared by dissolving 30.3 g of Tris (Affymetrix), 144 g glycine (Affymetrix), and 10 g of SDS in 1 L of UDW. The working buffer was made by diluting the 10x stock buffer to 1xbuffer using UDW.

9. Transfer buffer

Tris (3.03 g) and 14.4 mL glycine (Affymetrix) were dissolved in 900 mL of UDW. The preparation was added with 100 mL of methanol (Affymetrix) and mixed well.

APPENDIX G

1. Clone N11.1 alignment by Bio edit program

```

Alignment: C:\Users\Acer\Desktop\N11.1 new.1.1

      5      15      25      35      45      55
ATGC_AG086 AGCCGCCAT GGCGCAGGTT ACTCTGAAAAG AGTCTGGCCC TGGGATATTG CAGCCCTCCC
ATGC_AG086 AGCCGCCAT GGCGCAGGTT ACTCTGAAAAG AGTCTGGCCC TGGGATATTG CAGCCCTCCC

      65      75      85      95     105     115
ATGC_AG086 AGACCCCTCAG TCTGACTTGT TCTTTCTCTG GGTTTTCACT GAACACTTCT GGTATGGGTG
ATGC_AG086 AGACCCCTCAG TCTGACTTGT TCTTTCTCTG GGTTTTCACT GAACACTTCT GGTATGGGTG

      125     135     145     155     165     175
ATGC_AG086 TGAGCTGGAT TCGTCAGCCT TCAGGAAAAGG GTCTGSAAGTG GCTGGCACAC ATTTACTGGG
ATGC_AG086 TGAGCTGGAT TCGTCAGCCT TCAGGAAAAGG GTCTGSAAGTG GCTGGCACAC ATTTACTGGG

      185     195     205     215     225     235
ATGC_AG086 ATGATGACAA GCGCTATAAT CCATCCCTGA AGAGCCGGCT CACAATCTCC AAGGATACCT
ATGC_AG086 ATGATGACAA GCGCTATAAT CCATCCCTGA AGAGCCGGCT CACAATCTCC AAGGATACCT

      245     255     265     275     285     295
ATGC_AG086 CCAGAAACCA GTTATTCTCT AAGATCACCA GTGTGSAACAC TGCAGATACT GCCACATACT
ATGC_AG086 CCAGAAACCA GTTATTCTCT AAGATCACCA GTGTGSAACAC TGCAGATACT GCCACATACT

      305     315     325     335     345     355
ATGC_AG086 ACTGTGCTCG AACGGGGGAC TATGATTACG ACGACCCGGT TGCTTACTGG GGCCAAGGGA
ATGC_AG086 ACTGTGCTCG AACGGGGGAC TATGATTACG ACGACCCGGT TGCTTACTGG GGCCAAGGGA

      365     375     385     395     405     415
ATGC_AG086 CTCTGGTCAC TGTCTCTGCA GCCAAAACGA CACCCCAAAA GCTTGAAGAA GGTGAATTTT
ATGC_AG086 CTCTGGTCAC TGTCTCTGCA GCCAAAACGA CACCCCAAAA GCTTGAAGAA GGTGAATTTT

      425     435     445     455     465     475
ATGC_AG086 CAGAAGCACG CGTAGATATT GTGATAACCC AGSATGAACT CTCCAATCCT GTCACCTCTG
ATGC_AG086 CAGAAGCACG CGTAGATATT GTGATAACCC AGSATGAACT CTCCAATCCT GTCACCTCTG

      485     495     505     515     525     535
ATGC_AG086 GAGAATCAGT TTCCATCTCC TGCAGGTCTA GTAAGAGTCT CCTATATAAG GATGGGAAGA
ATGC_AG086 GAGAATCAGT TTCCATCTCC TGCAGGTCTA GTAAGAGTCT CCTATATAAG GATGGGAAGA

      545     555     565     575     585     595
ATGC_AG086 CATACTTGAA TTGGTTTCTG CAGAGACCAG GACAATCTCC TCACTCTCTG ATCTATTTGA
ATGC_AG086 CATACTTGAA TTGGTTTCTG CAGAGACCAG GACAATCTCC TCACTCTCTG ATCTATTTGA

      605     615     625     635     645     655
ATGC_AG086 TGTCCACCCG TGCATCAGGA GTCTCAGACC GGTTTAGTGG CAGTGGGTCA GSAACAGATT
ATGC_AG086 TGTCCACCCG TGCATCAGGA GTCTCAGACC GGTTTAGTGG CAGTGGGTCA GSAACAGATT

      665     675     685     695     705     715
ATGC_AG086 TCACCTGGA AATCAGTAGA GTGAAGGCTG AGSATGTGGG TGTGTATTAC TGTCAACAAC
ATGC_AG086 TCACCTGGA AATCAGTAGA GTGAAGGCTG AGSATGTGGG TGTGTATTAC TGTCAACAAC

      725     735     745     755     765     775
ATGC_AG086 TTGTAGAGTA TCCTCGCACG TTCGGAGGGG GGACCAAGCT GSAATAAAAA CGGGCTGATG
ATGC_AG086 TTGTAGAGTA TCCTCGCACG TTCGGAGGGG GGACCAAGCT GSAATAAAAA CGGGCTGATG

      785     795     805     815     825     835
ATGC_AG086 CTGCACCAAC TGTATCCGCG GCCGCTGGAT CCAAAGATAT CAGAGCTGAA ACTGTTGAAA
ATGC_AG086 CTGCACCAAC TGTATCCGCG GCCGCTGGAT CCAAAGATAT CAGAGCTGAA ACTGTTGAAA

      845     855     865     875     885     895
ATGC_AG086 GTTGTTTAGC AAAATCCCAT ACAGAAAATT CATTACTAA CGTCTGGAAA GACGACA
ATGC_AG086 GTTGTTTAGC AAAATCCCAT ACAGAAAATT CATTACTAA CGTCTGGAAA GACGACA

```

2.Restriction sites Muscfv

NcoI--VH--HindIII + linker + MluI--VL--NotI

2.1 Clone N11.1 alignment was checked restriction sites Muscfv of position.

AGCCGG **CCATGG**CGCAGGTTACTCTGAAAGAGTCTGGCCCTGGGATATTGCAGCCCTCCCAGA
 CCCTCAGTCTGACTTGTCTTTCTCTGGGTTTTCACTGAACACTTCTGGTATGGGTGTGAGCTG
 GATTCGTCAGCCTTCAGGAAAGGGTCTGGAGTGGCTGGCACACATTTACTGGGATGATGACAAG
 CGCTATAATCCATCCCTGAAGAGCCGGCTCACAATCTCCAAGGATACCTCCAGAAACCAGTTAT
 TCCTCAAGATCACCAGTGTGGACACTGCAGATACTGCCACATACTACTGTGCTCGAACGGGGGA
 CTATGATTACGACGACCGGTTTGCTTACTGGGGCCAAGGACTCTGGTCACTGTCTCTGCAGCC
 AAAACGACACCCCCA **AAGCTT**GAAGAAGGTGAATTTTCAGAAGC **ACGCGT**AGATATTGTGA
 TAACCCAGGATGAACTCTCCAATCCTGTCACTTCTGGAGAATCAGTTTCCATCTCCTGCAGGTC
 TAGTAAGAGTCTCCTATATAAGGATGGGAAGACATACTTGAATTGGTTTCTGCAGAGACCAGGA
 CAATCTCCTCAGCTCCTGATCTATTTGATGTCCACCCGTGCATCAGGAGTCTCAGACCGGTTTA
 GTGGCAGTGGGTCAGGAACAGATTTACCCCTGGAAATCAGTAGAGTGAAGGCTGAGGATGTGG
 GTGTGTATTACTGTCAACAACCTGTAGAGTATCCTCGCACGTTCCGGAGGGGGACCAAGCTGGA
 AATAAACGGGCTGATGCTGCACCAACTGTATCC **GCGGCCGCT**GGATCCAAAGATATCAGAGCT
 GAAACTGTTGAAAGTTGTTTAGCAAATCCCATACAGAAAATTCATTTACTAACGTCTGGAAAG
 ACGACA

2.2 DNA of clone N11.1 translate to amino acid summit online by

<https://web.expasy.org/translate/>

MAQVTLKESGPGILQPSQTLSTCSFSGFSLNTSGMGVSWIRQPSGKLEWLAHYIYWDD
 DKRYNPSLKSRLTISKDTSRNQLFLKITSVDTADTATYYCARTGDYDYDDRFAYWGQGLVTVSAA
 KTTTPKLEEGEFSEARVDIVITQDELSPVTSGESVVSISCRSSKSLLYKDGKTYLNWFLQRPQGSPQ
 LLIYLMSTRASGVSDRFSGSGSGTDFLTLEISRVAEDVGVVYCOQLVEYPRTFGGGTKLEIK

VITAE

Name-Surname Sukanya Ponphimai
Affiliation Bachelor of Public Health Program in community, Faculty of Allied Health Sciences, Nakhon Ratchasima College, Thailand
Present Positions Lecturer

Contact

TELEPHONE: 044 466 051
 MOBILE: 097 3371777
 FACSIMILE: 044 65668
 Email: Sukanya.p@g.sut.ac.th

Education:

2007 High school. Phimai Wittaya School Phimai District, Nakhon Ratchasima Province, Thailand
 2012 Bachelor of Science in Public Health (Public Health), Faculty of Public Health, Vongchavalitkul University, Thailand
 2017 Master of Public Health Program in Nutrition for Health, Faculty of Public Health, Khon Kaen University, Thailand
 2018-present Master of Science and Doctor of Philosophy Program in Translational Medicine (International Program), Suranaree University of Technology, Thailand

Employment History:

2013 Teaching Assistants, Faculty of Public Health Vongchavalitkul University, Nakhon Ratchasima Province, Thailand
 2018 Researcher, Parasitic Disease Research Center, Institute of Medicine, Suranaree University of Technology, Nakhon Ratchasima, Thailand

- 2020 Public health academic, Phimai District Public Health Office, Phimai District, Nakhon Ratchasima Province, Thailand
- 2024 Lecturer, Bachelor of Public Health Program in community, Faculty of Allied Health Sciences, Nakhon Ratchasima College, Thailand

Publications:

1. **Sukanya Ponphimai**, Nitchatorn Panoma Perception Regarding Supplementary Food Consumption Among Sung Noen Hospital Elderly Club, Nakhon Ratchasima, Thailand
2. Kaewpitoon SJ, Rujirakul R, Loyd RA, Panpimanmas S, Matrakool L, Tongtawee T, Komporn P, Norkaew J, Chavengkun W, Wakkhuwattapong P, Kujapun J, **Ponphimai S**, Phatisena T, Eaksunti T, Polsripradist P, Joosiri A, Sukkasam I, Padchasuwan N, Kaewpitoon N. Surveillance of Populations at Risk of Cholangiocarcinoma Development in Rural Communities of Thailand Using the Korat-CCA Verbal Screening Test. *Asian Pac J Cancer Prev.* 2016;17(4):2205-9. PubMed PMID: 27221919.
3. Kaewpitoon SJ, Rujirakul R, Sangkudloa A, Kaewthani S, Khemplila K, Cherdjirapong K, Kujapun J, Norkaew J, Chavengkun W, **Ponphimai S**, Polsripradist P, Padchasuwan N, Joosiri A, Wakkhuwattapong P, Loyd RA, Matrakool L, Tongtawee T, Panpimanmas S, Kaewpitoon N. Distribution of the Population at Risk of Cholangiocarcinoma in Bua Yai District, Nakhon Ratchasima of Thailand Using Google Map. *Asian Pac J Cancer Prev.* 2016;17(3):1433-6. PubMed PMID: 27039785.
4. Kaewpitoon SJ, Kaewpitoon N, Rujirakul R, Wakkhuwattapong P, Matrakool L, Tongtawee T, Loyd RA, Norkaew J, Kujapun J, Chavengkun W, **Ponphimai S**, Polsripradist P, Eksanti T, Phatisena T. Nurses and Television as Sources of Information Effecting Behavioral Improvement Regarding Liver Flukes in Nakhon Ratchasima Province, Thailand. *Asian Pac J Cancer Prev.* 2016;17(3):1097-102. PubMed PMID: 27039731.
5. Komporn P, Muang Karn R, Norkaew J, Kujapun J, Photipim M, **Ponphimai S**, Chavengkun W, Phong Paew S, Kaewpitoon S, Rujirakul R, Wakkhuwattapong P, Phatisena T, Eaksanti T, Joosiri A, Polsripradist P, Padchasuwan N, Kaewpitoon N. Population-Based Intervention for Liver Fluke Prevention and Control in Muang

- Yang District, Nakhon Ratchasima Province, Thailand. *Asian Pac J Cancer Prev.* 2016;17(2):685-9. PubMed PMID: 26925664.
6. Mongsawaeng C, Kokorn N, Kujapun J, Norkaew J, Kootanavanichpong N, Chavenkun W, **Ponphimai S**, Kaewpitoon SJ, Tongtawee T, Padchasuwan N, Pengsaa P, Komporn P, Kaewpitoon N. Knowledge, Attitude, and Practice Regarding Cervical Cancer among Rural Community Women in Northeast Thailand. *Asian Pac J Cancer Prev.* 2016;17(1):85-8. PubMed PMID: 26838259.
 7. Kaewpitoon SJ, Loyd RA, Rujirakul R, Panpimanmas S, Matrakool L, Tongtawee T, Kootanavanichpong N, Pengsaa P, Komporn P, Chavengkun W, Kujapun J, Norkaew J, **Ponphimai S**, Padchasuwan N, Polsripradist P, Eksanti T, Phatisena T, Kaewpitoon N. Helicobacter Species are Possible Risk Factors of Cholangiocarcinoma. *Asian Pac J Cancer Prev.* 2016;17(1):37-44. PubMed PMID: 26838240.
 8. Kaewpitoon SJ, Rujirakul R, Loyd RA, Panpimanmas S, Matrakool L, Tongtawee T, Komporn P, Norkaew J, Chavengkun W, Kujapun J, **Ponphimai S**, Phatisena T, Eksanti T, Polsripradist P, Padchasuwan N, Kaewpitoon N. Re-Examination of *Opisthorchis viverrini* in Nakhon Ratchasima Province, Northeastern Thailand, Indicates Continued Needs for Health Intervention. *Asian Pac J Cancer Prev.* 2016;17(1):231-4. PubMed PMID: 26838215.
 9. Kaewpitoon SJ, Loyd RA, Rujirakul R, Panpimanmas S, Matrakool L, Tongtawee T, Kootanavanichpong N, Komporn P, Chavengkun W, Kujapun J, Norkaew J, **Ponphimai S**, Padchasuwan N, Pholsripradit P, Eksanti T, Phatisena T, Kaewpitoon N. Benefits of Metformin Use for Cholangiocarcinoma. *Asian Pac J Cancer Prev.* 2015;16(18):8079-83. PubMed PMID: 26745042.
 10. Padchasuwan N, Kaewpitoon SJ, Rujirakul R, Wakkuwattapong P, Norkaew J, Kujapun J, **Ponphimai S**, Chavenkun W, Komporn P, Kaewpitoon N. Modifying Health Behavior for Liver Fluke and Cholangiocarcinoma Prevention with the Health Belief Model and Social Support Theory. *Asian Pac J Cancer Prev.* 2016;17(8):3721-5. Review. PubMed PMID: 27644606.
 11. Kaewpitoon SJ, Rujirakul R, Wakkuwattapong P, Benjaoran F, Norkaew J, Kujapun J, **Ponphimai S**, Chavenkun W, Komporn P, Padchasuwan N, Kaewpitoon N. Development of a Health Education Modification Program Regarding Liver Flukes and Cholangiocarcinoma in High-Risk Areas of Nakhon Ratchasima Province Using

- Self-Efficacy and Motivation Theory. *Asian Pac J Cancer Prev.* 2016;17(6):2947-51. PubMed PMID: 27356716.
12. Phatisena P, Eaksanti T, Wichantuk P, Tritipsombut J, Kaewpitoon SJ, Rujirakul R, Wakkhuwattapong P, Tongtawee T, Matrakool L, Panpimanmas S, Norkaew J, Kujapun J, Chavengkun W, Komporn P, Pothipim M, **Ponphimai S**, Padchasuwan N, Kaewpitoon N. Behavioral Modification Regarding Liver Fluke and Cholangiocarcinoma with a Health Belief Model Using Integrated Learning. *Asian Pac J Cancer Prev.* 2016;17(6):2889-94. PubMed PMID: 27356708.
 13. Chavengkun W, Komporn P, Norkaew J, Kujapun J, Pothipim M, **Ponphimai S**, Kaewpitoon SJ, Padchasuwan N, Kaewpitoon N. Raw Fish Consuming Behavior Related to Liver Fluke Infection among Populations at Risk of Cholangiocarcinoma in Nakhon Ratchasima Province, Thailand. *Asian Pac J Cancer Prev.* 2016;17(6):2761-5. PubMed PMID: 27356687.
 14. Kaewpitoon SJ, Rujirakul R, Wakkhuwattapong P, Matrakool L, Tongtawee T, Panpimanmas S, Kujapun J, Norkaew J, Pothipim M, **Ponphimai S**, Chavengkun W, Komporn P, Padchasuwan N, Sawaspol S, Phandee MC, Phandee W, Phanurak W, Kaewpitoon N. Overweight Relation to Liver Fluke Infection among Rural Participants from 4 Districts of Nakhon Ratchasima Province, Thailand. *Asian Pac J Cancer Prev.* 2016;17(5):2565-71. PubMed PMID: 27268631.

Training and certificate

1. "Fundamentals of raising and using animals for scientific purposes According to international standards" organized by The Center for Scientific and Technological Equipment Suranaree University of Technology during July 17, 2018
2. "Good clinical practice: GCP Training" organized by Suranaree University of Technology, Thailand during June 21-22, 2018
3. Has successfully and Passed the "CREATING HAPPINESS WITH POSITIVE PSYCHOLOGY" organized by Institute of Medicine, Suranaree University of Technology during October 10, 2019
4. Workshop: Iron and Blood Analysis organized by Thai Nguyen University of Medicine and Pharmacy Thai Nguyen, Vietnam during October 25t till 31, 2015
5. Human Ethics Committee of Thammasat University (Medicine)

Certifies that Has Complete the GCP online training (Computer-based)

"Good Clinical Practice (ICH-GCP: E6(R2))" This certificate is effective from February 20, 2024 to February 20, 2026

6. “ผู้ขออนุญาตใช้สัตว์เพื่องานทางวิทยาศาสตร์” organized by Institute for Animals for Scientific Purpose Development (IAD) National Research Council of Thailand (NRCT) during July 4-5, 2018
7. โครงการพัฒนาบุคลากรสู่ความเป็นเลิศทางวิชาการและนวัตกรรม คบสอ.พิมาย ปี 2563 หลักสูตรต่อเนื่อง เรื่องการวิจัย และ R2R คุณภาพ ณ โรงพยาบาลพิมาย ระหว่างวันที่ 15 มิถุนายน - 28 กันยายน 2563
8. การอบรมการจัดการน้ำหนักรเด็กวัยเรียน Smart kid Coacher ณ ศูนย์อนามัยที่ 9 นครราชสีมา ระหว่างวันที่ 15-16 ธันวาคม 2563
9. การฝึกอบรมตามหลักสูตร การอบรมจรรยาบรรณการใช้สัตว์เพื่องานทางวิทยาศาสตร์ขนาดเล็ก (หนูเมาส์ หนูแรท และกระต่าย) ณ ศูนย์เครื่องมือวิทยาศาสตร์และเทคโนโลยี มหาวิทยาลัยเทคโนโลยีสุรนารี ระหว่างวันที่ วันที่ 22 กันยายน 2564
10. การฝึกอบรมหลักสูตร "ความปลอดภัยทางชีวภาพ (Biosafety) และการรักษาความปลอดภัยทางชีวภาพ (Biosecurity)" (เลขทะเบียนรับรองหลักสูตรจากกรมวิทยาศาสตร์การแพทย์ที่ สธ 0621.06/140) ณ สถาบันวิจัยและพัฒนา มหาวิทยาลัยเทคโนโลยีสุรนารี วันที่ 24 พฤษภาคม 2565
10. การฝึกอบรมจริยธรรมการวิจัยในมนุษย์ หลักสูตร "จริยธรรมการวิจัยด้านสังคมและพฤติกรรมศาสตร์" ณ อาคาร C2-124 อาคารวิชาการ 2 มหาวิทยาลัยเทคโนโลยีสุรนารี วันพฤหัสบดีที่ 30 พฤษภาคม 2562
11. โครงการเตรียมความพร้อม ทางด้านวิชาการ ณ ห้องประชุมลำตะคองวิทยาลัยนครราชสีมา วันที่ 3 เมษายน 2567
12. โครงการอบรมอาจารย์ใหม่ ประจำปีการศึกษา 2566 ณ ห้องประชุมปักธงชัย วิทยาลัยนครราชสีมา วันที่ 4 เมษายน 2567
13. โครงการอบรมความรู้ ความเข้าใจในการนำ"เกณฑ์คุณภาพการศึกษาเพื่อการดำเนินการที่เป็นเลิศ (EdPEX)"มาใช้ในการบริหารจัดการศึกษา ณ ห้องประชุมลำตะคอง วิทยาลัยนครราชสีมา วันศุกร์ที่ 19 เมษายน พ.ศ.2567
14. โครงการเพิ่มพูนความรู้วิชาชีพการสาธารณสุขชุมชน Season 4 จัดโดย คกก.สภาการสาธารณสุขชุมชน ระหว่างวันที่ ๓๐ เมษายน - ๒ พฤษภาคม ๒๕๖๗

15. การอบรมเชิงปฏิบัติการการเขียนโครงสร้างองค์กร (Organizational Profile : OP) ตามแนวทางการพัฒนาคุณภาพการศึกษาสู่ความเป็นเลิศ(Education Criteria for Performance Excellence : EdPEx) ณ ห้องประชุมลำตะคอง วิทยาลัยนครราชสีมา ระหว่างวันที่ 8 - 9 พฤษภาคม พ.ศ.2567

International conference poster presentation

1. Effectiveness of 6 Steps Prevention and Control for Dengue Haemorrhagic Fever in Rural Community of Thailand. **Sukanya Ponphimai**. At Asian Symposium on Healthcare Without Borders (HWB 2rd 2015). Mitsui Garden Hotel, Hiroshima, Japan August 6th to 8th, 2015
2. Hospital Elderly Club, Nakhon Ratchasima, Thailand. **Sukanya Ponphimai**. At Asian Symposium on Healthcare Without Borders (HWB/ICT4HD 3rd 2016). The Clio Court Hotel, Fukuoka, Japan November 3-5. 2016
3. การพัฒนารูปแบบการส่งเสริมสุขภาพผู้สูงอายุในระดับพื้นที่กรุงเทพมหานคร.อนันตชัย อินทร์ธิดราช ดุษฎี เจริญสุข บัณฑิตา คงเจริญ ปาลพัชร เกื้อกุล เสาวลี แก้วช่วย **สุกัญญา ผลพิมาย** การประชุมวิชาการระดับชาติโครงการวันวิชาการคณะพลศึกษาบัณฑิตกรรมสุขภาพและกีฬา ครั้งที่ 6 ณ คณะพลศึกษา มหาวิทยาลัยศรีนครินทรวิโรฒ องครักษ์ วันศุกร์ที่ 23 กุมภาพันธ์ 2567

Area of Interest

Public Health Typing of health promotion, Nutrition, prevention, and control, NCD and Molecular Typing of proteins, antigen antibodies, development of immunodiagnostic for detect food contamination.

Research projects

Construction and characterization of murine single-chain variable fragment (MuscFv) antibody against acrylamide This work was supported by research grants Graduate Studies from the Office of the National Research Council of Thailand for the year 2021 (Grant number D-M6111380-1/2564).

Supervisor advisor of graduate students

Advisor

1. นายคมสันต์ บุญผูก นักศึกษาระดับปริญญาตรี หลักสูตร สาธารณสุขหัตถ์วิทยานิพนธ์
พฤติกรรม การดูแลสุขภาพตนเองของผู้สูงอายุที่ป่วยเป็นโรคความดันโลหิตสูง ตำบลไพล
อำเภอลำทะเมนชัย จังหวัดนครราชสีมา

Co-Advisor

1. นางสาวสุพรรณิ แสงจันทร์ นางสาวกนิษฐา ท่าเกษม นักศึกษาระดับปริญญาตรี หลักสูตร
สาธารณสุขหัตถ์วิทยานิพนธ์ ความรอบรู้ด้านสุขภาพและพฤติกรรม การดูแลสุขภาพตาม
หลัก 3อ2ส.ของอาสาสมัครสาธารณสุขประจำหมู่บ้าน (อสม.)

